

IMT School for Advanced Studies, Lucca

Lucca, Italy

Neurophysiological assessments of low-level and high-level interdependencies between auditory and visual systems in the human brain

PhD in Institutions, Markets and Technologies –
Curriculum in Cognitive, Computational and Social
Neurosciences

XXXII Cycle

By

Evgenia Bednaya

2022

The dissertation of Evgenia Bednaya is approved.

PhD Program Coordinator:

Prof. Maria Luisa Catoni, IMT School for advanced Studies Lucca, Italy

Advisor:

Prof. Davide Bottari, IMT School for advanced Studies Lucca, Italy

Co-Advisor:

Prof. Emiliano Ricciardi, IMT School for advanced Studies Lucca, Italy

The dissertation of Evgenia Bednaya has been reviewed by:

Dr. Velia Cardin, University College London (UCL), United Kingdom

Dr. Nicola Molinaro, Basque Center on Cognition, Brain and Language (BCBL), Spain

IMT School for Advanced Studies, Lucca

2022

Брату Юре

Content

List of Figures	vii
Acknowledgements	viii
Vita	x
Publications and Presentations	xi
Abstract	xii
Chapter 1	1
1.1 Background.....	1
1.2 Thesis Outline	8
Chapter 2	11
2.1 Introduction.....	11
2.1.1 Probing intramodal plasticity through neural oscillations	14
2.1.2 The present study	15
2.2 Methods	17
2.2.1 Participants	17
2.2.2 Stimuli and Procedure	17
2.2.3 EEG-recording and pre-processing.....	19
2.2.4 Spectral decomposition.....	20
2.2.5 Statistical approach.....	21
2.3 Results	22
2.3.1 Behavioral data	22
2.3.2 Repetition Suppression effects.....	23
2.3.3 Novelty Detection effects.....	25

2.4 Discussion.....	27
2.4.1 Altered RS in early deaf adults.....	28
2.4.2 Reduced ND response in early deaf adults.....	31
2.4.3 Is the greater RS a marker of modified predictive mechanisms in early deafness?.....	33
Chapter 3.....	36
3.1 Introduction.....	36
3.2 Methods	39
3.2.1 Participants.....	39
3.2.2 Experimental design and setup	40
3.2.3 Face-Object Categorization (Experiment 1)	41
3.2.4 Emotional Facial Expression Discrimination (Experiment 2).....	43
3.2.5 Individual Face Discrimination (Experiment 3).....	44
3.2.6 EEG acquisition.....	46
3.2.7 Data analysis in the frequency-domain.....	46
3.2.8 Data analysis in the time-domain.....	51
3.2.9 Source reconstruction.....	52
3.2.10 Behavioral data	54
3.3 Results	55
3.3.1 Experiment 1 (Face-Object Categorization, FO).....	55
3.3.2 Experiment 2 (Emotional Facial Expression Discrimination, EM).....	56
3.3.3 Experiment 3 (Individual Face Discrimination, ID).....	58
3.3.4 Base frequency	60

3.3.5 Source estimates for FO and ID experiments at Auditory ROIs.....	60
3.4 Discussion.....	62
Chapter 4.....	68
4.1 Introduction.....	68
4.2 Methods	70
4.2.1 Participants	70
4.2.2 Stimuli	70
4.2.3 Task and Experimental Procedure	74
4.2.4 EEG Recording.....	75
4.2.5 EEG Preprocessing	76
4.2.6 Extraction of Acoustic Envelope.....	77
4.2.7 Estimation of TRF	77
4.2.8 Regularization Parameter Estimation.....	78
4.2.9 Spatiotemporal Characteristics.....	79
4.2.10 Chance-level Estimation by Permutation Testing (Control).....	79
4.2.11 Source Estimation	79
4.2.12 Statistical Analysis.....	81
4.3 Results	82
4.3.1 Behavioral responses.....	82
4.3.2 Neural tracking	83
4.4 Discussion.....	88
4.4.1 Effects of low-level acoustic (SNR) processing on neural tracking of speech envelope.....	88

4.4.2 Effects of high-level linguistic (Semantic) processing on neural tracking of speech envelope.....	90
4.4.3 Two distributed networks are engaged in envelope tracking of continuous speech	91
4.4.4 Early visual cortex's entrainment to speech envelope in blindfolded individuals is reduced by background noise...	92
4.4.5 Limitations of the study	94
4.4.6 Conclusion	95
Chapter 5.....	96
Appendix A	101
Appendix B.....	103
B.1 Time-course of EEG data for each experiment	107
B.1.1 Face-selective response	109
B.1.2 Response to facial expression change	110
B.1.3 Identity discrimination response.....	110
B.2 Source analysis, within group results.	111
B.2.1 Face-Object Categorization experiment.....	111
B.2.2 Individual Face Discrimination experiment	112
Appendix C.....	114
C.1 Questionnaire.....	114
C.2 Choice of SNR level.....	116
C.3 Effect of Speech Rate, Intensity and Modulation Depth	120
Bibliography.....	121

List of Figures

Figure 2.1: Experimental paradigm	19
Figure 2.2: Repetition Suppression (RS; Induced Activity) in early deaf individuals and hearing controls	24
Figure 2.3: Zoom-in of RS-Theta effect.....	25
Figure 2.4: Novelty Detection (ND; Induced Activity) in early deaf individuals and hearing controls	26
Figure 2.5: Inter-trial phase coherence (ITPC) in early deaf individuals and hearing controls	27
Figure 3.1: Schematic illustration of the experimental paradigms	42
Figure 3.2: Experiment 1 (Face-Object Categorization)	56
Figure 3.3: Experiment 2 (Emotional Facial Expression Discrimination)	57
Figure 3.4: Experiment 3 (Individual Face Discrimination)	59
Figure 3.5: Source analysis performed in the time domain for the Face-Object Categorization experiment	61
Figure 3.6: Source analysis performed in the time domain for the Individual Face Discrimination experiment	62
Figure 4.1: Stimuli, Behavioral Responses, and Analysis Approach	73
Figure 4.2: Low-level acoustic (SNR) effect	84
Figure 4.3: High-level (Semantic) effect	86

Acknowledgements

This dissertation contains material based on the works either published in peer-reviewed journals or under submission, as follows:

The content of **Chapter 2** was published as (Bednaya, Pavani, Ricciardi, Pietrini, & Bottari, 2021) in *Cortex*, co-authored by **Evgenia Bednaya**, Francesco Pavani, Emiliano Ricciardi, Pietro Pietrini, and Davide Bottari.

CRedit taxonomy (<https://credit.niso.org/>) for Evgenia Bednaya: Formal analysis, Data Curation, Writing - original draft, Writing - review & editing, Visualization. This work was performed in collaboration between IMT School for Advanced Studies Lucca (Italy) and Center for Mind/Brain Sciences (CIMEC), University of Trento (Italy).

The content of **Chapter 3** was published as (Bottari, Bednaya, Dormal, Villwock, Dzhelyova, Grin, Pietrini, Ricciardi, Rossion, & Röder, 2020) in *NeuroImage*, co-authored by Davide Bottari, **Evgenia Bednaya**, Giulia Dormal, Agnes Villwock, Milena Dzhelyova, Konstantin Grin, Pietro Pietrini, Emiliano Ricciardi, Bruno Rossion, and Brigitte Röder.

CRedit for Evgenia Bednaya: Formal analysis, Writing - original draft, Writing - review & editing, Visualization. This work was performed in collaboration between IMT School for Advanced Studies Lucca (Italy), University of Hamburg (Germany) and Institute of Neuroscience, University of Louvain (Belgium).

The content of **Chapter 4** is under submission, with the following list of co-authors: **Evgenia Bednaya**, Bojana Mirkovic, Martina Berto, Emiliano Ricciardi, Alice Martinelli, Alessandra Federici, Stefan Debener, and Davide Bottari.

CRedit for Evgenia Bednaya: Conceptualization, Methodology, Formal analysis, Investigation, Data Curation, Writing - original draft, Writing - review & editing, Visualization. This work was performed in collaboration between IMT School for Advanced Studies Lucca (Italy) and University of Oldenburg (Germany).

Throughout the dissertation chapters, I use "we" to acknowledge the contribution of all the above-mentioned collaborators.

I want to thank:

- My supervisor, Davide Bottari, for his patience, help and guidance throughout these years, and for teaching me that PhD is a marathon - not a sprint;
- My co-supervisor, Emiliano Ricciardi, for supporting all the research ideas, as well as extra-curricular activities during my PhD;
- External referees, for their positive feedback and sincere suggestions on the thesis;
- IMT PhD office and administrative staff, for their help and assistance in getting through Italian bureaucracy easier;
- Dr. Alexander Arkhipenko, for being a true mentor and all the encouragement along this PhD journey from start to finish, from Bruges, Paris, Provence, and New York;
- My dear frolleagues from IMT - Ilaria, Laura, Hakan, Nilay, Niraj, Sampath, Matteo, Di, and Yuri, for the great time we spent together in Lucca, and for conversations we had during late-night dinners at StraVinSky;
- Vlad and Roman from StraVinSky, for a homely atmosphere and the best food, wine, and service in town;
- Members of Just Choir (aka non-official IMT choir), as well as current and former members of IMT Student and Alumni Association Executive Board, for the great teamwork and filling my PhD life outside the lab with social activities along with some administrative tasks and duties;
- My colleagues at the SEED research group - Alice, Martina, Alessandra, Chiara, and Marta, for their help and volunteering as a "lab buddy" for my EEG experiments;
- PhD students from the Neuropsychology Lab at the University of Oldenburg - Joanna, Yadwinder, Maria, Tatiana, and Nadine, for making my visiting period unforgettable;
- My old friends - Dasha, Sid, Grazia, Sasha B., and Katia D., for being always by my side and patiently listening to me whine about this and that;
- My family, for their love and unconditional support, no matter what;
- My partner's family, for their immense hospitality and showing me the beauty of Northern Italy;
- My partner Ste, for being there for me through my ups and downs, using motivational quotes from Iron Maiden, and reminding me that there is a light at the end of the tunnel.

Vita

- 10 July, 1988** Born in Sosnovy Bor (Leningrad Oblast), USSR
- 2005-2011** B.Sc., M.Sc. in Biology
Saint-Petersburg State University,
St. Petersburg, Russia
- 2008-2013** Junior Research Associate
Child Speech Research Group,
St. Petersburg, Russia
- 2011-2013** Teaching Assistant in Medical Biology
St. Petersburg State Pediatric Medical University,
St. Petersburg, Russia
- 2013-2015** M.Res. in Cognitive Neuroscience
Radboud University,
Nijmegen, The Netherlands
- 2015** Research Assistant
Donders Centre for Cognition,
Nijmegen, The Netherlands
- 2016-2022** Ph.D. in Cognitive, Computational and Social
Neurosciences
IMT Institute for Advanced Studies Lucca,
Lucca, Italy
- 2019** Visiting Researcher (supported by Erasmus+ Grant)
University of Oldenburg
Oldenburg, Germany

Publications (within this thesis)

1. **Bednaya, E.**, Mirkovic, B., Berto, M., Ricciardi, E., Martinelli, A., Federici, A., Debener, S., and Bottari, D. (2022). *Early visual cortex tracks speech envelope in the absence of visual input*. bioRxiv. <https://doi.org/10.1101/2022.06.28.497713>
2. **Bednaya, E.**, Pavani, F., Ricciardi, E., Pietrini, P., and Bottari, D. (2021). Oscillatory signatures of Repetition Suppression and Novelty Detection reveal altered induced visual responses in early deafness. *Cortex*, *142*, 138–153.
3. Bottari, D., **Bednaya, E.***, Dormal, G.*, Villwock, A., Dzhelyova, M., Grin, K., Pietrini P., Ricciardi E., Rossion B., and Röder, B. (2020). EEG frequency-tagging demonstrates increased left hemispheric involvement and crossmodal plasticity for face processing in congenitally deaf signers. *NeuroImage*, *223*, 117315. *Shared authorship

Presentations (during the PhD)

Face processing in congenitally deaf signers as revealed by fast periodic visual stimulation, *World Congress of Psychophysiology (IOP)*, Lucca, Italy, 2018.

Face processing in congenitally deaf signers, *WoRLD: Workshop on Reading, Language and Deafness*, San Sebastián, Spain, 2018.

Altered Neural Network Dynamics During the Visual Processing in Early Deaf Individuals, *Annual Meeting of Organization for Human Brain Mapping (OHBM)*, Rome, Italy, 2019.

Investigating the role of auditory deprivation in shaping the mechanisms of repetition suppression and novelty detection in the visual system, *XXVII Congress of Italian Society of Psychophysiology and Cognitive Neuroscience (SIPF)*, Ferrara, Italy, 2019.

Abstract

This dissertation investigates the functional interplay between visual and auditory systems and its degree of experience-dependent plasticity. To function efficiently in everyday life, we must rely on our senses, building complex hierarchical representations about the environment. Early sensory deprivation, congenital (from birth) or within the first year of life, is a key model to study sensory experience and the degree of compensatory reorganizations (i.e., neuroplasticity). Neuroplasticity can be intramodal (within the sensory system) and crossmodal (the recruitment of deprived cortical areas for remaining senses). However, the exact role of early sensory experience and the mechanisms guiding experience-driven plasticity need further investigation. To this aim, we performed three electroencephalographic studies, considering the aspects: 1) sensory modality (auditory/visual), 2) hierarchy of the brain functional organization (low-/high-level), and 3) sensory deprivation (deprived/non-deprived cortices). The first study explored how early auditory experience affects low-level visual processing, using time-frequency analysis on the data of early deaf individuals and their hearing counterparts. The second study investigated experience-dependent plasticity in hierarchically organized face processing, applying fast periodic visual stimulation in congenitally deaf signers and their hearing controls. The third study assessed neural responses of blindfolded participants, using naturalistic stimuli together with temporal response function, and evaluated neural tracking in hierarchically organized speech processing when retinal input is absent, focusing on the role of the visual cortex. The results demonstrate the importance of atypical early sensory experience in shaping (via intra- and crossmodal changes) the brain organization at various hierarchical stages of sensory processing but also support the idea that some crossmodal effects emerge even with typical experience. This dissertation provides new insights into understanding the functional interplay between visual and auditory systems and the related mechanisms driving experience-dependent plasticity and may contribute to the development of sensory restoration tools and rehabilitation strategies for sensory-typical and sensory-deprived populations.

Chapter 1

Introduction

1.1 Background

In 2017, while attending a summer school at Imperial College London, I met Noah Wall, then five-year-old. Noah was born with only 2 percent of his brain due to a severe form of fetal spina bifida, so his chance to survive long after the birth was minimal. However, by the age of three, after extensive training and rehabilitation procedures, Noah had grown about 80 percent of his brain back and learned how to walk, speak, and count as any other toddler. The grown-back brain of Noah is an example of thriving *neuroplasticity* – the ability of the brain to repair itself through growing new pathways and reorganizing to compensate for a loss (e.g., resulting from fetal anomalies, neonatal damage, or sensory deprivation early in life).

In everyday life, to survive and function effectively, it is essential to rely on our senses and build complex hierarchical representations about the environment. As dynamic creatures, humans rely heavily on vision in the constantly changing environment to analyze what happened in the past and predict what could happen in the future. These include both basic aspects, such as the ability to recognize familiar patterns and detect novel ones and orienting, and more complex ones, such as identifying familiar objects, and recognizing faces and emotional facial expressions for effective interpersonal communication. Along with vision, hearing and speech processing are crucial for our successful navigation and effective social communication in complex and challenging listening environments, which often comprise speech signals embedded into background noise. Visual and auditory systems are highly interconnected, and we greatly benefit from interactions between sensory modalities which alter each other's processing. Moreover, the brain has been hypothesized to have rather a metamodal structure (Alvaro Pascual-Leone & Hamilton, 2001), where cortical areas perform their specific computations regardless of the sensory input, selecting the optimal sensory modality from the competing ones. As a result, we can understand and segment incoming information quickly and with ease, even unconsciously.

Sensory-deprived individuals, relying heavily on their intact senses, can adapt to sensory loss and effectively manage their everyday life. Furthermore, sensory-deprived individuals even outperform their neurotypical counterparts in some tasks, demonstrating enhanced perceptual abilities. It becomes possible due to experience-dependent plasticity, a fundamental property of the brain to change and adapt in response to the environment because of experience.

Early sensory deprivation (i.e., the reduction or removal of input from one or more senses since birth or within the first year of life) is a key and unique model for understanding the role of early sensory experience in the brain development, the degree of adaptive structural and functional reorganizations in the brain that drive behavioral performance, as well as corresponding neuronal mechanisms (Ricciardi, Bottari, Pfito, Röder, & Pietrini, 2020). Numerous studies on human data and animal models showed that to compensate for the lack of sensory input, plastic reorganizations tend to happen during the early years of life and at multiple levels in the brain (Bavelier & Neville, 2002; Merabet & Pascual-Leone, 2010; Rauschecker, 1995, 2002; Ricciardi & Pietrini, 2011). Within the current dissertation, we focus on auditory and visual deprivations, which have been shown to induce partially common mechanisms (Bavelier & Neville, 2002; L. Bell et al., 2019; Merabet & Pascual-Leone, 2010; Pavani & Röder, 2012). These sensory deprivations are associated with crossmodal and intramodal changes in the brain (Bola et al., 2017; Heimler, Weisz, & Collignon, 2014; Merabet & Pascual-Leone, 2010; Striem-Amit, Bubic, & Amedi, 2012).

Crossmodal reorganizations in the brain reflect the recruitment of cortical areas of a deprived sensory modality to process input originating from the intact sensory modalities (Bavelier & Neville, 2002; Merabet & Pascual-Leone, 2010; Sharma, Campbell, & Cardon, 2015). Crossmodal plasticity in deaf or cochlear implanted individuals could be illustrated by the recruitment of parts of their brain that are typically considered for processing auditory input to process non-auditory ones, such as visual and tactile (Benetti et al., 2017; Bola et al., 2017; Bottari et al., 2014; Cardin et al., 2013; Finney, Clementz, Hickok, & Dobkins, 2003; Finney, Fine, & Dobkins, 2001; Karns, Dow, & Neville, 2012; Leonard et al., 2012; MacSweeney et al., 2002; Sandmann et al., 2012; Stropahl et al., 2015). Similarly, crossmodal plasticity in blind individuals encompasses the recruitment of the occipital cortex, ordinarily responsible for visual

processing, to process sound and touch (Bedny, Pascual-Leone, Dodell-Feder, Fedorenko, & Saxe, 2011; Bedny, Richardson, & Saxe, 2015; Collignon et al., 2011; Collignon, Voss, Lassonde, & Lepore, 2009; Gougoux, Zatorre, Lassonde, Voss, & Lepore, 2005; Merabet et al., 2008; Poirier et al., 2006; Ricciardi et al., 2007; Röder, Stock, Bien, Neville, & Rösler, 2002; Sadato et al., 1996).

In the context of sensory deprivation, intramodal reorganizations in the brain occur within a sensory modality, resulting from altered usage (increased or decreased) of that modality due to altered input availability. This is the case of responses in the visual cortex of deaf and cochlear implanted individuals (Bavelier et al., 2000, 2001; Bottari et al., 2014; Doucet, Bergeron, Lassonde, Ferron, & Lepore, 2006; Hauthal, Thorne, Debener, & Sandmann, 2014). Similarly, blind individuals demonstrate intramodal changes as a consequence of sensory deprivation through responses in their auditory cortex (Burton et al., 2002; Elbert et al., 2002; Gougoux et al., 2009; Röder, Rösler, & Neville, 1999; Röder et al., 2002). Furthermore, this type of plasticity is well known to happen also in the neurotypical population, following extensive training and learning, affecting a particular modality (see for the reviews: Chang, 2014; Münte, Altenmüller, & Jäncke, 2002). Intramodal plasticity effects are characterized by the reduction or expansion of cortical representations (Elbert et al., 1994; Rauschecker, 2002) and alterations of the functional tuning of neuronal responses (Huber et al., 2019).

Crossmodal and intramodal reorganizations have been linked to enhanced behavioral performance in the remaining modalities in deaf and blind individuals compared to non-sensory deprived individuals. Particularly, deaf individuals show an advantage over hearing individuals in specific visual tasks (Amadeo, Campus, Pavani, & Gori, 2019; Bavelier et al., 2000; Bottari, Caclin, Giard, & Pavani, 2011; Bottari et al., 2014; Bottari, Nava, Ley, & Pavani, 2010; de Heering, Aljuhanay, Rossion, & Pascalis, 2012; Nava, Bottari, Zampini, & Pavani, 2008; Proksch & Bavelier, 2002; Stoll et al., 2018; see for the reviews: Bavelier, Dye, & Hauser, 2006; Pavani & Bottari, 2012), whereas blind individuals outperform sighted individuals in a variety of non-visual task, including auditory and somatosensory, tasks (Arnaud, Gracco, & Ménard, 2018; Dietrich, Hertrich, & Ackermann, 2013; Muchnik, Efrati, Nemeth, Malin, & Hildesheimer, 1991; Nilsson & Schenkman, 2016; Röder, Rösler,

Hennighausen, & Näcker, 1996; Röder et al., 1999; see for the reviews: Kupers & Ptito, 2014; Pavani & Röder, 2012).

The subject of ongoing research is the functional interplay between the visual and auditory systems in the human brain and its degree of experience-dependent plasticity. In the last thirty years, the progress of neuroimaging techniques and analytic tools has led to the grown interest in the human sensory-deprived model, with the increasing number of studies investigating congenital, early, and late blindness and deafness in humans at both behavioral and neural levels (Ricciardi et al., 2020). However, to date, it is still an ongoing debate on how and to what extent the brain reorganizes itself following temporary or permanent atypical sensory experience. Furthermore, understanding which mechanisms may guide such neuroplasticity is scarce and needs further attention.

Therefore, in three different studies, this thesis addressed several *open research questions* to advance the current knowledge on the functional interplay between visual and auditory systems and the degree and mechanisms of experience-dependent changes in the human brain (each study is described below in section “1.2 Thesis Outline”). Answering these questions would let us get insights not only into how the brain functions in general (informing research on vision, audition, and audio-visual integration) but also into its potential to adapt to a sensory loss, which could contribute to the development of effective rehabilitation procedures (Collignon, Champoux, Voss, & Lepore, 2011; Heimler et al., 2014; Heimler & Amedi, 2020; Merabet & Pascual-Leone, 2010).

The following specific questions have been addressed in this thesis:

- (1) How the early auditory deprivation affects the oscillatory signatures of fundamental mechanisms of basic visual processing such as Repetition Suppression (RS) and Novelty Detection (ND)? To what extent the functional development of RS and ND responses is constrained within each sensory system, or does their functioning also depend on the input availability in the other senses?
- (2) Which aspects of face processing are experience-dependent? Whether and to what extent different functions of face processing encounter distinct neural adaptations to altered early auditory experience?

(3) What is the role of the visual cortex in different levels of continuous speech processing in the absence of competing retinal input?

Overall, using electroencephalography (EEG), we investigated the functional interplay between visual and auditory systems, the degree, and mechanisms of experience-dependent changes in the human brain. We considered three main aspects of sensory processing: 1) modality (auditory or visual), 2) hierarchy of the brain functional organization (low-level or high-level), and 3) sensory deprivation (deprived or non-deprived cortices). Moreover, in each of these three separate EEG-based studies, through collaborative efforts and shared expertise between research groups, we managed to test different though homogeneous population groups of participants and employ various experimental paradigms and methods of analysis. Thus, our research aims were probed from different angles.

Studying both neurotypical and early sensory-deprived populations allows for assessing the effects of experience on human brain development and its functioning. That is, we could better understand whether and which neuroplastic changes are specific for the sensory-deprived brain as a result of altered sensory experience or, instead, if it is a shared, general principle of neural organization and function in the brain (Ricciardi, Bonino, Pellegrini, & Pietrini, 2014). However, research involving sensory-deprived human models could be challenging due to the small size of the focus populations and difficulties with their recruiting (Cardin, Grin, Vinogradova, & Manini, 2020), as well as due to the high heterogeneity of their demographic and clinical variables (e.g., cause and onset of sensory deprivation, age, education) (Ricciardi et al., 2020). Therefore, nowadays, collaborations across laboratories are highly demanded (Cardin et al., 2020; Ricciardi et al., 2020).

As for the employed here experimental paradigms and methods of analysis, **time-frequency analysis** has become a widely used approach in the last two decades, offering several advantages over traditional neurophysiological methods (such as event-related potentials, ERPs) of the EEG data analysis. It provides essential information on the EEG signal regarding the dynamic changes in amplitude and phase of neural oscillations across multiple specific frequencies, which is neglected in traditional ERP analysis and Fourier-based analyses of power (Morales &

Bowers, 2022; Roach & Mathalon, 2008; Catherine Tallon-Baudry, Bertrand, Delpuech, & Pernier, 1997). Hence, optimal evoked (phase-locked) and induced (non-phase-locked) time-frequency representations of power could be computed and investigated, as well as inter-trial phase coherence, to measure the degree of phase consistency of the neural response across trials within conditions of interest.

Another recent methodological development is represented by the analysis of EEG data following Fast Periodic Visual Stimulation (FPVS) or **frequency-tagging**. Frequency-tagging approach could tell us about different aspects of neural processing in terms of information flow. It has been successfully employed to study selective stimulus responses in EEG experiments of the last decade, particularly for face processing in typically developed individuals (Dzhelyova, Jacques, & Rossion, 2017; Liu-Shuang, Norcia, & Rossion, 2014; Rossion, Torfs, Jacques, & Liu-Shuang, 2015; see Rossion, Retter, & Liu-Shuang, 2020 for a review). With frequency-tagging, a stimulus is presented repetitively at a fixed and fast periodic rate (i.e., frequency of interest), producing a robust steady-state evoked potential, and therefore, resulting in greater brain response at the tagged frequency. Thus, the frequency with which the stimulus is presented provides a frequency tag to identify the associated brain response. The advantages of this approach are in its sensitivity (i.e., very high signal-to-noise ratio), objectivity (i.e., responses are predefined by a stimulation frequency of interest), and the possibility to measure both low-level and high-level functions in the absence of explicit behavioral responses (e.g., Heinrich, 2009; Norcia, Appelbaum, Ales, Cottareau, & Rossion, 2015; Stothart, Quadflieg, & Milton, 2017; Vettori et al., 2019).

With the methodological progress, it also became possible to employ noninvasive magneto- and electroencephalography (M/EEG) techniques together with **system identification** approaches in order to relate continuous stimuli (e.g., speech) to ongoing brain activity in time (see for the reviews: Alday, 2019; Brodbeck & Simon, 2020; Holdgraf et al., 2017). Classic neuroscientific paradigms imply multiple repetitions of short and isolated stimuli (e.g., single words, syllables, and sentences) and averaging responses recorded from the brain to obtain a sufficient signal-to-noise ratio (SNR). These paradigms, though, are incapable of studying neural responses to continuous speech signal and thus has been criticized as being less informative and not naturalistic for studying how

the language is processed in the brain (Alexandrou, Saarinen, Kujala, & Salmelin, 2020; Hamilton & Huth, 2020). Naturalistic speech stimuli (such as movies or narratives in the presence of background noise) are complex and resemble dynamic everyday life listening conditions, engaging simultaneously multiple perceptual and cognitive processes. In the past decade, naturalistic and continuously presented stimuli, previously avoided in functional magnetic resonance imaging (fMRI) research (Willems & van Gerven, 2018), have been widely employed in fMRI studies together with the advanced statistical and computational methods, making it possible to assess hierarchically organized language processing at multiple cortical sites and different temporal windows (e.g., Huth, Lee, et al., 2016; Huth, Nishimoto, Vu, & Gallant, 2012; see for reviews: Hamilton & Huth, 2020; Jääskeläinen, Sams, Glerean, & Ahveninen, 2021; Willems & van Gerven, 2018). However, despite fMRI technique has significantly higher spatial resolution compared to those of M/EEG, the latter offer far superior temporal resolution.

Neurons can synchronize (or entrain) their activity to slow temporal fluctuations of an acoustic signal (i.e., envelope) (Luo & Poeppel, 2007). Such entrainment, or *neural tracking* of the speech envelope, has been considered a promising and more advanced tool for studying speech perception and comprehension (Giraud & Poeppel, 2012). For example, M/EEG studies on auditory selective attention widely employed the **temporal response function** (TRF) approach (Crosse, Di Liberto, Bednar, & Lalor, 2016) to identify an attended speaker in a more naturalistic multi-speaker, or cocktail-party (Cherry, 1953), scenario (Ding & Simon, 2012; Mirkovic, Debener, Jaeger, & De Vos, 2015; J. A. O'Sullivan et al., 2015; Zion Golumbic et al., 2013). Other recent studies used TRF to record the relationships between low-level acoustic features and high-level semantic representations of continuous speech (e.g., Brodbeck, Hong, & Simon, 2018; Broderick, Anderson, & Lalor, 2019; Broderick, Di Liberto, Anderson, Rofes, & Lalor, 2021; Etard & Reichenbach, 2019).

More specifically, TRF is a ridge regression-based system identification approach allowing to predict neural response from the stimulus (forward model/encoding), or vice versa, to reconstruct the stimulus from neural response (backward model/decoding). Forward TRF models describe how neural responses change as a function of a (or set of) specific stimulus feature(s) (for example, the envelope) and are advantageous over simple cross-correlation procedure when applied to

continuous speech, considering the autocovariance of the stimuli (Crosse et al., 2016). Forward modeling allows to minimize a common problem of temporal smearing of impulse response functions when averaging across time points, since the potential time delay between the stimuli and the recorded brain responses is taken into account (Crosse et al., 2016; Myers, Lense, & Gordon, 2019). Furthermore, unlike backward models, forward models are readily neurophysiologically interpretable (Haufe et al., 2014) and comparable (though not exactly identical) to cortical auditory evoked potentials (CAEPs) (Lalor & Foxe, 2010; Lalor, Power, Reilly, & Foxe, 2009).

1.2 Thesis Outline

The following three chapters contain EEG-based studies, and each chapter can be read independently from the other two chapters.

The first study (**Chapter 2**) aimed to explore how early deafness affects the oscillatory signatures of two fundamental mechanisms of low-level visual processing: Repetition Suppression (RS) and Novelty Detection (ND). It is an open question, to what extent the functional development of RS and ND responses is constrained within each sensory system, or whether their functioning also depends on input availability in the other senses. With this aim, we investigated modulations of oscillatory activity and their relation to feedback/feedforward processes in the brain, in line with the predictive coding theories of sensory processing. The EEG data were acquired from the group of early deaf participants and their hearing counterparts exposed to repeated and novel visual events in the oddball paradigm. Using the time-frequency analysis, we evaluated between-group differences in RS and ND. We compared the evoked and induced oscillatory activities and inter-trial phase coherence. The results revealed experience-dependent changes selectively in the induced responses: in theta band for RS and in alpha/beta bands for ND. The modulations of evoked responses and inter-trial phase coherence were comparable between the two groups. Selective changes in induced activity may indicate altered feedback processes in early deaf individuals and suggest a better functional tuning of the visual system in early deaf individuals.

The second study (**Chapter 3**) investigated the experience dependence of the cortical organization for hierarchically organized face processing – one of the most studied human brain functions. To this aim, we combined fast periodic visual stimulation with frequency-tagging EEG. The EEG recordings were obtained in the group of participants from a rare population of congenitally deaf signers and their control group of hearing non-signers. Participants watched a continuous stream of repeated visual stimuli presented at the base stimulation frequency, with target stimuli occurring at the oddball frequency and its harmonics. This paradigm allowed us to obtain objective face-selective neural responses (i.e., visual steady-state responses) with a high signal-to-noise ratio in a relatively short stimulation time. We performed a series of three experiments and evaluated face-selective responses separately in the frequency-domain and in the time-domain: (Experiment 1) Face-Object categorization, (Experiment 2) Emotional Facial Expression, and (Experiment 3) Individual Face discrimination. The results suggested that different aspects of the face processing system displayed specific experience-dependent functional organizations through partial adaptations in different ways (either intra- or crossmodal) to the altered early experience.

In the first two studies, we investigated the impact of the permanent lack of auditory experience on low-level and high-level processes within the visual system and the corresponding neural mechanisms that may underlie enhanced visual processing skills in deaf individuals. In the third study, we investigated to what extent the visual cortex participates in tracking auditory input in case of typical development but when the competing visual input is absent.

In particular, the third study (**Chapter 4**) assessed neural tracking in the hierarchy of continuous speech, focusing on the role of the early visual cortex. We recorded EEG responses of neurotypical blindfolded participants listening to meaningful and meaningless stories either in quiet or noise at different SNR. To assess neural speech tracking, we used linear mapping between the EEG data and corresponding stimuli to estimate temporal response function (TRF) to speech. We assessed low-level acoustic (SNR) effects by contrasting TRFs resulting from listening to stories in quiet vs. noise, as well as high-level linguistic (Semantic) effects by contrasting TRFs resulting from listening to meaningful vs. meaningless stories, both embedded in noise. To better understand the

origin of such effects, we performed source modeling of the TRFs, focusing on the visual cortex. Our findings revealed low-level acoustic and high-level linguistic effects on envelope tracking, involving broad networks of activation beyond the auditory cortex. Furthermore, our findings revealed that the early visual cortex of blindfolded participants was involved into speech envelope tracking, and the magnitude of such entrainment was affected by low-level speech features. These findings contribute to the characterization of the functional role of the visual cortex in speech processing in the sighted and blind.

Finally, a brief summary of the results, implications, limitations and future directions are outlined in **(Chapter 5)**.

Chapter 2

Oscillatory signatures of Repetition Suppression and Novelty Detection reveal altered induced visual responses in early deafness

2.1 Introduction

A fundamental property of the visual system is the ability to recognize familiar patterns and distinguish novel ones. This property unveils how neural dynamics are modulated by ongoing sensory processing on a short temporal scale (Kohn, 2007). When visual stimuli are repeated, the neural response is typically reduced. Such reduction, upon the second and subsequent stimulus presentations, has been usually referred to as Repetition Suppression (RS) or adaptation (Grill-Spector, Henson, & Martin, 2006). Repetition suppression is stimulus-specific, that is, it is not observed following the presentation of trains of physically different visual events (E. K. Miller, Li, & Desimone, 1993). Yet, a certain invariance to stimulus properties, such as size and location, has been described (Lueschow, Miller, & Desimone, 1994). Moreover, RS is known to interact with expectations of the repetition to occur (e.g., Summerfield, Wyart, Johnen, & de Gardelle, 2011), as well as with attentional processes (Hsu, Hämäläinen, & Waszak, 2014). The RS has been broadly studied in animal models (e.g., monkeys: Vinken, Op de Beeck, & Vogels, 2018; Vinken & Vogels, 2017; Vogels, 2016), and in humans, using multiple imaging tools, across different sensory modalities and multiple brain regions (see Gotts, Chow, & Martin, 2012; Webster, 2015 for the reviews).

On the contrary, novel visual stimuli are typically associated with an increase of the neural response/excitability, as compared to previous events (Ranganath & Rainer, 2003; Sokolov, 1990). This neural response increase is assumed to represent the automatic detection of unexpected events (File & Czigler, 2018; Schomaker & Meeter, 2014) and has been termed Novelty Detection (ND) or orienting response (OR) (Lange, Seer, Finke, Dengler, & Kopp, 2015; Sokolov, 1963, 1990). This neural response has been observed in very different contexts, from awake and sleeping

newborns and infants (Háden, Németh, Török, & Winkler, 2016; Kushnerenko, Ceponiene, Balan, Fellman, & Näätänen, 2002; Snyder & Keil, 2008) to comatose patients (Morlet & Fischer, 2014), and it is generally assumed to reflect an automatic change-detection mechanism. The ND response has been widely studied with oddball paradigms, in which an infrequent and non-predictable stimulus (i.e., Deviant) is presented within a stream of repeated stimuli (i.e., Standards; Garrido, Kilner, Stephan, & Friston, 2009; Näätänen et al., 2012; Näätänen, Paavilainen, Rinne, & Alho, 2007). The ND signature in the evoked response potentials (ERPs) has also been termed Mismatch Negativity (MMN), and it has been described as a sort of "primitive intelligence": it represents the ability to extract invariant elements of past patterns and assesses whether a violation of them occurs in sensory streams (Näätänen, Tervaniemi, Sussman, Paavilainen, & Winkler, 2001).

Typically, RS and ND are investigated as sensory-specific processes. Nonetheless, it is *an outstanding issue* to what extent the functional development of RS and ND responses are exclusively constrained within each sensory system (e.g., vision), or whether their functioning also depends on input availability in the other senses. To fill this gap, in the present study, we adopted the model of sensory deprivation to investigate the experience dependence of two basic properties of the visual system, namely the ability to recognize familiar patterns and distinguish novel ones. Specifically, we aimed to study whether long-term experience-dependent plasticity following an early-onset profound deafness can shape the oscillatory signatures underlying visual RS and ND, which remains an open question. To this aim, we compared evoked and induced oscillatory activity, as well as inter-trial phase coherence, in early deaf individuals and their age-matched hearing controls. Based on the assumption of enhanced visual processing in early deaf individuals, we hypothesized (see section "2.1.2. The present study") that early deaf individuals would display altered oscillatory signatures underlying RS and ND compared to hearing controls: increased RS and decreased engagement of the visual system for the ND. Furthermore, based on the literature (Bottari et al., 2016; Kral et al., 2017), we expected that RS and ND alterations would mainly involve induced activity and, thus, feedback processes.

In case a sensory input is missing since birth, neural circuits of the spared sensory modalities are known to reorganize (see Cardin et al.,

2020; Ricciardi et al., 2020 for the reviews). The term *intramodal plasticity* refers to the reorganization occurring within a sensory cortex when processing its typical sensory input (Bavelier & Neville, 2002; Striem-Amit, Dakwar, Reich, & Amedi, 2012). Among other causes, intramodal reorganizations are known to occur as a consequence of complete deprivation of other sensory modalities. This is the case of the responses in the auditory cortex when the visual inputs are lacking due to blindness (Huber et al., 2019) or the case of responses in the visual cortex when the auditory inputs are lacking due to deafness (e.g., Bavelier et al., 2000; Bottari, Bednaya, Dormal, Villwock, Dzhelyova, Grin, Pietrini, Ricciardi, Rossion, & Röder, 2020; Bottari et al., 2011, 2014; Hauthal et al., 2014; Smittenaar, MacSweeney, Sereno, & Schwarzkopf, 2016). Such neural plasticity effects are characterized by quantitative changes, such as the reduction or expansion of cortical representations (Elbert et al., 1994; Rauschecker, 2002), as well as alterations of the functional tuning of neuronal responses (Huber et al., 2019).

At the behavioral level, intramodal plasticity in the context of sensory deprivation in other modalities has been typically associated with improved performances compared to individuals without sensory deficits (e.g., Bavelier et al., 2000; Bottari et al., 2011; Recanzone, Merzenich, Jenkins, Grajski, & Dinse, 1992). In humans, a permanent lack of auditory input alters visual processing, both at the behavioral and the neural level. For instance, changes in visual skills have been documented in deaf humans in terms of faster detection of abrupt onsets (Bottari et al., 2010), altered representation of time (Amadeo et al., 2019; Nava et al., 2008), lower discrimination thresholds of motion directions (Hauthal, Sandmann, Debener, & Thorne, 2013), and improved analysis of events occurring in the periphery of the visual field (Proksch & Bavelier, 2002; see Pavani & Bottari, 2012; Pavani & Röder, 2012 for the reviews; also, see a recent study by Smittenaar et al. (2016), where the authors proposed that observed enhanced peripheral visual skills in deaf individuals could be linked to an increase in cortical population receptive field size rather than to a decrease in cortical thickness in the primary visual cortex). Moreover, a visual processing advantage has been typically described in deaf individuals under conditions of attentional load (Dye, Hauser, & Bavelier, 2009; Proksch & Bavelier, 2002); and when reorienting attentional resources (Stivalet, Moreno, Richard, Barraud, & Raphel, 1998). Similar behavioral advantages have

also been documented in deaf animal models (see Lomber, Meredith, & Kral, 2011 for a review).

At the neural level, intramodal changes in the visual cortex of deaf individuals were initially more elusive, especially in fMRI studies (Bavelier et al., 2000; Finney et al., 2001). However, investigations employing electrophysiological measures found that individuals with early deafness display reduced visual cortex responsiveness to the onset of visual motion, as compared to hearing controls (Bottari et al., 2014). Similar findings have been reported in the visual cortices of individuals with late-onset deafness who use a cochlear implant (CI) (Sandmann et al., 2012). Furthermore, enhanced RS following repeated visual stimuli was reported in the same population (L.-C. Chen, Stropahl, Schönwiesner, & Debener, 2017). These findings have been interpreted as indices of increased neural efficiency during visual processing as a result of auditory deprivation (Bottari et al., 2014; L.-C. Chen et al., 2017; Sandmann et al., 2012; see Stropahl, Chen, & Debener, 2017 for a review).

2.1.1 Probing intramodal plasticity through neural oscillations

Efficient development of neural representations demands well-tuned cortico-cortical connectivity, which is shaped from both feedforward and feedback projections (Kral, Yusuf, & Land, 2017a). Electrophysiological measurements allow to investigate feedforward and feedback connectivity indirectly through the characterization of neural oscillations, which represent how information is encoded, transferred, and integrated between distinct brain regions and across multiple temporal scales (Siegel, Donner, & Engel, 2012). Neural oscillations comprise the evoked activity that is phase-locked to stimulus onset (i.e., the classic and widely used Event-Related Potentials, ERPs) and the induced activity that is non-phase-locked to stimulus onset (David, Kilner, & Friston, 2006; Herrmann, Rach, Vosskuhl, & Strüber, 2014; Tallon-Baudry & Bertrand, 1999). The *evoked* neural oscillatory activities have been suggested to be mostly associated with feedforward mechanisms, reflecting bottom-up sensory processes, whereas the *induced* activity has been linked with the interaction between the processing of sensory input and the ongoing neural activity, including feedback (top-down) information (C.-C. Chen et al., 2012; Engel, Fries, & Singer, 2001; Klimesch, Sauseng, & Hanslmayr, 2007; Tallon-Baudry & Bertrand, 1999). The measure of the neural response phase-locking

across trials (Inter-Trial Phase Coherence, ITPC) has also been used to further characterize neural efficiency. ITPC is positively associated with stimulus evoked firing rates in the visual system (e.g., Zareian et al., 2020).

When focusing on induced activity, the frequency of neural oscillations and the latency of these neural responses are also considered indirect indices of feedforward and feedback processes. When processing visual events, theta (4-7 Hz) and gamma (> 30 Hz) activities in the first 100 ms after stimulus onset have been associated with low-level feedforward processes (e.g., Bastos et al., 2015; Busch, Debener, Kranczioch, Engel, & Herrmann, 2004; Fründ, Busch, Körner, Schadow, & Herrmann, 2007; Kienitz et al., 2021; Spyropoulos, Bosman, & Fries, 2018). On the contrary, modulations in theta, alpha (8-14 Hz) and beta (15-30 Hz) frequency bands, occurring at a later latency, have been mostly associated with high-level inhibitory feedback processes exerting top-down influences (Arnal & Giraud, 2012; Bastos et al., 2015; Klimesch, 2012; Klimesch, Fellinger, & Freunberger, 2011; Michalareas et al., 2016; Richter, Coppola, & Bressler, 2018; Van Kerkoerle et al., 2014). Thus, by investigating electrophysiological responses across multiple frequency bands and at different latencies, it is possible to infer whether they relate to feedback and/or feedforward processing. Notably, both bottom-up and top-down mechanisms have been proposed to play a role in RS and ND (Barbosa & Kouider, 2018; Garrido et al., 2009; Grill-Spector et al., 2006; Kaliukhovich & Vogels, 2012; Summerfield, Trittschuh, Monti, Mesulam, & Egnér, 2008; see Grotheer & Kovács, 2016 for a review), hence they are directly relevant for the scopes of the present study.

2.1.2 The present study

In hearing individuals, RS and ND have been linked with modulations of the power in various frequency bands. RS has been associated with a gradual power decrease of the induced gamma band (Engell & McCarthy, 2014; Gruber, Giabbiconi, Trujillo-Barreto, & Müller, 2006; Gruber, Malinowski, & Müller, 2004) as well as with a decrease of the induced alpha band (Engell & McCarthy, 2014). The comparison of repeated and novel (or unrepeated) stimuli has also revealed power modulations of both induced (Barbosa & Kouider, 2018; T. Yan et al., 2017) and evoked (Hesse, Schmitt, Klingenhoefer, & Bremmer, 2017) theta band activity, as well as a modulation of the

induced alpha oscillations (Hesse et al., 2017). Overall, these effects have been linked to a sharpening of the neural response when representing a repeated visual event and to the orienting of attentional resources to novel stimuli – i.e., a combination of feedforward and feedback components. Whether early auditory deprivation affects neural oscillation to visual RS and ND, however, remains an open question. Addressing this question would allow to move beyond the general notion that intramodal plasticity occurs, to start unraveling how it manifests. In particular, it would allow to examine if feedforward and feedback mechanisms are altered by long-term auditory deprivation.

A recent study demonstrated the differential role of developmental experience on evoked and induced activity in the auditory cortex of congenitally deaf cats, suggesting that induced activity might be particularly affected by the lack of sensory experience and linking this finding to feedback processes (Yusuf, Hubka, Tillein, & Kral, 2017). Similar results were found in the visual cortex of humans who missed visual experience in early development (Bottari et al., 2016), but to date, this type of evidence lacks in deaf humans (see e.g., Land et al., 2016; Land, Radecke, & Kral, 2018 for studies in the animal model). Here we used electroencephalography to measure oscillatory neural activity in early deaf and hearing control individuals while they observed a stream of visual stimuli comprising both repeated and novel events whose occurrence could not be predicted. To measure automatic mechanisms, participants were engaged in an orthogonal visual task implying the detection of an infrequent visual target, which was perceptually dissociated from the occurrence of both repeated and novel events.

With the aim to assess whether early deafness impacts feedforward as well as feedback components of RS and ND, we specifically investigated evoked and induced aspects of the oscillatory neural activity occurring in response to repeated and novel visual events. In addition, we studied inter-trial phase coherence to further pinpoint feedback and/or feedforward processing. Based on the assumption of more efficient visual processing in early deaf individuals, we expected altered/increased RS, as well as a reduced engagement of the visual system for the ND, in early deaf individuals compared to hearing controls. Considered previous findings indicating that developmental sensory experience affects induced cortical responses (Bottari et al., 2016;

Kral et al., 2017), we expected RS and ND alterations to mainly involve induced oscillations and, thus, feedback processes.

2.2 Methods

We report how we determined our sample size, all data exclusions, all inclusion/exclusion criteria, whether inclusion/exclusion criteria were established prior to data analysis, all manipulations, and all measures in the study.

2.2.1 Participants

A group of eleven early deaf adults (ED; mean age = 36.6 years, SD = 9.99, range 20-45 years; 7 females) was recruited at the National Association for Deaf, in Trento (Italy). All subjects had bilateral profound hearing loss (at least 90 dB in the better ear) and had acquired deafness within the first 9 months of life (eight of them had congenital deafness). None of them became deaf due to systemic causes that could also affect vision; none received a cochlear implant. All deaf participants were proficient users of the Italian Sign Language by self-report. Eleven hearing individuals, matched in age and gender, served as the controls (HC; mean age = 33.1 years, SD = 6.85, range 25-45 years; 6 females). None of the hearing participants was familiar with sign language. All participants reported to be right-handed and to have normal or corrected-to-normal vision. None of the participants tested was excluded from our data analysis. Our sample size was based on the maximum available number of participants we could retrieve in our focus group: i.e., early deaf individuals (born profoundly deaf or with profound deafness acquired before reaching the age of one) who use Italian Sign Language as their primary language for communication. The study was approved by the Ethical Committee at the University of Trento (Italy). All participants signed a written informed consent prior to testing. The study protocol adhered to the guidelines of the Declaration of Helsinki (2006).

2.2.2 Stimuli and Procedure

All the stimuli were delivered using Presentation program (Neurobehavioral Systems, Inc.). The stimuli consisted of a circle continuously transitioning into an ellipse, either in the horizontal or in

the vertical direction (see Figure 2.1; for detailed information on the original stimuli, see (Giard & Peronnet, 1999)). The circle, with a diameter of 4.55 cm, was centrally presented in white on a black background and subtended 2° of visual angle. Between each deformation, the circle remained visible on the screen. Relative to the diameter of the circle, the deformation changed its shape by 33% and lasted 107 ms. The amount of time required to recover to the original shape was equal (i.e., 107 ms). The stimulus onset asynchrony (SOA) was 587 ms. Additionally, a small white cross was presented at the center of the circle (subtending 0.2° of visual angle) and served both as a fixation point and as a target. Participants were sitting at a viewing distance of 130 cm and were instructed to keep their gaze at the fixation cross and press a button as fast as possible after its disappearance (17% of the trials). The cross disappeared briefly (for a duration of 133 ms) at unpredictable moments during each block. The task was performed to ensure that the participants were paying attention to the visual stream. All trials including button-press responses following the fixation cross disappearance were excluded from the analysis.

The experiment was divided into 8 blocks. In each block, in 76% of the trials, the circle deformed in one direction (Standard) and, in the remaining 14% of the trials, it deformed in the opposite direction (Deviant). In half of the blocks, Standards and Deviants were swapped to account for physical differences between them, therefore the obtained responses could be generalized to both vertical and horizontal changes. Standard and Deviant stimuli appeared in pseudo-randomized order. That is, a Deviant was always preceded by *at least three* Standard stimuli. Moreover, a Deviant stimulus could never follow a trial including the fixation cross disappearance, nor appear in conjunction to it (e.g., Besle, Hussain, Giard, & Bertrand, 2013; Bottari et al., 2014). While Standard trials were designed to assess adaptation to repeated visual stimuli, Deviant trials were used to investigate the response to an unpredicted change in the visual stream.

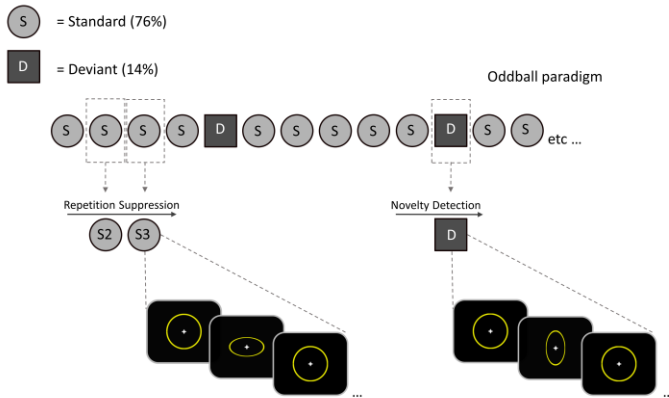


Figure 2.1: Experimental paradigm. The stimuli consisted of a circle continuously transitioning into an ellipse, either in the horizontal or in the vertical direction. A white cross at the center of the circle served both as a fixation point and as a target. In 76% of the trials, the circle deformed in one direction (Standard, S; vertical deformation in the example) and, in 14% of the trials, it deformed in the opposite direction (Deviant, D; horizontal deformation in the example). A Deviant stimulus was always preceded by at least three repetitions of a Standard stimulus (i.e., S1, S2, S3). The epochs were selected from the original EEG data around the second and third presentation of a Standard stimulus in order to test the Repetition Suppression effect (S2 minus S3), and around the Deviant stimulus in order to test Novelty Detection effect.

2.2.3 EEG-recording and pre-processing

The EEG data were recorded (bandwidth: 0.1-200 Hz, sampling rate: 1000 Hz) from 34 electrodes placed according to the extended 10-20 system (<http://www.easycap.de>). All scalp channels were referenced to the nose. Horizontal eye-movements were monitored from two additional electrodes placed at the outer canthi of the eyes. All data pre-processing and analysis were performed using EEGLab (Delorme & Makeig, 2004) and FieldTrip (Oostenveld, Fries, Maris, & Schoffelen, 2011) toolboxes, together with custom written MATLAB (The MathWorks, Inc., version R2018b) code. Raw data were low-pass filtered at 110 Hz, downsampled to 250 Hz, and then high-pass filtered at 0.1 Hz

(in both cases, using FIR filter implemented in EEGLab). Components that clearly resembled the eye blinks/-movements and heartbeat artifacts were identified using Independent Component Analysis (ICA) decomposition (with runica, infomax ICA algorithm implemented in EEGLab) and were manually removed after visual inspection of each component (its time-course, topography, and power spectrum). The average number of removed components in the early deaf group was 1.9 (range: 1-4; SD = 0.95), that is around 5% (on a total of 36 independent components which were extracted in each participant), and 3.1 (range: 2-5; SD = 0.84), that is around 9% of total independent components, in the group of hearing controls. Channels with an excessive noise (identified by ICA) were also removed and interpolated.

We selected events-of-interest (see Figure 2.1) and epoched the data into two seconds segments: [-0.88 s, +1.12 s]. The data were epoched according to two analysis strategies. (1) In order to assess Repetition Suppression effects, epoching was performed considering the second and third repetitions of the Standard stimulus (S2, S3). Note that the first Standard stimulus (S1) of each series of Standards was not considered in the analysis as it followed a Deviant, and thus elicited a response to a physically novel stimulus as compared to the previous one. (2) In order to estimate the ND response, epoching was also performed for Deviant stimuli (D). Finally, any epoch in which electrical signals exceeded ± 100 μV was eliminated.

2.2.4 Spectral decomposition

At the single-trial level, we obtained time-frequency representations of power (TFR) by applying a Hanning taper to an adaptive window which included 4 cycles for each frequency in the range [4 Hz, 30 Hz] in steps of 1 Hz, over the entire epochs including Standard and Deviant stimuli [-0.88 s, +1.12 s], in steps of 0.02 s. This approach provides optimal control over spectral leakage that may cause substantial smearing of the spectrum at frequencies lower than 30 Hz (Jensen et al., 2014). These long epochs were adopted for the spectral decomposition to minimize boundary distortion effects within the time window of interest. Provided the relatively fast occurrence of stimuli, only the data within the time window [-0.1 s, +0.4 s] were further analyzed and statistically compared within and between participants. Trials were then averaged, providing an estimate of the total power TFR, which included

both evoked and induced activity (Herrmann, Grigutsch, & Busch, 2004; Herrmann et al., 2014). The averaging across trials was performed by comprising both directions of the ellipse transition (vertical or horizontal) within each relevant condition (Standard S2, Standard S3, and Deviant); thus, all results were independent of motion direction. Evoked TFR was computed on averaged time-locked data (Mouraux & Iannetti, 2008; T. R. Schneider, Lorenz, Senkowski, & Engel, 2011), using the same procedure as for the total power TFR described above. Induced TFR of power was obtained by subtracting evoked TFR from total power TFR (Herrmann et al., 2014).

Additionally, we computed the inter-trial phase coherence (ITPC)/phase-locking factor (Delorme & Makeig, 2004; Tallon-Baudry, Bertrand, Delpuech, & Pernier, 1996) to measure the degree of phase consistency of the neural response across trials within conditions of interest. Following computation of the Evoked TFR, ITPC was computed for each trial with previously validated methods (e.g., Van Diepen & Mazaheri, 2018). That is, phase-locking values were calculated as the absolute values of the ITPC, for each time point of the epoch and each frequency, in a range from 0 (no phase-locking over trials) to 1 (perfect phase-locking over trials). The evoked TFRs, ITPCs, and induced TFRs, were normalized as the relative change (in %) with respect to a baseline (constrained by the fast periodicity of stimulation), defined as [-0.1 s, -0.02 s] relative to stimulus onset as follows: $P(t,f)_{corrected} = 100 * ((P(t,f)_{activity} - P(f)_{baseline}) / P(f)_{baseline})$. For the RS analysis, at the single-subject level, we computed the difference of normalized TFRs and ITPCs between second and third repetitions of a Standard stimulus (S2 minus S3). The resulting difference was used as an objective index of RS.

2.2.5 Statistical approach

Behavioral analysis. We measured response time (RT) for the simple detection of cross disappearance. Trials with false alarms (mean false alarms, ED: 0.75%; HC: 0.97%) and trials with no response (mean misses, ED: 2.33%; HC: 2.51%) were not considered. The following trials were excluded from the analysis: trials with RTs below 100 ms (0.04% for ED, 0.04% for HC) and higher than three standard deviations above the individual median (mean outliers, ED: 1.40%; HC: 1.48%). For each participant, we calculated the median of RTs and compared these values between the two groups by means of a t-test for independent samples.

EEG analysis. The same parsimonious statistical model was employed to compare between groups (HC, ED) the Repetition Suppression to visual stimuli (S2 minus S3), and the Novelty Detection (Deviant) effects. To characterize the subtending neurophysiological changes, analyses were performed on the following measures of interest: (i) induced and (ii) evoked TFRs, and (iii) ITPC. To this end, a series of non-parametric cluster-based permutation tests (Maris & Oostenveld, 2007) were used to estimate group differences. This approach allows to identify clusters of significant effects in time, frequency and space, and controls for multiple comparisons. Cluster-based permutation analyses were run without a bias from any prior assumptions about specific frequency bands, regions of interest (ROI), or time intervals: thus, across all frequencies (4-30 Hz), channels, and time-points (0-0.4 s) after stimulus presentation. To this end, we used non-parametric permutation tests (Monte Carlo sampling method, 1,000 iterations, cluster alpha = 0.05, maxsum criterion, minimum spatial extent = 2 adjacent channels (Maris & Oostenveld, 2007)). In case the cluster-based p-value was less than 0.025 (corresponding to critical alpha level of 0.05 for two-tailed testing, accounting for both positive and negative clusters), we rejected our null hypothesis that there were no group differences. For illustrative purposes, we plotted the results averaged over a cluster of posterior electrodes (Pz-P7-P3-PO3-O1-P8-P4-PO4-O2) comprising both hemispheres (e.g., Kimura, Ohira, & Schröger, 2010; Stefanics, Kimura, & Czigler, 2011). In summary, to study RS and ND effects in early deaf individuals and in hearing controls, we compared between groups the following measures: (i) induced components of neural activity as indices of feedback processes and, (ii) evoked components of neural activity (phase-locked to stimulus onset) together with (iii) inter-trial phase coherence of evoked activity, as indices of feedforward processes.

2.3 Results

2.3.1 Behavioral data

A t-test for independent samples revealed no difference in RTs between ED and HC in the ability to detect the disappearance of the central fixation cross (two-tailed t-test; $p = 0.94$; mean RTs ED: 392 ms, SE = 13.25 ms; HC: 391.41 ms; SE = 13.42 ms).

2.3.2 Repetition Suppression effects

First, we assessed whether early deafness had an impact on the visual RS effect. To this aim, a between-group comparison across all frequencies (4-30 Hz), channels, and time-points (0-0.4 s) was performed on the difference of power (evoked and induced) measured in response to repeated visual events (i.e., S2 minus S3). The cluster-based permutation analysis revealed a significant between-group difference selectively in the induced power (positive cluster, $p = 0.011$, see Figure 2.2). The significant effect involved a large portion of electrodes (mostly pronounced over posterior electrodes in the right hemisphere and over frontal-central areas in the left hemisphere) and was found in the theta (4-7 Hz) frequency range, for the whole time window (see Figure 2.2). Within this time window and frequency range, the change of induced theta power occurring for the response difference S2 minus S3 was greater in the group of early deaf than in the group of hearing controls (ED: +12.58%, vs. HC: -3.21%) (see Figure 2.3).

To interpret the between-group effect (S2 minus S3), we performed within-group cluster-based permutation analyses across all frequencies (4-30 Hz), channels, and time-points (0-0.4 s). For early deaf, a significant theta power reduction relative to baseline emerged, for S3 as compared to S2 ($p = 0.018$; for the whole time window). Conversely, only a tendency toward significance emerged for the hearing control group (all p -values > 0.056). Note that the direction of theta power change between S2 and S3 has opposite directions in the two groups. These results are compatible with an altered RS in early deaf compared to hearing controls.

The between-group cluster-based permutation analysis on the evoked power, on the difference of response between S2 and S3, did not reveal any significant effect of stimulus repetition (all p -values > 0.4 ; see Supplementary Figure A.1), suggesting that evoked power to RS were comparable in the two groups. Similarly, the same statistical model performed on ITPC on the difference of response between S2 and S3 did not show significant between-group differences (all p -values > 0.2 ; see Figure 2.5).

RS (Induced Activity)

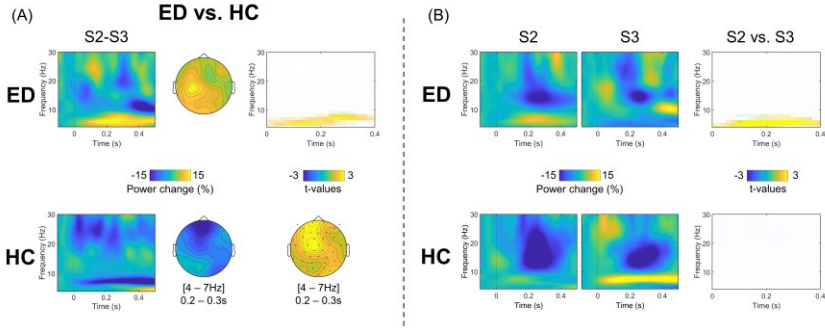


Figure 2.2: Repetition Suppression (RS; Induced Activity) in early deaf individuals and hearing controls. (A) Relative changes of induced spectral power for the S2 - S3 difference and statistical results of the comparison between early deaf (ED) and hearing controls (HC); time-frequency plots display data averaged across posterior electrodes (Pz-P7-P3-PO3-O1-P8-P4-PO4-O2). Topography plots represent the averaged activity within the theta range [4-7 Hz] and over the [0.2-0.3 s] time window after stimulus onset. The plot of statistics (with t-values) highlights significant between-groups differences, identified by the cluster-based permutation testing ($p < 0.025$) and corresponding topography plot (bottom) of t-values, averaged for theta range [4-7 Hz] and over [0.2-0.3 s] time window: electrodes belonging to the cluster in which the effect was significant are highlighted with black dots. (B) Relative changes of induced spectral power for each stimulus (S2 and S3) and results of their statistical comparison, for the early deaf individuals (ED) and hearing controls (HC). Each plot represents the averaged data across posterior electrodes (Pz-P7-P3-PO3-O1-P8-P4-PO4-O2). Plots of statistics (with t-values) highlight significant with ingroup differences, identified by the cluster-based permutation testing ($p < 0.025$).

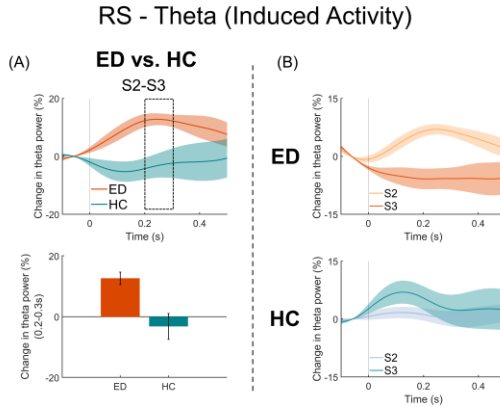


Figure 2.3: Zoom-in of RS-Theta effect. (A) The relative power changes in the theta range for the RS (S2-S3) displayed for each group and averaged across posterior electrodes (Pz-P7-P3-PO3-O1-P8-P4-PO4-O2); shaded areas represent the standard error of the mean; the dashed black box indicates the time window in which group differences were found to be maximally significant in the cluster-based permutation (see Figure 2.2; ~ 0.2-0.3 s after stimulus onset); The bar plot (bottom) displays for each group the relative power change in the theta band (in % from baseline), averaged across posterior electrodes and over the time range indicated by the dashed black box. (B) Relative changes of induced spectral power in the theta range [4-7 Hz] for each stimulus (S2, S3) displayed separately for each group (ED and HC), averaged across posterior electrodes; shaded areas represent the standard error of the mean.

2.3.3 Novelty Detection effects

Next, we evaluated whether early deafness has an impact on the oscillatory neural activity in response (evoked and induced) to a novel, unexpected visual stimuli. Between-group comparison was performed on the power obtained in response to novel visual events (i.e., Deviants). The cluster-based permutation analysis revealed a significant between-group difference selectively in the induced power (positive cluster, $p = 0.023$; see Figure 2.4). The effect involved a broad range of posterior and central electrodes and, it was found in the alpha (8-12 Hz) and beta (13-25 Hz) frequency ranges, from 200 to 300 ms after stimulus onset (see

Figure 2.4). For this time window and frequency ranges, hearing controls had a significantly greater alpha-beta desynchronization in response to novel stimuli as compared to early deaf individuals (HC: -5.81% vs. ED: $+0.68\%$) (see Figure 2.4).

The cluster-based permutation test on evoked power (see Supplementary Figure A.2), as well as on ITPCs (see Figure 2.5), did not reveal any between-group effect in response to Deviant stimuli (all p -values > 0.13), suggesting similar modulation of evoked power and ITPC for the ND in the two groups.

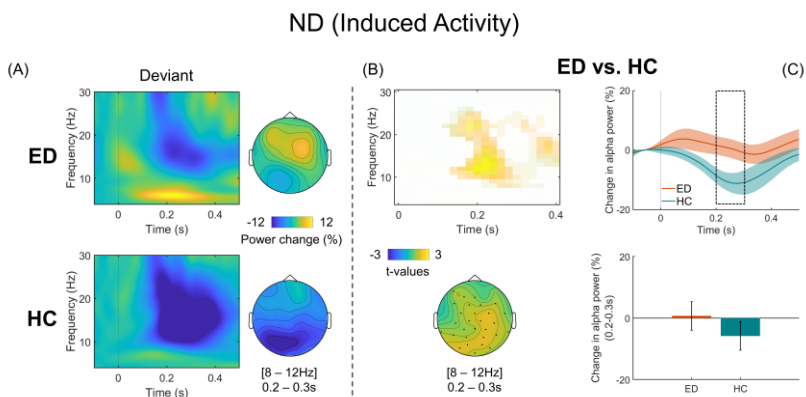


Figure 2.4: Novelty Detection (ND; Induced Activity) in early deaf individuals and hearing controls. (A) Relative changes of induced spectral power in response to a novel stimulus (Deviant) as a function of time and frequency, in early deaf (ED) and hearing controls (HC); time-frequency plots display data averaged across posterior electrodes (Pz-P7-P3-PO3-O1-P8-P4-PO4-O2). Topography plots represent the averaged activity within the alpha range [8-12 Hz] and over the [0.2 - 0.3 s] time window after stimulus onset. (B) The plot of statistics (with t-values) highlights significant between-groups differences, identified by the cluster-based permutation testing ($p < 0.025$) and corresponding topography plot (bottom) of t-values, averaged for alpha range [8-12 Hz] and over [0.2-0.3 s] time window: electrodes belonging to the cluster in which the effect was significant are highlighted with black dots. (C) The relative power changes in the alpha range for the Deviant displayed for each group and averaged across posterior electrodes (Pz-P7-P3-PO3-O1-P8-P4-PO4-O2); shaded areas represent the standard error of the mean; the dashed black box indicates the time window

in which group differences were found to be maximally significant in the cluster-based permutation (see Figure 2.4B; ~ 0.2 - 0.3 s after stimulus onset); The bar plot (bottom) displays for each group the relative power change in the alpha band (in % from baseline), averaged across posterior electrodes and over the time range indicated by the dashed black box.

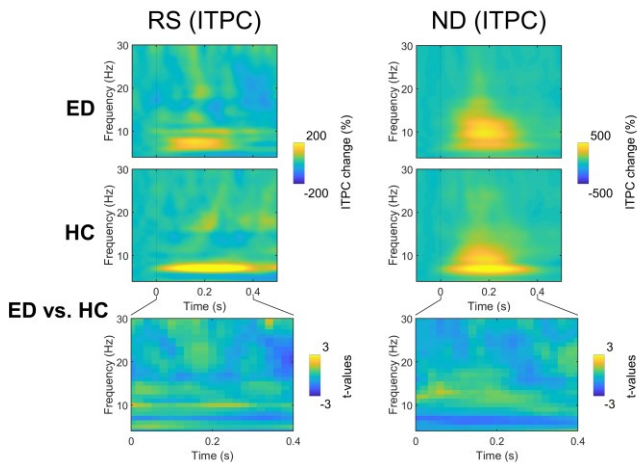


Figure 2.5: Inter-trial phase coherence (ITPC) in early deaf individuals and hearing controls. Left column: ITPC changes for RS (S2 minus S3). Right column: ITPC changes for ND (Deviant). Upper and middle panels: Relative changes of ITPC (in %, from the baseline), in early deaf (ED) and hearing controls (HC), averaged across posterior electrodes (Pz-P7-P3-PO3-O1-P8-P4- PO4-O2). Bottom panels (left and right columns): Time-frequency plots of statistics (with t-values) showing the results of cluster-based permutation testing; note, there were no significant differences in ITPC between the two groups, neither for RS nor for ND.

2.4 Discussion

In the present study, we investigated the impact of auditory deprivation on visual Repetition Suppression (RS) and Novelty Detection (ND) by studying the neural oscillations associated with these two fundamental mechanisms of visual processing in early deaf and in age-matched hearing controls. We found three main results. First, we

observed greater attenuation of the response to repeated visual stimuli in individuals with early deafness compared to controls. This effect emerged selectively for the induced oscillatory activity in the theta band (4-7 Hz, RS-theta). Conversely, a tendency toward an increase of theta oscillations was found for repeated stimuli in hearing controls. Second, early deaf individuals had reduced alpha/beta modulations (i.e., desynchronization) following a novel event as compared to hearing controls. This effect was found selectively for the induced activity in the alpha and beta range (8-12 Hz and 13-25 Hz). Third, between-group differences did not emerge either for the evoked oscillatory activity or for ITPC in both RS and ND, across the whole frequency range (4-30 Hz). Taken together, these findings suggest that the oscillatory signatures that underlie the visual processing of repeated and novel events are altered in auditory deprived individuals. Moreover, these results further suggest that intramodal plasticity effects found on both RS and ND may be mostly driven by alteration of feedback signals in early deaf individuals.

2.4.1 Altered RS in early deaf adults

Individuals with early deafness showed altered RS effects in the theta band for repeated stimuli compared to hearing controls. The topography of this effect was distributed over a large portion of the scalp and encompassed posterior electrodes, which are typically associated with visual cortex responses. Although the EEG technique does not allow for precise localization of the sources due to its relatively poor spatial resolution, our data are compatible with a change in the excitability of cortical visual neurons following repeated visual events in early deaf individuals. This effect was not observed in hearing controls, where the RS-theta showed, in fact, a trend in the opposite direction. Previous studies on visual RS have found both increase (Barbosa & Kouider, 2018; Summerfield et al., 2011) and decrease of theta oscillations (e.g., Rigoulot et al., 2017). While the inconsistency of previous results in hearing adults might depend on specific paradigms/stimuli employed and on the type of analysis conducted (comparison between the repeated stimuli or selective analysis of the repeated event), here we clearly showed a substantial reorganization of the neural responses to repeated visual events following early deafness.

The neural mechanisms underlying RS are still debated, and different accounts have been proposed. When interpreted as the result of bottom-up mechanisms, RS would represent the consequence of processing at the sensory level driven by stimulus-specific physical properties. Among potential mechanisms, it has been proposed that with prolonged stimulus repetition, the membrane excitability of cortical neurons is changed, resulting in a strong hyperpolarization (Grill-Spector et al., 2006). In this context, RS represents a dynamic modulation of neuronal responses within sensory cortical areas. Thus, the present finding can be interpreted within the framework of intramodal neural plasticity occurring in the visual cortex (Röder & Neville, 2003). Reduced responsiveness in the visual cortex of deaf individuals has been previously reported, both in individuals that experienced no auditory input (as in the present work) and in subjects whose access to auditory input was partially restored using cochlear implants (CIs). ERP studies in humans have consistently shown that following a visual onset, the amplitude of the visual response is reduced in individuals with early-onset deafness (Bottari et al., 2014) and in individuals with late-onset deafness who use CIs, as compared to hearing controls (L.-C. Chen et al., 2017; Sandmann et al., 2012). This evidence supports the possibility that visual processing in early deaf individuals may be functionally better tuned and operate with greater efficiency, as compared to hearing controls. Our findings expand this account by showing that long-term experience-dependent plasticity can also emerge as a more efficient inhibition of neural responses in case of repeated visual events.

Intramodal plasticity effects have not been found only in the case of auditory deprivation. Extended tonotopic maps in the auditory cortex, as well as extended sensorimotor representations in the somatosensory cortex, have been documented in blind compared to sighted individuals (Elbert et al., 2002; Pascual-Leone, Wassermann, Sadato, & Hallett, 1995; Pascual-Leone & Torres, 1993). Moreover, in auditory and somatosensory tasks, neural responses in blind individuals are characterized by shorter latencies and shorter refractory periods of ERPs than those in sighted controls (Niemeyer & Starlinger, 1981; Röder et al., 1996, 1999). Intramodal plasticity seems to represent a general mechanism of adaptation occurring in sensory cortices (Bavelier & Neville, 2002). At the physiological level, recent studies suggest that intramodal plasticity originates from the strengthening of thalamo-

cortical synapses within the spared sensory systems (Petrus et al., 2014, 2015; see Lee & Whitt, 2015 for a review).

In our study, the between-group RS-theta effect emerged selectively for the induced oscillatory activity (non-phase locked), which has been reliably linked to feedback processing (Van Kerkoerle et al., 2014; see Jensen, Mathilde, Marshall, & Tiesinga, 2015 for a review). In line with this idea, RS-theta modulation in our study was also found at frontal-central electrode sites, particularly in the left hemisphere. This scalp distribution of theta modulations during processing of repeated visual stimuli is in line with the existing literature (e.g., Barbosa & Kouider, 2018). At the functional level, induced frontal theta activity has been associated with conflict and error detection and with cognitive control of upcoming stimuli (Cavanagh, Frank, Klein, & Allen, 2010; Cohen & Donner, 2013; Duprez, Gulbinaite, & Cohen, 2020). It has also been proposed that frontal theta represents a mechanism for cognitive control across brain regions (see Cavanagh & Frank, 2014 for a review). Importantly, regardless of the RS-theta effect topography, we did not find any significant difference neither in the evoked activity nor in the ITPC, which instead have both been associated with feedforward mechanisms (C.-C. Chen et al., 2012; Lakatos et al., 2009). Sensory processing (associated to stimulus-specific physical properties) and higher cognitive control of repetitions could both play a role in the observed effects. While the present data do not allow to disentangle between these interpretations, the differences found selectively in induced oscillatory activity and not in the evoked activity or in the ITPC suggest that feedback processing occurring in RS is altered as a result of early deafness (Kral, Dorman, & Wilson, 2019).

Studies in the animal model have extensively explored the role of evoked and induced neural oscillatory activity in the auditory cortex of congenitally deaf cats with cochlear implants (Kral et al., 2019). Results revealed that the induced responses were substantially reduced in animals with complete absence of auditory experience compared to animals with hearing experience, in both secondary and primary auditory cortices (Yusuf et al., 2017). This, in turn, demonstrated the differential role of auditory experience on evoked and induced activity in the auditory cortex, suggesting that induced activity might be particularly affected by early deafness. These results further supported previous findings, which have indicated that top-down interactions are

particularly affected in case of congenital deafness (Kral, 2013; Kral, Yusuf, & Land, 2017). The investigation of cortical columns has revealed reduced cortical thickness in the auditory cortex of congenitally deaf cats in layers IV-VI (Berger, Kühne, Scheper, & Kral, 2017), which are the major source and target of feedback projections (e.g., Callaway, 1998; Galaburda & Pandya, 1983). Conversely, supragranular layers, which are known to be mostly involved in sensory feedforward processing, appeared preserved (Berger et al., 2017). Such a specific top-down deficit was also confirmed in a recent study that analyzed connectivity measures between primary and higher-order auditory fields (Yusuf et al., 2021).

When considered in the light of these studies in deaf cats, our findings extend in humans and beyond the auditory cortices (specifically, in visual cortices) the observation that changes in sensory processing may reflect more an alteration of top-down/feedback signals, rather than a modification of bottom-up/feedforward mechanisms.

2.4.2 Reduced ND response in early deaf adults

The evaluation of ND revealed an additional alteration of basic visual mechanisms induced by early deafness. Following a novel visual stimulus (i.e., the Deviant) strong desynchronization of the alpha/beta activity was found in hearing controls. On the contrary, early deaf participants did not show such a pattern. The two groups differed in the alpha/beta desynchronization over a broad portion of electrodes comprising posterior and central scalp locations.

While the exact role of the alpha activity remains to be clarified (Clayton, Yeung, & Cohen Kadosh, 2018; Palva & Palva, 2011), it has been closely linked with attention and cognitive control (Foxe & Snyder, 2011; see Klimesch, 2018; Sadaghiani & Kleinschmidt, 2016 for the reviews). The modulation of alpha power has been commonly considered as a functional mechanism of selection or gating of information in the visual cortex (Van Diepen, Foxe, & Mazaheri, 2019). Under the popular gating-by-inhibition hypothesis (Jensen & Mazaheri, 2010), alpha activity has been suggested to reflect the amount of functional suppression of neuronal resources that are not currently in use (Klimesch et al., 2007; Mazaheri & Jensen, 2006; but see Foster & Awh, 2019). Moreover, alpha synchronization has been found to reflect inhibition of irrelevant information, whereas alpha and beta

desynchronizations have been associated with (task-relevant) release from such inhibition or, more generally, to reflect cortical excitation (see Klimesch, 2012 for a review). While the development of alpha oscillations has already been associated with the availability of visual input in the first developmental phases (Bottari et al., 2016), our study is the first to reveal an alteration of alpha/beta activity as a result of auditory deprivation in humans. Similar findings have been previously reported in congenitally deaf cats (Yusuf et al., 2017). Following auditory stimulations, an extensive reduction of neural activity in higher-order auditory fields, selectively in the induced responses and most prominently in the alpha/beta band, was found starting from 150 ms after stimulus onset. The present study provided supporting evidence that the absence of auditory experience alters induced oscillatory responses also in humans. Moreover, it reveals that early deafness can have an impact on induced oscillatory activity in the visual system.

Novel unexpected events are known to attract attention (C. J. Howard & Holcombe, 2010). Moreover, they are more easily encoded into memory than expected stimuli (Kafkas & Montaldi, 2018). A distributed cortical network for ND has been proposed (see Ranganath & Rainer, 2003 for a review). A recent study in hearing controls using a visual Mismatch Negativity (vMMN) paradigm found a strong alpha desynchronization for Deviant visual stimuli, broadly distributed across the scalp (Stothart & Kazanina, 2013). This response was strongest at right occipital and parietal electrode sites, between 400 and 600 ms, and was attributed to the rareness of Deviant events (Stothart & Kazanina, 2013). In the present work, the reduced alpha/beta desynchronization in response to Deviants in deaf participants suggests an alteration of the mechanisms underlying ND and possibly indicates a reduced early-automatic response to distracting unexpected visual information. It is noteworthy that, in the present task, participants were asked to detect an infrequent visual event – the fixation cross disappearance – which was dissociated from the occurrence of the Deviant.

One account for this finding is that deaf individuals may deploy less attentional resources when detecting unexpected visual changes. However, several studies have suggested that early deaf individuals possess greater attentional resources as compared to hearing controls (Dye et al., 2009; Hauthal et al., 2013), in line with the account of a greater functional tuning of the visual processing in deaf individuals (Bavelier

et al., 2006; see e.g., Land et al., 2016 for visual processing in the animal model). An alternative account for our findings could suggest that deaf individuals may be better at inhibiting the automatic response to the non-relevant task events. However, this seems unlikely as it is in contrast with ample evidence from previous studies. While congenital and early deaf individuals were found to outperform hearing controls in orienting visual attention from one location to another (Bosworth & Dobkins, 2002), they have been more susceptible to distractors (Dye, Baril, & Bavelier, 2007; Proksch & Bavelier, 2002; see Dye, Hauser, & Bavelier, 2008 for a review). Notably, consistently with the RS-theta effect, between-group differences associated to the ND effect were found selectively in oscillatory induced activity and not in evoked activity nor in ITPC. The fact that for both RS and ND no effects emerged, in the same frequency bands and time-range for both evoked and induced activity suggests that if leakage of power between induced and evoked responses occurred it did not have a major impact on results. Overall, consistently with previous suggestions (Berger et al., 2017; Kral et al., 2019; Kral & Eggermont, 2007; Kral & Sharma, 2012; Yusuf et al., 2017), these results further support the idea that feedback processes, but not forward processes, that are changed in the deaf individuals.

2.4.3 Is the greater RS a marker of modified predictive mechanisms in early deafness?

As we previously highlighted, differences in the induced theta might reflect an alteration of the oscillatory activity that underlies the prediction of errors. In this respect, RS has been linked to the predictive coding (PC) framework (Friston, 2005). Within this theoretical context, RS was hypothesized to reflect mechanisms of perceptual learning (Grill-Spector et al., 2006), as brain predictions about upcoming stimuli are continuously modulated with repetitions of events. From the PC perspective, RS may result from a reduction of the activity that represents the prediction error of incoming events, through a top-down mechanism that influences perceptual expectations (Auksztulewicz & Friston, 2016).

Until now, the anticipative (i.e., predictive) abilities in deaf and in CI individuals have been overlooked or only studied as a property of the auditory system. According to a recent review (Kral et al., 2017), current data indicate that as a result of congenital deafness, a reduced cortico-

cortical functional coupling between auditory areas occurs for both bottom-up and top-down streams. The same authors proposed that congenital deafness could be associated with a deficit in predictive coding mechanisms occurring within the auditory cortex, which would emerge as an impairment in auditory learning following late cochlear implantations (see also "the connectome model" of deafness, Kral et al., 2016). The altered RS effect found here in early deaf individuals, and in similar studies on post-lingually deaf CI users (L.-C. Chen et al., 2017), suggests the possibility that compensatory enhanced predictive mechanisms emerge in the visual system in these populations. Thus, an enhanced ability to benefit from environmental statistical information regarding stimuli occurrence could be expected in these individuals. It is noteworthy that early deaf participants have been found to differently take advantage of posterior probability changes regarding stimuli occurrence (Bottari et al., 2011). When asked to detect visual stimuli that were occurring either after a short or a long inter-stimulus-interval (ISI) from a visual warning, hearing controls showed the typical pattern of slower RTs to visual events occurring at the shorter rather than the longer ISI. This effect relates to the posterior probability increase that was associated to the long ISI. Conversely, deaf individuals did not, and revealed a strong RTs advantage as compared to hearing controls, responding to visual stimuli presented at the short ISI. Moreover, faster RTs in a simple visual detection task correlated with visual evoked potential amplitudes at an earlier latency in deaf individuals (P1), as compared to hearing controls (Bottari et al., 2011).

The results of the present work outline a new working hypothesis in this direction, suggesting that either the visual system in early deaf individuals effectively anticipates the prediction of an upcoming visual event or, alternatively, that visual attention taps at an earlier latency, or both. Additionally, a recent ERP study revealed that early deaf individuals have a shorter latency of the N1 wave, as compared to hearing controls, during the processing of moving stimuli (Hauthal et al., 2014). Overall, previous findings have indicated faster visual processing as a result of deafness. While this certainly helps shortening the time of processing, it can, in turn, be of help to prompt the anticipation of upcoming visual information. While similar temporal thresholds emerged between deaf individuals and hearing individuals,

early deafness was associated to faster responses during the discrimination of the temporal order of visual events (Nava et al., 2008).

Overall, our results indicate that in the case of early auditory deprivation, the development of fundamental mechanisms of visual processing, such as Repetition Suppression and Novelty Detection, are altered. The data show, in the context of RS and ND, the existence of selective changes in oscillatory patterns, which might suggest alterations of feedback processes in early deaf individuals. Overall, these findings are in agreement with conclusions resulting from animal studies and provide novel insights on the potential oscillatory mechanisms that may underlie specific superior visual processing in early deaf individuals.

Chapter 3

EEG frequency-tagging demonstrates increased left hemispheric involvement and crossmodal plasticity for face processing in congenitally deaf signers

3.1 Introduction

Face processing belongs to the most studied human brain functions, most likely due to the fact that faces play a unique role in social interactions (Calder et al., 2011). Faces convey crucial information about, e.g., the identity, sex, age, and emotional state of a person. The processing of faces recruits a network of brain regions which responds more strongly to faces than to other visual stimulus categories, mainly in the ventral occipito-temporal cortex (VOTC) and posterior superior temporal sulcus (pSTS) (Haxby et al., 2000; Duchaine & Yovel, 2015; Grill-Spector et al., 2017). Newborns display a bias for visual stimuli that encompass general statistical properties present in faces (e.g., "top-heavy patterns", Macchi Cassia et al., 2004; Simion et al., 2008). The face processing system specializes over an extended developmental period to the faces most often encountered (Macchi Cassia et al., 2009; Anzures et al., 2013).

An unsolved question is the extent to which different functions of the face processing system are shaped by experience. Here we investigated three sub-functions of face processing, in congenitally deaf individuals who all had learned a sign language as first language. Faces are of particular relevance to this population since on the one hand, facial cues are of special importance in sign languages and for lip reading, and on the other hand, deaf individuals miss vocal information to assess the emotional tone or identity of other people.

Following auditory deprivation, neural circuits which are associated with the deprived sensory system (i.e., the auditory cortex) as well as neural circuits, which represent the intact sensory input (e.g., the visual cortex) have been found to reorganize (Bavelier & Neville, 2002; Merabet & Pascual-Leone, 2010; Pavani & Röder, 2012; Heimler et al., 2014). These

phenomena are called crossmodal and intramodal plasticity, respectively. Both crossmodal and intramodal plasticity have been linked to enhanced visual abilities in deaf individuals (Bavelier et al., 2000; Bavelier et al., 2006; Lomber et al., 2010; Hauthal et al., 2013).

Studies on face processing in congenitally deaf signers have revealed both crossmodal and intramodal plasticity (McCullough et al., 2005; Stropahl et al., 2015; Benetti et al., 2017). A recent functional magnetic resonance (fMRI) study in congenitally deaf signers by Benetti et al. (2017) has investigated brain regions of the right superior temporal sulcus (STS), which have been suggested to comprise neural systems for voice processing (temporal voice area, TVA) in hearing individuals (Belin et al., 2000; Belin & Zatorre, 2003). Results revealed that the response of this area to faces was enhanced in deaf individuals as compared to both hearing signers and hearing non-signers. The authors interpreted their results in favor of the view that crossmodal plasticity follows the functional specialization of neural systems (Lomber et al., 2010): brain regions supporting person processing in one modality support person processing based on the remaining intact sensory modalities if the typical modality input is missing. Moreover, the results of this study indicated that such crossmodal response could not be explained by the use of a sign language. McCullough et al. (2005) observed a change in the typical lateralization of ventral visual areas (specifically the fusiform gyrus) following congenital deafness: while emotional facial expressions elicited a bilateral activation of the fusiform gyrus (FG) in hearing controls, the activation was left lateralized in congenitally deaf signers (McCullough et al., 2005). This result suggests intramodal in addition to crossmodal changes of face processing in deaf individuals. Crucially, hearing native signers did not show a similar change in lateralization, suggesting that sign language experience alone was not responsible for these cortical changes (Emmorey & McCullough, 2009). In sum, these studies provide evidence that the human face processing system depends on early experience (Bettger et al., 1997; McCullough et al., 2005; Weisberg et al., 2012; Letourneau & Mitchell, 2013; Benetti et al., 2017). In concordance with a change in the lateralization of neural systems related to face processing, behavioral studies have shown a reduced left visual field (LVF) bias in early deaf individuals when judging emotional facial expressions of the gender of faces (Letourneau & Mitchell, 2013; Dole et al., 2017). By contrast, the

typical LVF bias was observed in deaf signers for face identity judgments (Letourneau & Mitchell, 2013) suggesting that changes in laterality are task dependent.

However, which face processing functions are experience-dependent and whether different functions encounter distinct neural adaptations is yet unknown. To address these questions, the same subjects must be tested for different face processing functions. This approach was implemented in the present study by employing Fast Periodic Visual Stimulation (FPVS) and recording triggered changes in the electroencephalography (EEG) in a group of congenitally deaf signers and a group of hearing controls. The two groups were compared in three functions of face processing: (1) the ability to discriminate faces from non-face objects, i.e., Face-Object Categorization, (2) the ability to discriminate changes in facial expression i.e., Emotional Facial Expression Discrimination, and (3) the ability to individuate face identities, i.e., Individual Face Discrimination. We used FPVS-EEG since visual stimuli presented at periodic rates typically elicit high signal-to-noise ratio (SNR) responses over the human scalp which can be objectively quantified in the frequency-domain (see Norcia et al., 2015; Rossion et al., 2020 for reviews). In recent years, this approach has been successfully used to provide sensitive and objective measures of face processing in typically developed individuals (Rossion et al., 2020 for a recent review). This technique allowed us here to measure rapidly and objectively robust discriminative responses within the same participants and within the same experimental session. We exploited this powerful technique to investigate the combined impact of a congenital auditory deprivation and the use of a sign language since birth on different face processing functions.

All experiments implemented in the present study were previously validated in hearing individuals (Liu-Shuang et al., 2014; Rossion et al., 2015; Dzhelyova et al., 2017). Pictures were presented at a fixed rate of 6 Hz (six images/s) with a target stimulus being presented every five stimuli (i.e., $6/5 = 1.2$ Hz). The target was defined as a face among other objects in experiment 1; a face with an emotional expression among neutral faces in experiment 2 and the image of a face having a different identity among images of faces having the same identity in experiment 3. In experiment 2 and experiment 3, images were selected from the same dataset, but stimulus categories were orthogonally organized: while in

the Emotional Facial Expression Discrimination experiment the identity of the faces was randomized across facial expressions, in the Individual Face Discrimination experiment emotional facial expressions were randomized across face identities. Therefore, by using the same set of stimuli, we were able to directly compare neural correlates of emotion vs. identity processing between congenitally deaf signers and hearing adults. For each of the three experiments, neural responses at the target frequency (1.2 Hz) and its harmonics were extracted from the EEG frequency-domain representation. The overall discriminative response was compared between the two groups. Based on previous findings (McCullough et al., 2005; Letourneau & Mitchell, 2013), we predicted a relatively stronger involvement of the left hemisphere for face categorization and for aspects of face processing related to sign language (the processing of facial expressions) but not to identity. Crossmodal plasticity, that is, a stronger activation of the auditory cortex in response to face stimuli, was assessed with distributed sources modelling. We hypothesized that congenitally deaf signers would activate the auditory cortex more than controls during face processing (Benetti et al., 2017; Stropahl et al., 2015).

3.2 Methods

3.2.1 Participants

Twelve congenitally deaf adults (from now on referred to as "CD", eight men, mean age = 25.15 years, SD = 4.02, range: 21-33 years; all of them completed secondary schools) participated in the present study. All CD participants were right-handed and had a profound bilateral hereditary deafness with a hearing loss greater than 100 dB in the better ear since birth. All participants had learned a sign language as first language. Ten deaf participants had acquired German Sign Language (Deutsche Gebärdensprache, DGS; Kubus et al., 2015) as their first language while the two remaining participants had learned Turkish or Russian Sign Language as their first language. These two participants had acquired DGS as a second sign language and used DGS as their main language. DGS proficiency was assessed with the German Sign Language Repetition Task (DGS-SRT; adapted from the ASL-SRT (American Sign Language Sentence Repetition Task); e.g., Hauser, Paludneviene, Supalla, & Bavelier, 2008) by two deaf experts who were

native signers. According to the DGS-SRT evaluation, all deaf participants owned native-like DGS competence. All CD participants were recruited from the North German region, had normal or corrected-to-normal vision, and none of them reported a history of a neurological disorder.

A control group of twelve hearing non-signers (from now on referred as "HC", eight men, mean age = 25.36 years, SD = 3.54, range: 20-32 years) matching the CD individuals in age, gender, and handedness, was recruited from the local community of the city of Hamburg, Germany. All hearing participants had normal or corrected-to-normal vision and reported that they had never suffered from any neurological disorder. The study was approved by the ethical committee of the German Society of Psychology and was conducted in accordance with the seventh revision of the Declaration of Helsinki. Prior to testing, all participants received instructions about the experimental procedure (for the CD individuals, the explanation was provided in written form and in a DGS video) and gave their written informed consent.

3.2.2 Experimental design and setup

The study consisted of three previously validated EEG experiments: (1) Face-Object Categorization (FO; from Rossion et al., 2015), (2) Emotional Facial Expression Discrimination (EM; from Dzhelyova et al., 2017) and (3) Individual Face Discrimination (ID; from Liu-Shuang et al., 2014; as extensively reviewed in Rossion et al., 2020).

Each participant performed all three experiments during one session, in a dimly lit room in the Biological Psychology and Neuropsychology lab of the University of Hamburg. The order of the experiments was the same for every participant: FO, ID, and EM. However, we report methods and results of each experiment with the following order FO, EM, ID as it better represents the hierarchy within the face processing system. The stimuli were delivered on a Dell computer monitor with 1680 × 1050 resolution and a refresh rate of 60 Hz, by adopting a sinusoidal contrast modulation (0-100%) at 6 Hz using the Sinstim Toolbox created in Matlab 2009 (MathWorks Inc., Natick, MA). Thus, each stimulation cycle lasted 167 ms. The full luminance value of each pixel of an image was reached around 83 ms after the onset of a stimulus, that is, at half cycle.

During EEG recording, participants were comfortably sitting at 80 cm viewing distance from the computer screen. Prior to testing, participants were instructed to adopt a relaxed sitting position, to refrain from moving and to continuously fixate on a small black cross (16 pixels resolution, 5 mm in size, 0.35° of visual angle) shown at the center of the flickering stimuli (the fixating cross was located between the eyes of the faces). Participants were asked to detect infrequent changes (from black to red) of the fixation cross and to press the spacebar of a keyboard (placed in front of them) with the index finger of the right hand whenever the fixation cross changed its color. Participants were instructed to perform this color detection task without ignoring the stream of images in the background. Color changes occurred 10 times per stimulation sequence at random times. Response times (RT) and accuracy (percentage correct) to color changes were recorded. During the EEG session, a webcam continuously monitored participants to guarantee continuous communication between them and the experimenter. Participants were invited to take regular breaks every 10–15 min and to shortly rest after each sequence (see Procedure). When a participant was ready for the next sequence, he/she made a sign towards the camera upon which the experimenter started the next sequence. The sequence order was randomized for each participant. The total testing time, including three experiments with EEG application/removal, breaks, took about 3 h.

3.2.3 Face-Object Categorization (Experiment 1)

3.2.3.1 Stimuli

Fifty-one photographic images of faces and 254 photographic images of various objects (animals, plants, houses, and human-made objects) were used as stimuli (see Experiment 1 in Figure 3.1). All images were in greyscale, equalized in luminance and contrast, 200×200 pixels in size (for the details on the stimuli dataset, see Rossion et al., 2015). The stimuli were shown on the screen within an area of 7.3×7.3 cm at the resolution of 259×259 pixels, resulting in a 5.22° of visual angle (VA) when viewed at a distance of 80 cm. The faces were unknown to the participants, and they had not seen any of the object pictures prior to the experiment.

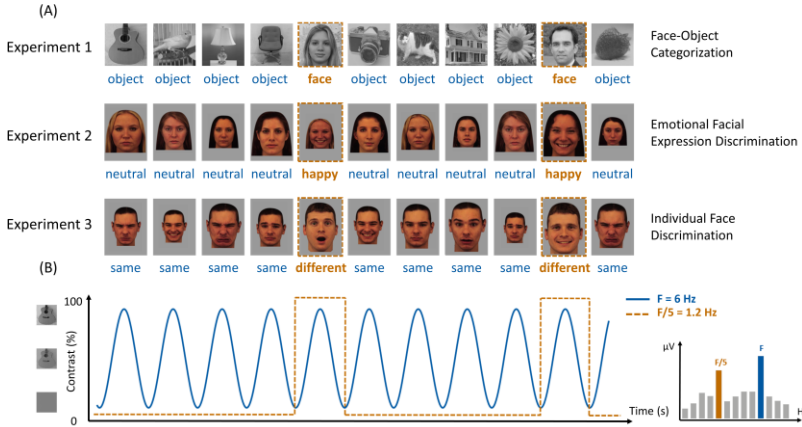


Figure 3.1: Schematic illustration of the experimental paradigms (for details, see Liu-Shuang et al., 2014; Rossion et al., 2015; Dzhelyova et al., 2017). **(A)** All three experiments shared a similar design. Stimuli were presented at a base frequency of 6 Hz (solid blue line in **B**). Key stimuli appeared periodically every fifth image, that is, at a rate of 1.2 Hz (dashed orange line in **B**). Experiment 1: Face-Object Categorization (FO). Stimuli included grey-colored images of non-face objects from ten different categories and images of faces. The stimulus appearing every 5 stimuli was always a face. Experiment 2: Emotional Facial Expression Discrimination (EM). Neutrally expressive faces of different identities were presented at the base frequency, whereas expressive faces with another emotion (disgust, fear, or happiness) appeared at the oddball frequency (identity was changing for each image). Experiment 3: Individual Face Discrimination (ID). Stimuli included Face images of different identities with neutral or expressive emotions (fear, disgust, happiness). At the base frequency, different expressions of the same face-identity were presented, while at the oddball frequency, a novel identity was used (emotional facial expression was changing for each image). In all three experiments, participants continuously monitored a color-change of a small cross located at the center of the visual stimuli to which they had to respond with the button-press. **(B)** An illustration of the sinusoidal contrast modulation used for stimuli presentation and the periodic response (that is, a periodic EEG response to a fast periodic visual stimulation, appearing at the same frequency as the stimulation); the response at the base frequency is indicated with the blue color, whereas the oddball response is indicated with the orange color. Note: responses at the corresponding harmonics are not shown on the figure.

3.2.3.2 Procedure

Stimulus presentation was controlled using Matlab 2009. Fast Periodic Visual Stimulation (FPVS, Rossion, 2014) was applied, with sinusoidal contrast modulation at the base frequency of 6 Hz. A face image appeared after four images of other objects, that is, at a frequency of 1.2 Hz. To compose a sequence, the stimulus selection for both stimulus categories was random. Frequencies of interest included the base frequency (6 Hz), the oddball frequency (1.2 Hz), and harmonics for the oddball frequency (e.g., 2.4 Hz, 3.6 Hz, etc.). Stimulation sequences were shown to test the ability to discriminate between the face-stimuli and other objects from other categories. Since multiple object identities were used, categorization required generalizing across multiple face exemplars and objects. The amplitude of the EEG signal at the 1.2 Hz frequency and its harmonics was considered as an indicator of category discrimination and generalization (Rossion et al., 2018). Each sequence was repeated twice for each participant. Each sequence lasted for 64 s, including 60 s of stimulation, 2 s of fading-in and 2 s of fading-out, at the beginning and at the end of stimulation. Only these 60 s of "pure" stimulation were further analyzed. Each sequence start was preceded by the appearance of a small black fixation cross against the grey blank background for 2-5 s (randomly jittered in length), in order to setup and maintain the participants' eye-fixation.

3.2.4 Emotional Facial Expression Discrimination (Experiment 2)

The stimuli used in experiment 2 and experiment 3 were selected from the same stimulus set. For Emotional Facial Expressions Discrimination, neutrally expressive faces were presented at the base frequency, while a face expressing disgust, fear or happiness was shown at the oddball frequency (see Experiment 2 in Figure 3.1). For both the base and the oddball frequency the identity of the face was randomized; gender was kept constant.

3.2.4.1 Stimuli

Due to time constraints, we limited the investigation to the discrimination of three emotional facial expressions (namely, fear, disgust, and happiness) with respect to a neutral facial expression. Fourteen full colored front face pictures from the Karolinska Directed Emotional Faces dataset were selected (Lundqvist et al., 1998)

comprising 7 males and 7 female identities with 4 facial expressions: 3 emotional expressions corresponding to fear, disgust, and happiness plus 1 neutral. Therefore, 56 stimuli were used in total. Participants were unfamiliar with the pictures prior to testing. Each face picture had an equalized mean pixel luminance during stimulation. The original background was replaced with a grey color.

3.2.4.2 Procedure

The base frequency was generated by presenting images randomly selected from 7 different identities (either from the male or female pool) with a neutral emotional facial expression. Every fifth stimulus (oddball), a face with one of three emotional expressions was shown (while the identity of the face was random). Within a stimulation sequence, the same emotional facial expression was used as oddball images (that is either disgust, fear, or happiness). To avoid low-level repetition effects, the size of the pictures was randomly varied between 90% and 110% at every stimulation cycle (Dzhelyova & Rossion, 2014a, 2014b).

The number of sequences was 6: 3 oddball emotional expressions (disgusted, fearful, and happiness) and 2 experimental conditions (upright and inverted). Each sequence was repeated 4 times (2 sequences of male identities and 2 of female identities), resulting in a total of 24 randomized sequences. The inverted condition was used as a control. Stimulus selection for both stimulus categories was random. All images were 300×450 pixels in size. The stimuli were shown on the screen within an area of 8.5×12.7 cm, resulting in 6° of visual angle (VA) when viewed at a distance of 80 cm. Each sequence lasted 54 s, including 50 s of stimulation, 2 s of gradual fading-in at the beginning and 2 s of gradual fading-out at the end of stimulation. Only 50 s of stimulation were included in the data analysis. The remaining procedure was as for experiment 1. Without counting breaks, the duration of the experiment lasted for about 21 min (24 sequences \times 54 s).

3.2.5 Individual Face Discrimination (Experiment 3)

3.2.5.1 Stimuli

For Individual Face Discrimination (experiment 3), at the base frequency different expressions of the same identity were presented, whereas at the oddball frequency, a novel identity was used. The stimuli

were extracted by the same set of stimuli which was used in experiment 2. To maximize the generalizability of the identity discrimination across the largest possible sets of different images, we used all emotional facial expressions which were available in the set of stimuli: 7 males and 7 female identities, each with 7 facial expressions (fear, angry, disgust, happiness, neutral, sad, and surprised). Thus, in total 98 pictures were employed. Participants were unfamiliar with the pictures prior to testing. Images were presented with the same size as in experiment 2, all other parameters were as in experiments 1 and 2.

3.2.5.2 Procedure

Two conditions were implemented (upright and inverted) with four repetitions per condition (2 sequences with male identities and 2 sequences with female identities), resulting in a total of 8 randomized sequences. The base frequency was generated by presenting images randomly selected among 7 different facial expressions of the same identity; every fifth face, another identity (oddball frequency; $6 \text{ Hz}/5 = 1.2 \text{ Hz}$) was shown. At the start of each sequence, the base identity was randomly selected from four possible identities. The face identities presented at the oddball frequency were randomly selected from the remaining pool (i.e., from 42 pictures: 6 different identities with 7 different emotional expressions each).

To avoid low-level repetition effects, the size of the pictures was randomly varied between 90% and 110% at every stimulation cycle (Dzhelyova & Rossion, 2014a, 2014b). To further isolate face individuation responses that cannot be accounted merely by physical differences between images, we used an inverted face presentation as a control condition, in which the same face stimuli were used albeit upside-down (note: Figure 3.1 shows only upright condition of experiment 3).

Each sequence lasted 54 s, including 50 s of stimulation, 2 s of gradual fading-in at the beginning and 2 s of gradual fading-out at the end of stimulation. Only the 50 s of stimulation were included to further data analysis. The remaining procedure was as described for Experiment 1 and 2. Without counting breaks, the duration of the experiment lasted for about 7.2 min (8 sequences \times 54 s)

3.2.6 EEG acquisition

The EEG was recorded with 74 Ag/AgCl passive electrodes (EasyCap) referenced to the right earlobe and acquired using the BrainVision software (Brain Products, GmbH). The sampling rate was 500 Hz (hardware bandpass filter with a passband of 0.032-200 Hz). Electrode positions included standard international 10-20 system locations and additional intermediate positions (see Supplementary Figure B.1).

3.2.7 Data analysis in the frequency-domain

The analysis in the frequency domain was performed in Letswave 6 (Matlab-based toolbox; <http://www.nocions.org/letswave>). The same pre-processing procedures (tuned for the Fast Periodic Visual Stimulation) were applied to the datasets of all three experiments, according to most recent studies with such paradigms (e.g., X. Yan et al., 2019; Retter et al., 2020; see also the review of Rossion et al., 2020). First, a Butterworth bandpass filter was applied to the EEG data (fourth-order, 0.1-120 Hz cut-off), which was down-sampled from 500 to 250 Hz and segmented from 2 s to 66 s in order to include 2 s of recording before the first stimulus onset and 2 s after the end of each sequence. For each participant, recording sequences of each experiment were concatenated (separately for each experiment). Biological artefacts related to eye movements and eye blinks were removed by applying an independent component analysis on the extended Infomax (A. J. Bell & Sejnowski, 1995; Jung, Makeig, Humphries, et al., 2000; Jung, Makeig, Westerfield, et al., 2000). Components were extracted and then inspected for their spectral properties, scalp distribution, and distribution across sequences. ICA components indicating one of the artefacts listed above were removed. Noisy channels were replaced by interpolating 3 neighbouring channels (Experiment 1 (FO): 3 channels in total across 2 CD participants and 8 channels in total across 6 HC participants; Experiment 2 (EM): 13 channels in total across 9 CD participants and 9 channels in total across 6 HC participants; Experiment 3 (ID): 7 channels in total across 5 CD participants and 4 channels in total across 4 HC participants). All channels were finally re-referenced to a common average reference. At the single participant level, each epoch was further segmented to an integer number of 1.2 Hz cycles, starting at the onset of the sequence and lasting 60 s (corresponding to 72 cycles, 15,000 time points in total, in FO

experiment) or 50 s (corresponding to 60 cycles, 12,500 time points in total, in EM and ID experiments). This procedure was applied to avoid spectral leakage to neighbouring frequencies. The number of bins for a frequency of interest was computed through a Matlab custom made script intercycle, multiplying the value of the sampling rate by the length of the segment. To increase SNR, epochs corresponding to stimulation sequences of the same condition were averaged in the time domain, separately for each participant. Fast Fourier Transform (FFT) was applied to each of the averaged segments, converting the EEG data to the frequency domain. The FFT transformation yielded a spectrum ranging from 0 to 250 Hz with a spectral resolution (i.e., frequency bins) of 1/60 s, i.e., 0.017 Hz for FO experiment and 1/50 s, i.e., 0.02 Hz for the EM and the ID experiments.

To quantify the responses of interest, we first identified in each experiment whether there was a significant response at the frequency of interest (e.g., 1.2 Hz) and its harmonics. To this aim, we computed the FFT grand averaged data across participants, conditions, and groups, separately for each experiment. The amplitude of the FFT data was further averaged across all electrodes. The amplitude value at the fundamental frequencies of interest (1.2 Hz or 6 Hz) and their harmonics (2.4 Hz, 3.6 Hz, etc.; 12 Hz, etc.) was compared to the distribution calculated on the amplitude of the FFT grand averaged data measured at 20 surrounding bins (of each frequency of interest). We excluded the 2 bins (one on the left and one on the right side) immediately adjacent to the frequency of interest, to exclude potential amplitude leakage across adjacent bins (Dzhelyova & Rossion 2014a, 2014b; Retter & Rossion 2016). Z-values were then computed separately for each frequency of interest, against the surrounding noise (note that, in both groups and across all experiments and conditions, the distributions of the amplitudes of surrounding bins were normally distributed). Z-values were calculated as follows: the amplitude at the frequency of interest (e.g., 1.2 Hz) *minus* the average of surrounding bins / standard deviation of surrounding bins. This procedure measures the deviation of the amplitude of the frequency of interest with respect to the mean of the surrounding bins, expressed in terms of standard deviations from this mean. Frequency bins with a z-value larger than 1.64 (corresponding to a one-tailed p-value of $p < 0.05$) were considered as deviating significantly from noise. A one-tailed liberal statistical threshold was

used at this stage to select the highest number of harmonics to obtain an accurate quantification of the signal, with a one-tailed testing due to the directionality of the hypothesis (i.e., signal > noise level; see Rossion et al., 2020; see also Supplementary Material for a data analysis performed using a more stringent z-value of 3.29, corresponding to a two-tailed p-value of $p < 0.001$ with similar results). Once significant responses at the frequencies of interest (e.g., 1.2 Hz, 2.4 Hz, and so on) were identified, we returned to the raw single subject data and computed baseline-correction for each participant and condition. Only for frequencies which differed from surrounding noise (in the FFT grand averaged data across participants, conditions and groups) the baseline correction was computed at the single participant level as follows: from the frequency of interest the averaged amplitude of 20 surrounding frequency bins (10 from each side) was subtracted (we did not consider immediately adjacent bins, which might contain power in the frequency of interest due to a spectral leakage, and the local maximum and minimum amplitude bins as in (Dzhelyova & Rossion 2014a, 2014b; Retter & Rossion 2016). Moreover, for visualization purposes, the SNR was calculated for each participant and condition as follows: the amplitude at the frequency of interest was divided by the average amplitude of 20 surrounding bins (we did not consider the same bins which were excluded in the baseline-correction procedure, see above). This procedure was implemented to correct for the overall noise level and to better visualize the data (Dzhelyova et al., 2017).

For each frequency of interest, we then identified the set of consecutively significant baseline-corrected harmonics in the FFT grand averaged data across participants, conditions, and groups. Harmonics of the 1.2 Hz oddball frequency, which corresponded to the base frequency or its harmonics, the 5th (6 Hz), 10th (12 Hz), and 15th (18 Hz) were not considered, because the responses to stimuli presented at both base and oddball frequencies are confounded at these frequencies. These significant harmonics were then combined into a summed oddball response at the single participant level. Once the summed oddball response was averaged for each participant, it was used as a dependent measure for further statistical analyses (see Dzhelyova et al., 2017). In the FO experiment (experiment 1), 14 consecutive harmonics (i.e., 1.2 Hz to 20.4 Hz; see Supplementary Material) were significant. In the EM experiment (experiment 2) 18 consecutive harmonics (i.e., 1.2 Hz to 26.4

Hz; see Supplementary Material) were significant. The summed oddball response across emotional facial-expressions was calculated by averaging the summed oddball response calculated at the level of single Emotional Facial-Expressions in each group. Finally, for in the ID experiment, the significant summed oddball response was composed by the average first 6 harmonics (i.e., 1.2 to 8.4 Hz; see Supplementary Material; see also Rossion et al., 2020). Finally, we computed grand averages of both baseline-corrected and SNR data across participants for each group and condition.

The main aim of the frequency domain analyses was to perform between group comparisons of the summed oddball responses. The analysis focused on the average of the response across posterior electrodes in the left and right hemisphere, which for both groups comprised the highest baseline-corrected amplitudes in each experiment (see Supplementary Figure B.1). Data inspection revealed a strong consistency between the scalp topographies measured in the present sample of HC individuals and previous studies using the same paradigms (e.g., Liu-Shuang et al., 2014; Rossion et al., 2015; Dzhelyova et al., 2017). Electrode selection included four pairs (P7-P8, PO7-PO8, P9-P10, PO9-PO10) covering the posterior lateral portions of left and right hemispheres. At the single participant level, data were averaged across selected electrodes separately for each hemisphere. The resulting amplitude values were used for statistical comparisons. For each of the three experiments, we separately ran a mixed-design analyses of variance (ANOVAs; IBM SPSS Statistics V21.0.0) with group (CD, HC) as between-participant factor and the following within participant factors: For FO experiment: Hemisphere (left, right); for EM experiment: Condition (upright, inverted), Hemisphere (left, right); for ID experiment: Condition (upright, inverted), Hemisphere (left, right).

For the FO experiment, the analyses at posterior electrodes aimed at specifically testing for the two-way Hemisphere*Group interaction effect (Condition as a factor was not present in this experiment) and, we limited the analysis to this pre-specified effect (as opposed to investigating all main effects and interactions as it is done in exploratory analyses; see Cramer et al., 2016). For EM and ID experiments, at posterior electrodes we aimed at testing for the two-way Hemisphere*Group and, for the three-way Hemisphere*Condition*Group interaction effects, and the analyses were

limited only to these pre-specified effects (see Cramer et al., 2016). P-values were corrected for multiple comparisons across selected F tests (i.e., interactions listed above) using the false discovery rate (FDR; Benjamini et al., 2001). Moreover, for each participant, a laterality index (LI) was calculated separately for each experiment as follows: Laterality Index = $(L - R) / (|L| + |R|)$. Negative and positive values indicate a greater involvement of the right and of the left hemisphere, respectively (see e.g., Seghier et al., 2008). At the single participant level, L and R represent the EEG responses measured over each hemisphere averaged across the selected posterior electrodes. For both EM and ID experiments the LI was assessed only for the upright face conditions. At the group level, LI greater than a threshold of $|0.2|$ indicated that there is at least a 50% higher activity in one hemisphere than in the other hemisphere. This threshold has been previously suggested as indicating hemispheric dominance (see Seghier et al., 2008).

Prior to performing the analysis in the source space, we assessed at the scalp level potential crossmodal activations in the CD group by analyzing the responses measured at the vertex cluster comprising the midline electrodes FCz, Cz and CPz (that is, electrodes typically measuring the maximal responses from the auditory cortex; see Supplementary Figure B.1). The same statistical models were run as for the posterior electrodes albeit without the factor Hemisphere. The two-way ANOVAs which were run for vertex responses in the experiments EM and ID aimed at exclusively testing for a possible Condition*Group interaction (see Cramer et al., 2016). In the result section we reported only these pre-specified effects. For Post hoc analyses conducted to further analyze significant pre-specified interactions we used planned pairwise comparisons (Bonferroni-corrected). Since the analysis at the vertex was explorative before employing source modelling, we did not apply a correction for running two-mixed-design ANOVAs within the same experiment.

As control analyses, for each of the three experiments we ran ANOVAs using as dependent measure the response measured at the base frequency (6 Hz and its harmonics, 12 Hz and 18 Hz). This analysis focused on the same electrodes used for the summed oddball response.

3.2.8 Data analysis in the time-domain

The time-domain analysis was conducted with two main aims: (a) to visualize the time-course of the EEG response in all three experiments; (b) to perform an analysis in the source space (source modelling). The latter was not performed in the EM experiment as different emotional expressions are known to elicit different scalp topographies (Dzhelyova et al., 2017; Leleu et al., 2018) and source modelling of each emotional facial expression was beyond the scope of the present study.

The time-domain analysis was performed by implementing the pipeline used by Stropahl et al. (2015), Stropahl et al. (2018). Raw EEG data were pre-processed with EEGLAB 13.6.5 b (Delorme & Makeig, 2004). First, a low-pass filter (windowed sinc FIR filter, cut-off frequency 40 Hz, filter order 500) as well as a high-pass filter (windowed sinc FIR filter, cut-off frequency 1 Hz, filter order 100; (Widmann et al., 2015) were applied. Data were resampled to 250 Hz. In order to remove non-stereotypical artefacts (such as sudden increases of muscle activity) from the data, continuous datasets were segmented into consecutive epochs with a length of 1 s. Segments displaying a joint probability of activity (Delorme et al., 2007) larger than three standard deviations (SD) were removed before performing the ICA. To remove typical artefacts such as eye movements and eye blinks, an independent component analysis based on the extended Infomax (A. J. Bell & Sejnowski, 1995; Jung, Makeig, Humphries, et al., 2000; Jung, Makeig, Westerfield, et al., 2000) was performed. In order to reduce computational time, the number of decomposed components was reduced from 74 to 50. The ICA weights were then associated to the raw EEG (continuous and unfiltered data). ICA components representing artefacts were identified with the semi-automatic algorithm CORRMAP (Viola et al., 2009). Following artefact-related component removal the data were segmented accordingly to stimulus presentation. Consecutive epochs with a length of 0.7 s (0.2 to 0.5 s) were generated. Epochs were time-locked to the 0% contrast time-point in the sinusoidal contrast modulation. In the ID experiment, epochs were calculated for the presentation of all face stimuli, but only for the upright condition. In order to match the SNR-level between the brain responses to different stimulus categories, in the FO experiment, only object images presented immediately before face stimuli were selected. Analogous to the FO experiment, only the face stimuli having the same identity, presented immediately before the face having a new

identity were considered. Epochs having a joint probability of activity greater than four standard deviations (Stropahl et al., 2018) were automatically rejected (mean epochs removed per condition and group were: FO: CD = 9.2%, SD = 3.3; HC = 8.1%, SD = 2.1; ID: CD = 8.9%, SD = 1.5; HC = 8.6%, SD = 1.8). Finally, the data were baseline corrected using the 100 to 0 ms pre-stimulus period, and digitally filtered (low-pass filter with a 40 Hz upper cut-off, order 100).

To visualize the time-course of the EEG signals, consecutive epochs with a length of 5.6 s (0 to 5.6 s) were extracted from the data after artefact-related component removal. The first 15 cycles of stimulation from the start of each sequence (3 times AAAAB sequences) were discarded from analyses, to only include EEG signal in which the periodic response had already been built. Each 5.6 s segment included 6 repetitions of the AAAAB sequence. At the individual subject level, epochs were averaged and low-pass filtered at 20 Hz (note that for both groups all significant harmonics occurred below 20 Hz). The data extraction was carried at the individual level separately for each experiment and condition. Data were then averaged at the group level for visualization (see Supplementary Figures B.3–B.5). EEG segments revealed a highly structured non-linear response in the time domain.

3.2.9 Source reconstruction

Source estimation was performed using Brainstorm software (Tadel, Baillet, Mosher, Pantazis, & Leahy, 2011), which is based on a distributed dipoles model fitting approach. Sources were extracted by applying a dynamic statistical parametric mapping (dSPM; Dale et al., 2000), which has been shown to provide a better localization of deep sources than standard minimum norm procedures (Lin et al., 2006). The dSPM adopts minimum-norm inverse maps to estimate the locations of scalp electrical activities. Before source estimation, the EEG data were re-referenced to the common average reference (Michel et al., 2004). Moreover, the activity was normalized by an estimate at the individual level of the noise standard deviation at each electrode location (Hansen et al., 2010). To this end, for each participant and location, noise covariance matrices and individual noise standard deviations were calculated using single trials baseline intervals data (100 to 0 ms). The boundary element method (BEM) provided in OpenMEEG was adopted as a head model (default parameters in Brainstorm were selected). The BEM provides

anatomical information by three realistic layers (Gramfort et al., 2010; Stenroos et al., 2014). Source estimation was performed by selecting the option of constrained dipole orientations (Tadel et al., 2011). Single-trial data were averaged for each individual, then the estimate of active sources was calculated at the individual level.

Based on the existing literature (Finney et al., 2001; Sandmann et al., 2012; Cardin et al., 2013; Bottari et al., 2014; Stropahl et al., 2015) an Auditory region of interest (ROI) was defined a priori in each hemisphere before any statistical comparison was run (see Supplementary Figure B.2). Estimated activations of this ROI were used to compare congenitally deaf individuals (CD) and hearing controls (HC). The ROIs were defined by using the Destrieux-atlas (Destrieux, Fischl, Dale, & Halgren, 2010; Tadel et al., 2011), as implemented in FreeSurfer (<http://ftp.nmr.mgh.harvard.edu/fswiki/CorticalParcellation>), which is available in Brainstorm and adopts an automatic parcellation performed by a surface-based alignment of the cortical folding (Destrieux et al., 2010). The Auditory ROI was defined by combining three areas to include Brodmann areas 41 and 42 (Destrieux: *G_temp_sup-G_T_transv*, *S_temporal_transverse* and *G_temp_sup-Plan_tempo*). The so defined Auditory ROI has repeatedly shown crossmodal activations in deaf individuals (Finney et al., 2003; Sandmann et al., 2012; Cardin et al., 2013; Bottari et al., 2014; Stropahl et al., 2015).

First, source estimates in the Auditory ROIs were analyzed for the FO and the ID experiments within each group. For the FO experiment we compared, separately for each hemisphere, the source estimates in response to faces and to objects within the 200-300 ms time window (see Supplementary Figure B.6) and, for the ID experiment the source estimates in response to the different and the same face identities within the 300-400 ms time window (see Supplementary Figure B.7). Two-sided t-tests for dependent samples were performed at each time-point within these preselected time windows. False discovery rate (FDR; Genovese et al., 2002) was used to correct for multiple comparisons. FDR bound (q-value) was set at 0.05 (Genovese et al., 2002). Note that, in the FO experiment, the latency of the source peak in response to faces was consistent with the original ERP result found in the study by Rossion et al. (2015) at posterior scalp location (i.e., 220 ms).

Second, source estimates of the evoked response to faces in the FO experiment and in response to different face identities in the ID experiment were compared between groups in the auditory ROIs. A specific hypothesis was tested in both FO and ID experiments. Based on previous evidence, we hypothesized that the CD group would show greater activations of the auditory cortex as compared to the HC group (Bottari et al., 2014; Stropahl et al., 2015; Benetti et al., 2017). To test this hypothesis, direct comparisons were performed between source activations measured in the Auditory ROIs, separately for each hemisphere. Local maxima (i.e., the absolute peak magnitude of source activations measured in Auditory ROIs) of the responses to faces (FO experiment) and different face identities (ID experiment) occurred for both groups, within the significant within-group effects (faces vs. objects: see Supplementary Figure B.6; same vs. different face identities: see Supplementary Figure B.7). Thus, local maxima for faces and different face identities were used as landmarks for the between group comparisons. One-sided t-tests for independent samples were performed at each time-point within 50 ms time windows which comprised for each experiment the local maxima of both groups. For the FO experiment, the 50 ms time window was between 210 and 260 ms and for the ID experiment between 340 and 390 ms. False discovery rate (FDR; Genovese et al., 2002) was used to correct for multiple comparisons. FDR bound (q-value) was set at 0.05 (Genovese et al., 2002). For all analyses, tests with p-values smaller than the FDR-corrected p-values were considered as significant.

3.2.10 Behavioral data

For each participant and experiment, we calculated the mean accuracy (percentage of correct responses) and the mean RT for the detection of the color change of the fixation cross. As control analyses, two separate ANOVAs (IBM SPSS Statistics V21.0.0) were run using as dependent measures of accuracy and RT for each experiment (FO, EM, ID). For both EM and ID experiments, the ANOVAs included Condition (upright and inverted) as within-participants factors and Group (CD and HC) as between-participants factor.

3.3 Results

3.3.1 Experiment 1 (Face-Object Categorization, FO)

3.3.1.1 Behavioral results

Two separate one way ANOVAs with Group (CD and HC) as between participants factor revealed that CD and HC groups did not differ in the mean accuracy or in mean detection times (mean accuracy: all p-values > 0.1; CD group = 97.9%, SD = 0.03%; HC group = 99.6%, SD = 0.01%; mean RTs: all p-values > 0.3; CD = 416 ms, SD = 59 ms; HC = 396 ms, SD = 45 ms).

3.3.1.2 Face-selective response

As expected, based on previous studies, the face-selective response appeared predominantly in the right hemisphere in HC (mean amplitudes: left hemisphere = 3.1 μV ; SE = 0.42; right hemisphere = 3.6 μV ; SE = 0.44). In contrast, the face-selective response was more pronounced in the left hemisphere in the CD group (left hemisphere = 3.5 μV , SE = 0.55; right hemisphere = 2.9 μV , SE = 0.28; see Figure 3.2). This observation was confirmed by an ANOVA with Hemisphere (left and right) as within-participants factors and Group (CD and HC) as between participants factor, showing a significant interaction between the two factors ($F(1,22) = 4.4$, $p < 0.05$, $\eta_p^2 = 0.17$). Despite the significant interaction, post-hoc pairwise comparisons did not reveal a greater response in the left hemisphere for the CD group than in the HC group, and no greater response in the right hemisphere for the HC group compared to the CD group (all p-values > 0.1, corrected). Moreover, post-hoc pairwise comparisons did not reveal a greater response in the left hemisphere vs. the right hemisphere for the CD group, nor a greater response in the right hemisphere as compared to the left hemisphere for the HC group (all p-values > 0.1, corrected; LI was below the |0.2| threshold for both the CD and the HC group). No between group differences emerged at the vertex (see methods section; all p-values > 0.8).

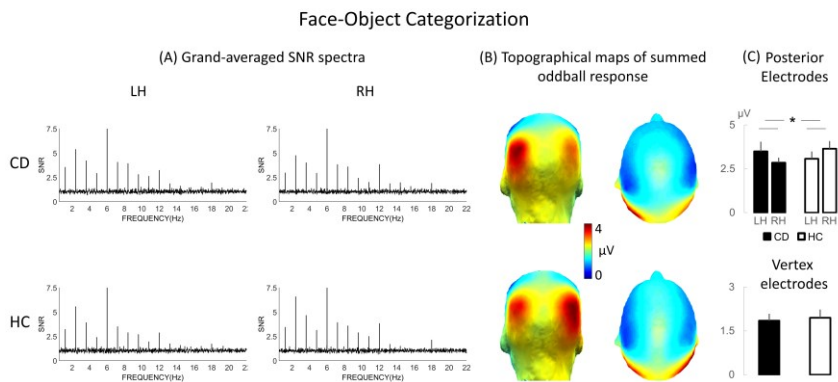


Figure 3.2: Experiment 1 (Face-Object Categorization). CD, congenitally deaf group; HC, hearing control group. **(A)** Grand-averaged SNR spectra across posterior electrodes in the left and in the right hemisphere. **(B)** Topographical maps (from back and top views) of the grand-averaged summed oddball response (baseline-subtracted amplitudes). **(C)** Upper panel: the bar plot shows the response measured at left and right hemispheres at the posterior electrodes for the summed oddball response to face stimuli for both groups. Bottom panel: the bar plot displays the response measured in each group at the vertex. Error bars represent standard errors of the mean. The statistically significant interaction is marked with "*" ($p < 0.05$).

3.3.2 Experiment 2 (Emotional Facial Expression Discrimination, EM)

3.3.2.1 Behavioral results

The ANOVAs with Condition (upright and inverted) as a within participants factor and Group (CD, HC) as between-participants factor did not reveal an effect of Group, neither for accuracy (all p -values > 0.08 ; CD = 96.2%, SD = 6.3%; HC = 97.8%, SD = 2.9%); nor for mean detection times (all p -values > 0.1 ; mean RT: CD = 431 ms, SD = 60 ms; HC = 419 ms, SD = 46 ms).

3.3.2.2 Response to facial expression change

In HC, the facial expression response appeared as bilateral over posterior electrodes (left hemisphere = 0.8 μV , SE = 0.24; right hemisphere = 0.8 μV , SE = 0.13), whereas it appeared as being predominantly involving the left hemisphere in the CD group (left hemisphere = 1.1 μV , SE = 0.18; right hemisphere = 0.8 μV , SE = 0.05; see Figure 3.3). The mixed-design ANOVA with Condition (upright and inverted) and Hemisphere (left and right) as within-participants factors, and Group (CD and HC) did not reveal significant effects for Hemisphere and Group interaction or the Hemisphere, Condition and Group interaction (all p -values > 0.1; see Figure 3.3). However, planned pairwise comparisons revealed that the HC group had a bilateral response for both upright and inverted conditions (left vs. right hemisphere comparison for upright: $F(1,22) = 0.14$, $p > 0.7$, $\eta_p^2 = 0.01$, corrected; inverted: $F(1,22) = 0.56$, $p > 0.4$, $\eta_p^2 = 0.02$, corrected) while a tendency toward a stronger involvement of the left hemisphere was found in the CD group selectively for the upright conditions (left vs. right hemisphere comparison for upright: $F(1,22) = 3.5$, $p = 0.07$, $\eta_p^2 = 0.14$, corrected; inverted: $F(1,22) = 0.11$, $p > 0.7$, $\eta_p^2 = 0.01$, corrected; see Figure 3.3C; LI was below the |0.2| threshold for both CD and HC groups). Finally, no significant interaction between the factors Condition and Group emerged at the vertex (all p -values > 0.7).

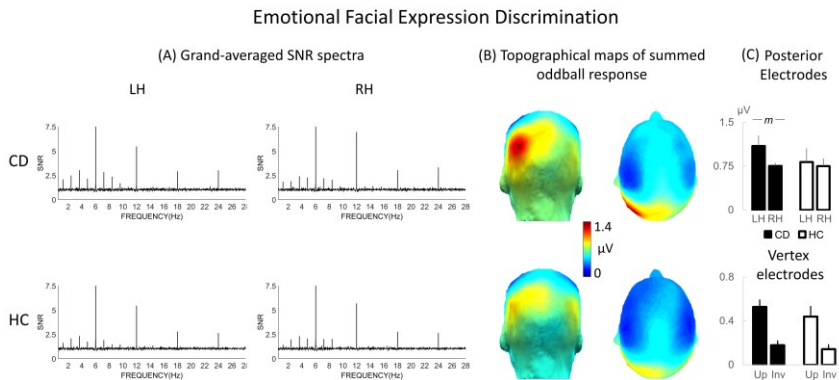


Figure 3.3: Experiment 2 (Emotional Facial Expression Discrimination). Response to changes across facial expressions (from neutral to either fear,

happiness, or disgust). CD, congenitally deaf group; HC, hearing control group. **(A)** Grand-averaged SNR spectra averaged across emotional facial-expressions (disgust, fear, and happiness), in the upright condition for across posterior electrodes in the left and in the right hemisphere. **(B)** Topographical maps (from back and top views) of the grand averaged summed oddball response (baseline-subtracted amplitudes), averaged across emotional facial-expressions, in the upright condition for both groups. **(C)** Upper panel: The bar plot shows the response measured across posterior electrodes in the left and right hemispheres of the grand-averaged summed oddball response mean amplitudes, averaged across emotional facial-expressions, in the upright condition for the two groups. Bottom panel: displays the grand-averaged summed oddball response mean amplitudes measured at the vertex for each Group as a function of Condition (upright and inverted). Error bars represent standard errors of the mean. The tendency towards a significant post-hoc comparison is marked with "m".

3.3.3 Experiment 3 (Individual Face Discrimination, ID)

3.3.3.1 Behavioral results

A mixed-design ANOVA with Condition (upright and inverted) as within-participants factor and Group (CD, and HC) as between participants factor did not indicate any significant main effect or interactions involving the factor Group for accuracy or RT measures (mean accuracy: all p-values > 0.08; CD = 97.3%, SD = 4.1%; HC = 96.4%, SD = 3.8%; mean RT: all p-values > 0.2; CD = 437 ms, SD = 51 ms; HC = 426 ms, SD = 53 ms).

3.3.3.2 Identity discrimination response

The scalp topographies indicated a slight increase in amplitude over the right compared to the left hemisphere for HC (left hemisphere = 0.87 μV , SE = 0.20; right hemisphere = 1.04 μV , SE = 0.16) this was also found in the CD group (left hemisphere = 1.07 μV , SE = 0.13; right hemisphere = 1.13 μV , SE = 0.11; see Figure 3.4). The mixed ANOVA with Condition (upright and inverted), Hemisphere (left and right) as within-participants factors, and Group (CD and HC) as between participants factor did not reveal significant pre-selected interactions involving the factors Hemisphere and Group (all p-values > 0.4; see Figure 3.4). Planned pairwise comparisons revealed that for both the HC group (HC left vs. right hemisphere, upright: $F(1,22) = 1.4$, $p > 0.2$, $\eta_p^2 = 0.06$, corrected; inverted: $F(1,22) = 3.9$, $p > 0.05$, $\eta_p^2 = 0.15$; corrected) and the

CD group (CD left vs. right hemisphere, upright: $F(1,22) = 0.2$, $p > 0.6$, $\eta_p^2 = 0.01$, corrected, inverted: $F(1,22) = 2.2$, $p > 0.1$, $\eta_p^2 = 0.09$, corrected) the response in the left and right hemispheres did not differ (see Figure 3.4C, upper panel; LI was below the $|0.2|$ threshold for both CD and HC groups). However, a significant interaction between the factors Condition and Group emerged at the vertex ($F(1,22) = 4.7$, $p < 0.05$, $\eta_p^2 = 0.17$). Post-hoc pairwise comparisons showed that both groups had a greater response for the upright as compared to inverted Condition ($p < 0.001$, corrected). Moreover, post-hoc pairwise comparisons did not reveal a between group effect for either the upright or for the inverted Condition (all p -values > 0.1 , corrected). Thus, the CD group displayed a greater difference between the response to the upright and the inverted conditions (CD: mean upright minus inverted = $0.61 \mu\text{V}$, $\text{SE} = 0.09$) compared to the HC group (HC: upright minus inverted: mean = $0.35 \mu\text{V}$, $\text{SE} = 0.08$; see Figure 3.4C, lower panel).

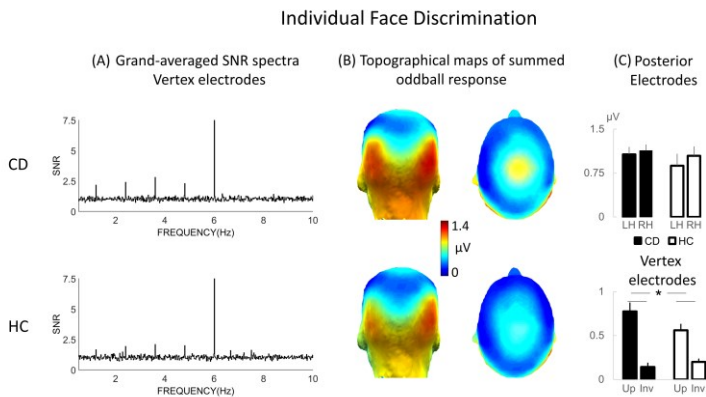


Figure 3.4: Experiment 3 (Individual Face Discrimination). Response to face identity change. **(A)** Grand-averaged SNR spectra for the central electrode FCz in the upright condition. **(B)** Topographical maps (from back and top views) of the grand-averaged data show the summed oddball response (baseline-subtracted amplitudes) to a face identity change, in the upright condition. **(C)** The bar plot shows the grand averaged summed oddball response associated to face identity change, (Upper panel) at posterior electrodes for left and right hemispheres (in the upright condition), and (Bottom panel) at the central cluster of electrodes for upright and inverted conditions in congenitally deaf (CD) and

hearing (HC) participants. Error bars represent standard errors of the mean. Statistically significant interaction involving the Group factor is marked with "*" ($p < 0.05$).

3.3.4 Base frequency

As complementary analyses, a series of ANOVAs with Hemisphere (left and right) and, if appropriate, Condition (upright and inverted, for the EM and the ID experiment) as within-participant factors and Group (CD and HC) as between-participant factor were run for each experiment for the responses measured at the base frequency. No significant interactions involving the factor group emerged (all p -values > 0.2). The same analyses performed at the vertex found no significant difference between group (all p -values > 0.3).

3.3.5 Source estimates for FO and ID experiments at Auditory ROIs

For each experiment, direct between group comparisons were performed with running t -tests between source activations measured in the Auditory ROI of each hemisphere (significant effects were FDR-corrected). Comparisons were performed within a 50 ms time window comprising local maxima of both groups (time windows: FO: 210-260 ms; ID: 310-360 ms; see Method section; for within group comparisons see Supplementary Material). Source estimates of the two groups were compared for the response to faces in the FO experiment and for the response to different face identities in the ID experiment. The analyses aimed at assessing whether a greater response at the pre-defined Auditory ROIs was found in the CD group as compared to the HC group.

Experiment 1 (Face-Object Categorization, FO)

No significant differences emerged for the between group comparison performed on the sources estimated in the Auditory ROIs (see Figure 3.5).

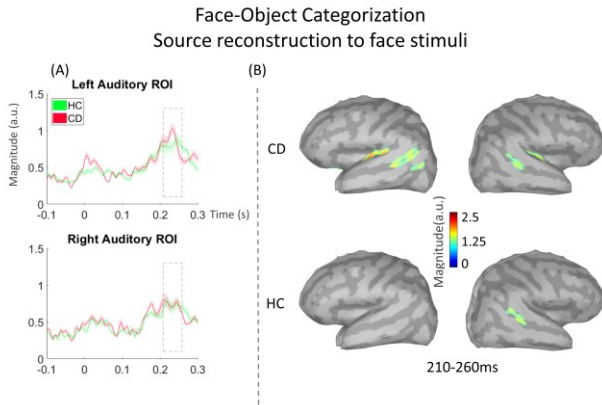


Figure 3.5: Source analysis performed in the time domain for the Face-Object Categorization experiment. Activity is shown in response to face stimuli. **(A)** From top to bottom: the time course of the activity measured for each group at left and right Auditory ROIs. Grey dashed boxes represent the time window of interest (210-260 ms). **(B)** Source activities averaged within the 210-260 ms time window for CD group (top) and HC group (bottom). Source activities are represented as absolute values and in arbitrary units based on the normalization within the dSPM algorithm. The color bar indicates the magnitude of activation. No between-group differences emerged.

Experiment 3 (Individual Face Discrimination, ID)

The between-group comparison of the estimated source activity in the Auditory ROIs revealed that congenitally deaf individuals displayed a greater activation to different face identities as compared to hearing controls in the right hemisphere (time points with $p < 0.05$, FDR-corrected are highlighted in grey in Figure 3.6A).

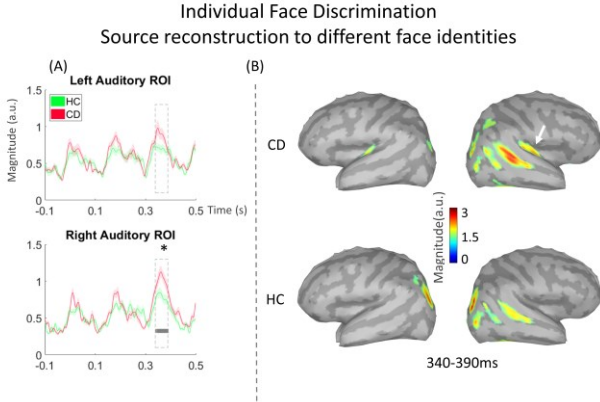


Figure 3.6: Source analysis performed in the time domain for the Individual Face Discrimination experiment. Activity is shown in response to the change of face identity. **(A)** From top to bottom: the time course of the activity measured for each group at left and right Auditory ROIs. Grey dashed boxes represent the time window of interest (340-390 ms). **(B)** Source activities averaged within the 50 ms time window (340-390 ms) for the CD group (top) and the HC group (bottom). The grey box highlights the duration of significant group differences (FDR-corrected). The CD group revealed a greater response to changes of face identity in the right Auditory ROI compared to the HC group. Source activities are represented as absolute values and as arbitrary units based on the normalization within the dSPM algorithm. The color bar indicates the magnitude of activation. Statistically significant effects are marked with "*" ($p < 0.05$, corrected).

3.4 Discussion

The present study investigated the experience dependence of the development of three aspects of face processing: (i) Face-Object Categorization (faces vs. objects of different categories; experiment 1), (ii) Emotional Facial Expression Discrimination (emotional faces vs. neutral faces; experiment 2), and (iii) Individual Face Discrimination (different vs. same face identities; experiment 3). To this end, we recorded the EEG in three experiments involving fast periodic visual stimulation (FPVS; Rossion, 2014; Rossion et al., 2015) in a group of

congenitally deaf signers (CD) and a group of matched hearing controls (HC).

There is evidence that face processing has distinct neural correlates in deaf signers compared to hearing controls (McCullough et al., 2005; Benetti et al., 2017). However, a systematic assessment of the neural correlates of different aspects of face processing in the same individuals has been lacking. Here, for each experiment, we compared the neural response of the two groups at posterior lateral electrode locations, which have been demonstrated to best capture the responses associated to face categorization, emotional facial expression and identity discrimination (see Liu-Shuang et al., 2014; Rossion, 2014; Rossion et al., 2015; Dzhelyova et al., 2017). This approach allowed us to investigate the functional organization of different aspects of face processing within the same subjects. Face categorization elicited a relatively stronger involvement of the left hemisphere in the CD group than the HC group. The same trend was observed for the EM experiment but not for the ID experiment.

Changes in the relative hemispheric involvement of neural systems such as for motion processing (Bavelier et al., 2001; Bosworth & Dobkins, 2002; Brozinsky & Bavelier, 2004), visual spatial attention (Neville & Lawson, 1987a) and language processing (Neville & Bavelier, 1998) have previously been observed in congenitally deaf signers. For instance, in a visual spatial attention task, a left hemispheric dominance was found in deaf individuals (Neville & Lawson, 1987b), which was only partially related to the usage of a sign language - hearing native signers displayed the typical right hemispheric dominance (Neville & Lawson, 1987a, 1987c). In contrast, changes in visual field dominance for motion processing have been found in both deaf and hearing signers, but not in hearing non-signers, suggesting a crucial role of sign languages for the development of the neural representations of visual motion (Bosworth & Dobkins, 2002). Furthermore, in an fMRI study, deaf signers did not display the typical hemispheric dominance of left-hemisphere language regions (e.g., inferior frontal gyrus, posterior superior temporal gyrus) during a reading task, but a rather bilateral response in the middle temporal and temporo-parietal cortices (Neville et al., 1998). However, more recent studies have suggested that language proficiency might explain some of these results: deaf individuals who were highly proficient users of both a sign language and a written language have

displayed a typical left hemispheric dominance for reading (MacSweeney et al., 2002; Skotara et al., 2012; Hänel-Faulhaber et al. 2014).

Changes in the responses measured in the two hemispheres for face processing have been previously observed in congenitally deaf native signers (McCullough et al., 2005; Weisberg et al., 2012). In an fMRI study, Weisberg et al. (2012) showed a reduced selectivity to faces relative to houses in deaf signers as compared to hearing non-signers in the right fusiform gyrus, whereas the two groups had a similar response in the left fusiform gyrus. However, Benetti et al. (2017) did not report lateralization differences between early deaf individuals and hearing control for face categorization (faces vs. houses). These inconsistent results might be accounted for the different deaf individuals who took part in these experiments. While in the first study (Weisberg et al., 2012) congenitally deaf individuals were native users of a sign language, in the study of Benetti et al. (2017) deaf participants had acquired a sign language at different years of age. Our sample resembled the deaf participants of Weisberg et al. (2012), and so did the observed shift towards a greater involvement of the left hemisphere for face categorization. These results might indicate that a combination of native acquisition of a sign language and congenital deafness results in a change of the representation of face categorization.

In the fMRI study of McCullough et al. (2005) brain activation in response to emotional and linguistic facial expressions was assessed in deaf native signers and hearing non-signers. The authors found that in deaf signers, both tasks elicited a left-lateralized fusiform gyrus activation, whereas hearing non-signers displayed a bilateral activation. The authors speculated that this change in functional lateralization might be due to the crucial role of facial movements in expressive sign language (McCullough et al., 2005). However, the finding that hearing native signers did not show a similarly alternated lateralization later questioned this interpretation (Emmorey & McCullough, 2009). The results of both the FO and EM experiments from the present study support an increased involvement of the left hemisphere for face processing in congenitally deaf native signers. Given that we did not test a group of hearing individuals who started acquiring a sign language from birth, we are not able to disentangle the effects of deafness and of early sign language acquisition on the neural representation of face

processing. Future research including hearing native signers should address the specific impact of the analyses of linguistic facial expressions occurring in sign languages on the neural representation of face processing. Moreover, because we analyzed neural responses at predefined scalp locations, we might have missed additional group differences, such as enhanced amygdala responses which have been previously observed (Weisberg et al., 2012).

Studies on the role of literacy in shaping the functional organization of the brain have provided evidence that learning to read has an impact on the neural organization of other parts of the visual system than only those typically associated with reading (Dehaene et al., 2015). Specifically, while the right hemispheric lateralization for face categorization emerges in infancy well before reading acquisition (de Heering & Rossion, 2015), competition with the processing of written text when children start to read seems to further contribute to the right hemisphere specialization for face processing (Dehaene et al., 2010). The neural competition hypothesis was supported by the observation that in children, high reading proficiency was accompanied by a stronger right lateralization of face categorization (Dundas et al., 2015; Lochy et al., 2019). A recent EEG study tested deaf individuals and hearing controls, who were matched in their reading abilities (Emmorey et al., 2017). Interestingly, higher reading skills were associated with a stronger left hemispheric activity in hearing individuals but with a stronger right hemispheric activity in deaf individuals. The authors interpreted these findings as supporting the phonological mapping hypothesis, which proposes that left hemispheric processing of word-form predominantly emerges to link orthography and phonology, that is visual word form areas (VWFA) and auditory language regions (McCandliss & Noble, 2003). In sum, these results might suggest that the lack of speech input changes the cerebral organization with regard to reading and in turn alters the lateralization of the face processing system in congenitally deaf individuals. However, not all results have been in consistency with this view. No differences in the VWFA activation have been found in response to written text in congenitally deaf signers and hearing controls, suggesting that in deaf individuals the neural correlates of reading are not necessarily altered (Waters et al., 2007; Emmorey et al., 2013; Xiaosha Wang et al., 2015). Moreover, it is noteworthy that the hemispheric specialization for face categorization does not follow a

linear development (Lochy et al., 2019). From being right lateralized in newborns (de Heering & Rossion 2015), it seems to encounter a bilateral phase in 5-year-old children (Lochy et al., 2019; but see Cantlon et al., 2011) before resulting in the adult-like right hemispheric dominance. The associated developmental trajectory as well as the impact of literacy need yet to be further investigated in deaf individuals.

The Individual Face Discrimination experiment revealed other group differences between the CD and the HC group than the Face Object categorization and Emotional Facial Expression Discrimination experiments. No differences were found between groups in the hemispheric responses. A previous behavioral study (Letourneau & Mitchell, 2013) showed a left visual field (LVF) bias for both an emotional facial-expressions judgement and a face identity classification task in hearing individuals. By contrast, deaf signers showed an RVF bias for the judgments of emotional facial-expressions, but the typical LVF bias for face Identity judgments. The present study possibly provides the neural correlates for these behavioral group differences. The lack of group differences in the lateralization for face identity processing of the present study suggests either less experience dependence or no dependence on auditory input or speech. Facial cues play a dominant role in person recognition (Sheehan & Nachman, 2014). In fact, not all patients with lesions in the right ventral cortex have additional difficulties recognizing others from their voices (Gainotti & Marra, 2011); some patients with prosopagnosia have been found to even outperform healthy controls in voice recognition tasks (Hoover et al., 2010).

However, Individual Face Discrimination selectively yielded responses compatible with crossmodal plasticity in the right auditory cortex of CD individuals. This result is in accordance with findings of right auditory cortex activation in deaf individuals in response to visual stimuli (Finney et al., 2001; Sandmann et al., 2012). Furthermore, it is in line with the results of a recent fMRI adaptation study, in which a group of early deaf individuals showed a higher selectivity for face individuation in the right temporal voice area (TVA; Belin & Zatorre, 2003) compared to hearing controls (Benetti et al., 2017). However, in the present study the Auditory ROI was defined by combining three areas to include Brodmann areas 41 and 42 (Finney et al., 2003; Sandmann et al., 2012; Cardin et al., 2013; Bottari et al., 2014; Stropahl et al., 2015), which are located less laterally and ventrally with respect to the right

temporal voice area (TVA). Finally, it is noteworthy that the time-course of source estimates of the present study depends on the paradigm used, which comprised (i) periodic stimulations and (ii) periodic contrast changes (rather than abrupt onsets). Thus, the time-course of source estimates cannot be directly compared to other studies with different stimulation methods (see Rossion et al., 2015 for a discussion on this aspect).

In sum, our results suggest that different aspects of the neural systems associated with face processing show specific experience dependent functional organizations - they adapt partially in different ways to altered experience. These adaptations comprise intramodal plasticity (changes in the hemispheric involvement of the visual cortex) or crossmodal plasticity (stronger activation of what is typically auditory cortex).

Chapter 4

Early visual cortex tracks speech envelope in the absence of visual input

4.1 Introduction

Neuronal populations developed the ability to synchronize their activity (through aligning the phase) to temporal regularities of a continuous input (Lakatos et al., 2019; Obleser & Kayser, 2019). This neural entrainment influences several aspects of processing, including language. In this context, neural activity entrained to amplitude modulations over time of continuous speech (that is, the envelope) has been consistently reported (Ding & Simon, 2014). The exact functional meaning of the entrainment to the speech envelope is still unclear. Several studies showed that intelligible speech is not mandatory for neural tracking (M. F. Howard & Poeppel, 2010; Luo & Poeppel, 2007). However, during comprehension, phase-locked responses to speech in the auditory cortex are enhanced (Gross et al., 2013; Peelle et al., 2013). Moreover, the entrainment to an attended speaker's speech envelope in noisy environments appears to play a role in solving the so-called cocktail-party (Cherry, 1953) problem (Ding, Chatterjee, & Simon, 2014; Riecke, Formisano, Sorger, Baskent, & Gaudrain, 2018). Based on this evidence, entrainment to speech envelope may be involved in promoting the perception of linguistic information (Poeppel & Assaneo, 2020) and facilitating speech comprehension (Ahissar et al., 2001; Luo & Poeppel, 2007), especially in challenging acoustic environments (e.g., Kerlin, Shahin, & Miller, 2010; Zion Golumbic et al., 2013). Importantly, neural entrainment to temporal dynamics of speech is modulated by low-level acoustic features (Ding et al., 2014) as well as high-level meaningful linguistic units, such as phonetic information, phrases, and sentences (Di Liberto, O'Sullivan, & Lalor, 2015).

Neural entrainment does not only occur for the auditory input of speech (A. E. O'Sullivan, Crosse, Liberto, Cheveigné, & Lalor, 2021; Plass, Brang, Suzuki, & Grabowecy, 2020). Recent magnetoencephalography (MEG) studies revealed that the early visual

areas entrain even to silent lip movements (Bourguignon, Baart, Kapnoula, & Molinaro, 2018, 2020; Hauswald, Lithari, Collignon, Leonardelli, & Weisz, 2018). This neural tracking is modulated by audio-visual congruences and boosts speech comprehension in noisy conditions (Park, Kayser, Thut, & Gross, 2016). The contribution of visual cortices in language processing is not limited to visual or audio-visual representations of spoken language. There is scattered evidence that the early visual cortex is also active during purely auditory stimulation (Brang et al., 2022; Petro, Paton, & Muckli, 2017; Vetter, Smith, & Muckli, 2014) and while listening to spoken language (e.g., Martinelli et al., 2020; Seydell-Greenwald, Wang, Newport, Bi, & Striem-Amit, 2021; Wolmetz, Poeppel, & Rapp, 2011). Importantly, such activations cannot be explained by semantic-based imagery alone but rather seem to reflect genuine responses to language input; in fact, the visual cortex also responds to abstract concepts with low imaginability rates (Seydell-Greenwald et al., 2021). Overall, this evidence highlights a putative role of the visual cortex in mapping temporal modulations of incoming sounds, especially in the absence of competing retinal input (Martinelli et al., 2020; Vetter et al., 2014). However, the exact role of the visual cortex in the hierarchy of speech processing remains unclear.

Here, we investigated the neural tracking of speech envelope when visual input is absent. Using electroencephalography (EEG), we recorded neural responses of blindfolded individuals while they were listening to stories presented in isolation (Quiet) or combined with multi-talker babble noise at different signal-to-noise ratios (SNR; Noise). Stories comprised either meaningful (speech) or meaningless (jabberwocky) narration. We used a temporal response function (TRF) to model neural tracking of broadband speech envelope (in 2-8 Hz range; as in: Hausfeld, Riecke, Valente, & Formisano, 2018; Mirkovic, Debener, Jaeger, & De Vos, 2015; J. A. O'Sullivan et al., 2015). TRF approach allows linear mapping between neurophysiological responses and continuous speech stimuli (Crosse, Di Liberto, Bednar, & Lalor, 2016; Crosse et al., 2021) and has been used to measure entrainment to speech in both clear and challenging listening conditions (e.g., Decruy, Vanthornhout, & Francart, 2019; Di Liberto et al., 2015; Ding et al., 2014; Ding, Melloni, Zhang, Tian, & Poeppel, 2016; Ding & Simon, 2014; Legendre, Andrillon, Koroma, & Kouider, 2019; J. A. O'Sullivan et al., 2015).

To disambiguate the effects of lower-level acoustic and higher-level linguistic processing using continuous naturalistic stimuli, we built a hierarchical model. We specifically assessed the effects of (i) low-level acoustic features by contrasting TRFs resulting from listening to stories presented in quiet vs. in noise, and (ii) high-level linguistic information by contrasting TRFs resulting from listening to meaningful (speech) vs. meaningless (jabberwocky) stories, both embedded in noise. Finally, we tested how low-level and high-level information effects are distributed at the source level, with a focus on whether and how speech envelope information is mapped in the visual cortex in the absence of competing visual information.

4.2 Methods

4.2.1 Participants

Nineteen native speakers of the Italian language took part in the study (N = 19; age: median = 28; min = 22; max = 32; females = 12; all right-handed). We excluded one participant because of an error in the presentation script during EEG acquisition and three more participants due to their inability to complete the experiment, resulting in a final sample of fifteen participants (N = 15; age: median = 28; min = 22; max = 30; females = 10). All participants self-reported the absence of any hearing problems and neurological disorders. The experimental protocol was approved by the local ethics committee and conducted following the Declaration of Helsinki. All participants were informed in advance that they would be blindfolded during the experiment, signed written informed consent prior to the study and received monetary compensation for their participation.

4.2.2 Stimuli

We used two types of target stories: (i) meaningful (speech) and (ii) meaningless (jabberwocky) narration. Meaningful stories were extracted from the fiction book for teens *Polissena del Porcello* by (Pitzorno, 1993). Meaningless stories were extracted from the books containing nonsense, metasemantic (jabberwocky) poems and texts: *Gnòsi delle fànfole* by (Maraini, 2019) and *Esercizi di Stile* by (Queneau, 1947/1983). Note that

syntactic information is preserved in jaberwocky stories, whereas semantic information is absent or significantly reduced.

Target stories were narrated by a trained Italian actress. We registered stories in a soundproof booth, using a video camera with an external condenser microphone (Olympus ME51S) at sampling frequency of 48000 kHz. To create stimuli for our EEG experiment, we extracted the audio material from the recorded files and edited them in Audacity® software (version 2.3.0, <https://www.audacityteam.org/>) and with a custom code using Signal Processing toolbox incorporated in MATLAB (version R2018b, Natick, Massachusetts: The MathWorks Inc.). Specifically, we: (i) inspected raw audio files for pronunciation errors and long breaths, consequently removing them, (ii) downsampled audio to 44100 Hz, set to 16-bit and converted from Stereo to Mono, (iii) truncated long pauses and silent periods exceeding 0.5 ms to 0.5 s, (iv) trimmed resulting files to the same length (~ 15 min), (v) identified the noise floor of the frequencies comprising the noise via “Get Noise Profile” feature and subsequently removed low-amplitude background noise with the Noise Reduction built-in feature based on an algorithm using Fourier analysis, (vi) normalized resulting files to the same common root-mean-square (RMS) value to ensure no variation of loudness across stories. Natural variations of loudness within each story were preserved.

We combined the target stories with a five-talker babble to construct stimuli in which the target story was embedded in the noise. Here, we used the babble noise, which is a non-stationary noise that works well both as an energetic and informational masker, efficiently reducing intelligibility and speech quality (Brungart, 2001; Xianhui Wang & Xu, 2021). The babble noise was a mixture of five different voices (2 females, 3 males, all native Italian speakers). Every speaker was recorded in the soundproof booth, reading several non-related extracts from the fiction book *La Strada* by (McCarthy, 2006/2014). These individual recordings were registered and edited with the similar routine described above for the target stimuli. Then, individual recordings were superimposed, resulting in multi-talker babble. Finally, the initial 500 ms of the multi-talker babble got discarded to eliminate a part that did not contain all five talkers.

The first 5 s of the resulting multi-talker babble were set to zero/"muted," followed by 5 s of fade-in to make it easier for the participants to identify and track the target stories in the multi-talker babble noise. Then, with custom MATLAB scripts, we normalized the target stories and the babble to a common RMS value to make sure there would be no story or any of its segments standing out from the noise, and then superimposed the stories and the babble at two SNR levels (SNR1 = +3.52 dB, – for both meaningful and meaningless stories, and SNR2 = +1.74 dB, – for meaningful story only; see Supplementary Material for details). As the last step, we normalized all the resulting audio files for all conditions once again to a common RMS value to achieve equal loudness across the stimuli and consequently verified each file's spectrogram in Audacity.

Altogether, we constructed stimuli to generate four experimental conditions: 1) *Speech-in-Quiet*, with speech without noise, 2) *Speech-in-Noise at SNR1*, 3) *Speech-in-Noise at SNR2*, and 4) *Jabberwocky-in-Noise at SNR1* (see Figure 4.1A). Each experimental condition contained a particular story divided in three parts of around 5 min, therefore the total duration of continuous speech stimuli to per condition was approximately 15 min.

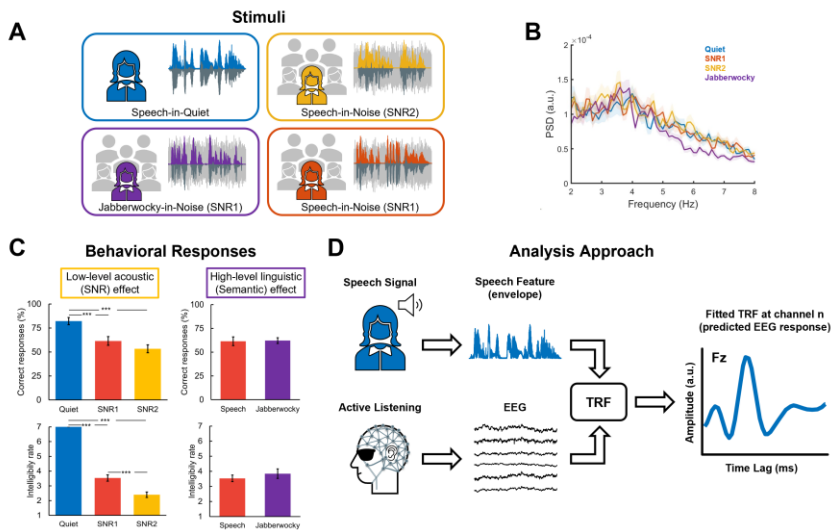


Figure 4.1: Stimuli, Behavioral Responses, and Analysis Approach. (A) Stimuli consisted of continuous (i) meaningful (Speech) and (ii) meaningless (Jabberwocky) stories presented either in quiet (Quiet) or as embedded in the multi-talker babble noise at a different signal-to-noise ratio (SNR1; SNR2). The babble noise was a mixture of five voices (2 females, 3 males) reading extracts from a book. The acoustic envelopes were extracted for further analysis through the Hilbert transform and filtering in the range between 2 and 8 Hz. (B) Power spectra density estimates of normalized acoustic envelopes were obtained using Welch's method with a 10 s Hamming window and half-overlap. Bold lines indicate average across trials, shaded areas indicate standard error of the mean. (C) Behavioral Responses represented by correct responses (Top) and intelligibility rates (Bottom). Barplots display mean \pm SE across participants. Asterisks indicate statistically significant differences ($***p < 0.001$). (D) Neural tracking of the speech envelope was estimated using the forward encoding approach – Temporal Response Function (TRF). Ridge regression-based linear models (TRFs) were fitted to participants' neural data, obtained during active listening, to predict EEG response for of a given EEG channel from speech envelope.

To test the effect of low-level acoustic (SNR) information, we compared neural tracking in *Speech-in-Quiet* condition and *Speech-in-Noise at SNR2* condition. To test the effect of high-level linguistic (semantic)

information, we compared neural tracking in *Speech-in-Noise at SNRI* condition and *Jabberwocky-in-Noise at SNRI* condition.

4.2.3 Task and Experimental Procedure

Participants performed four blocks, each consisted of one experimental condition. During the first block, they always listened to the story without background noise (i.e., *Speech-in-Quiet* condition). This was done to help the participants habituate both to the (target) narrator's voice and the experimental design since this condition was the easiest to attend. The order of the remaining three blocks was randomized across participants. Each of the four blocks consisted of a story that lasted about 15 min divided into three parts around 5 min each (see Supplementary Material for further details). Participants listened to each part of the story only once, without repetition, therefore avoiding the possibility of predicting the content of the story. To maintain the continuity of the storyline within each block, each part within each story followed the previous part chronologically.

We instructed participants to attentively listen to the target story (narrated by the female voice and guided by the first 5 s of the audio) while ignoring babble noise in the background. To ensure that the participants were actively attending to the stimuli, at the end of each part, they answered three specific Yes/No questions about the part of the story that they just listened to (for example, "Il cane di Lucrezia è un San Bernardo? [Is Lucrezia's dog a Saint Bernard?]" ; see Supplementary Material for the full list of questions). If they were not sure about the correct answer between the two, they had to choose the answer that seemed to them as the most probable. To answer, participants pressed corresponding buttons on the response panel with their index and middle fingers. At the end of each part, we asked participants to self-report intelligibility rates of the target story on a Likert scale (where 1 = *absolutely non-intelligible*, 7 = *very intelligible*) and let them have a short break lasting around 2 min. We also ensured that none of the participants was familiar with or recently exposed to the target stories. Moreover, we informally assessed a participant's comfort, alertness, and motivation to continue the experiment during short and long breaks. We removed the blindfolding mask during the breaks between the blocks (every 15 min) for the participants' comfort and to avoid inducing short term crossmodal plasticity effects resulting from the prolonged visual

deprivation (Landry, Shiller, & Champoux, 2013; Lazzouni, Voss, & Lepore, 2012; Merabet et al., 2008).

The experiment was controlled with E-Prime® software (version 3.0, W. Schneider et al., 2002). All instructions and speech stimuli were presented through a single front-facing loudspeaker (Bose Companion® series III multimedia speaker system, USA) placed in front of the participants with approximately 1 m distance from their head. Stimuli were delivered at ~ 60 dB sound pressure level (SPL), measured at the participant's ear, and reported by all the participants as comfortable volume.

To accurately measure the actual onset time of our stimuli, we administered a timing-test using Audio/Visual (AV) Device (Electrical Geodesics, Inc.) compatible with E-Prime software and NetStation system. The measured average delay in time was constant and about +5 ms regarding the stimulus onset.

4.2.4 EEG Recording

Before starting the experiment, each participant received a brief instruction and had a short (~ 1 min) training session on how to control over muscular artifacts through monitoring their EEG signal displayed on the computer screen. Then, we applied the blindfolding mask to the participant, and they were reminded to keep their eyes open during the EEG recordings, though blinking was permitted whenever they wanted. Moreover, we recorded resting-state EEG data for about 2 min at the beginning of each experiment while the participant kept their eyes open. Obtained resting-state data served as calibration data to attenuate EEG artifacts during the preprocessing step.

During the tasks, the participants were seated comfortably in a chair in a dark, soundproofed booth (BOXY, B-Beng s.r.l., Italy). The EEG recordings were acquired at a sampling rate of 500 Hz using NetStation5 software together with a Net Amps 400 EGI amplifier connected to 64 electrodes HydroCel Geodesic Sensor Net (Electrical Geodesics, Inc.), all signals referenced to vertex (additional channel E65/Cz). For data visualization purposes only, the data were band-pass filtered online using the digital filter from 1.0 to 100 Hz, and online digital anti-alias filter aligning EEG recordings with real-time events was kept on.

Electrode impedances were kept below 50 k Ω and were checked between the blocks (when the blindfolding mask was reapplied).

Participants were encouraged to take a break after each block and get enough rest before continuing. They also were reminded about the importance of staying attentive, keeping eyes open while blindfolded and avoiding excessive movements during the EEG recordings.

4.2.5 EEG Preprocessing

We preprocessed continuous EEG raw data offline using custom MATLAB (version R2018b, Mathworks Inc., Natick, MA) scripts together with EEGLAB toolbox (version 14.1.2b, Delorme & Makeig, 2004) for MATLAB.

First, the EEG data were submitted to cleaning with Artifact Subspace Reconstruction (ASR) - an automated artifact attenuation algorithm (clean_rawdata plug-in, version 2.1) available in EEGLAB toolbox. We applied the default flatline criterion of 5 s, together with default transition band parameters [0.25, 0.75]. ASR algorithm was chosen due to its objective and reproducible evaluation of artifactual components in EEG data. ASR is based on Principal Component Analysis (PCA) sliding window and effectively attenuates high-variance signal components in the EEG data (including eye blinks, eye movements, and motion artifacts). Specifically, first, the algorithm automatically identifies the most artifact-free part of the data (here, the resting-state data) to use it as the calibration data to compute the statistics. Next, a 500 ms PCA sliding window with 50% overlap is applied across all the channels to identify "bad" principal components. Then, the algorithm identifies the subspaces in which the signal exceeds 5 standard deviations away from the calibration data as corrupted and rejects them. Finally, it reconstructs the high variance subspaces using a mixing matrix calculated based on the calibration data.

The artifact attenuated EEG data were preprocessed as follows: (i) re-referenced from E65/Cz electrode to a common average reference, (ii) band-pass filtered from 0.1 to 40 Hz (low-pass: FIR filter, filter order: 100, window type: Hann; high-pass: FIR filter, filter order: 500, window type: Hann), (iii) downsampled to 250 Hz, (iv) epoched according to the onset of acoustic stimuli (related to each part of the story), adjusting to measured +5 ms onset delay in time and discarding the first 5 s of target-

speech alone and 5 s of fade-in for the babble noise, (v) band-pass filtered between 2 and 8 Hz (filter type and parameters the same as described above), (vi) downsampled to 64 Hz, (vii) EEG data corresponding to each of the three (~ 5 min) parts of the story were concatenated, (viii) and segmented into 1 min long trials, resulting in 12 trials per block per subject (N = 12). The preprocessed EEG data for each trial were z-scored to optimize cross-validation procedure during encoding (Crosse et al., 2016).

4.2.6 Extraction of Acoustic Envelope

First, audio files containing relevant parts of the target stories were concatenated and segmented into corresponding 1 min long trials, resulting in 12 trials per speech envelope per subject (N = 12) (see Figure 4.1B). Next, the acoustic envelope per each trial was obtained taking the absolute value of the Hilbert transform of the original target stories (i.e., without babble noise) followed by a low-pass filtering using a 3rd-order Butterworth filter with a cut-off frequency of 8 Hz (*filtfilt* function in MATLAB) and downsampling the resulting signal to 64 Hz, so to be matched with the EEG data (e.g., Mirkovic et al., 2015; J. A. O’Sullivan et al., 2015). Finally, the resultant extracted envelopes were normalized by dividing by maximum value.

4.2.7 Estimation of TRF

We modeled where and how the neural response to the speech envelope of the target stories is encoded in the brain, using a linear prediction approach known as temporal response function (TRF) (see Figure 4.1D). The TRF approach, incorporated in mTRF toolbox (Crosse et al., 2016), allows to predict previously unseen EEG response from the stimulus and has been used to model the neural tracking of acoustic and linguistic properties of naturalistic continuous speech (Drennan & Lalor, 2019; Obleser & Kayser, 2019).

The TRF is a mathematical function that is based on the ridge regression and could be described as follows:

$$r(t, n) = \sum_{\tau} w(\tau, n) s(t - \tau) + \varepsilon(t, n),$$

where $t = 0, 1, \dots, T$ is time, $r(t, n)$ is the EEG response from an individual channel, $s(t)$ is the stimulus feature(s) (e.g., speech envelope), τ is the

range of time-lags between s and r , $w(\tau, n)$ are the regression weights over time-lags, and $\varepsilon(t)$ is a residual response at each channel not explained by the TRF model (Crosse et al., 2016). Specifically, TRF can be viewed as a filter that describes the linear relationship between a continuous speech stimulus and a continuous neural response for a specified range of time-lags related to stimulus occurrence (Crosse et al., 2016).

The important assumptions about the TRF include the fact that it reflects the same neural generators as cortical auditory evoked potentials (CAEPs) resulting in their comparable topographies and that it can be used to measure neural tracking of speech envelope (Lalor & Foxe, 2010; Lalor et al., 2009). We fitted separate models (TRFs) to predict response in each EEG channel, using time-lags from -100 to 600 ms related to stimulus onset, typically used to capture CAEP components. Here we estimated the TRF using the envelope estimated between 2 and 8 Hz as previously performed (Legendre, Andrillon, Koroma, & Kouider, 2019; Mirkovic et al., 2015; J. A. O'Sullivan et al., 2015).

The TRF models were trained using a leave-one-out cross-validation procedure, keeping all but one trial for training the model to predict EEG response from the stimuli and using a left-out trial for testing. Thus, a prediction model was obtained for every single trial, and then the final averaging across trials, within participants and conditions was performed resulting in a grand average TRF model.

4.2.8 Regularization Parameter Estimation

Regression models are exposed to overfitting the training data, that is, fitting the random noise rather than true relationships between variables and failing to generalize to unseen data. The problem of overfitting needs to be accounted for before making any interpretations from the resulting model since it could be misleading. Ridge regularization prevents the model from overfitting by penalizing the model weights, forcing them to be smaller, towards 0, so the model could become better generalized.

To control for model overfitting, we empirically identified the optimal regularization parameter (λ) of TRF models through leave-one-out cross-validation procedure, using a grid of ridge values ($\lambda = \{10^6, 10^5, \dots, 1, 10, \dots, 10^5, 10^6\}$), for time-lags from -100 to 600 ms. The

regularization parameter λ was determined based on the mean squared error (MSE) value between the actual and predicted EEG responses. The optimal regularization parameter was the one yielding the lowest MSE on the testing data (here, identified as $\lambda = 10^3$) and kept constant across channels, participants, and conditions allowing to generalize across them at the group level.

4.2.9 Spatiotemporal Characteristics

Forward model weights are directly physiologically interpretable (Haufe et al., 2014) and allow us to get an insight about which channels contribute most to neural tracking of the speech envelope. The resulting topographical plots with TRF weights obtained per each individual time-lag window can be interpreted similarly to CAEPs in terms of both amplitude and direction (Lalor, Pearlmutter, Reilly, McDarby, & Foxe, 2006; Lalor et al., 2009). We investigated spatiotemporal characteristics of forward model weights by fitting the TRFs at different individual time-lags between the EEG response and the speech envelopes, using a sliding time-lag window of 45 with 30 ms overlap in a time-lag range from 115 to 620 ms. Finally, the estimate of forward model weights allowed us to directly transfer the data into source space avoiding further transformations (Haufe et al., 2014).

4.2.10 Chance-level Estimation by Permutation Testing (Control)

To assess the ability of TRF models to predict neural responses (i.e., neural tracking) and verify that neural tracking was well above chance, we computed null-distributed TRF model (Combrisson & Jerbi, 2015). We used a permutation-based approach with *mTRFpermute* function incorporated in mTRF-toolbox (Crosse et al., 2016, 2021). Specifically, this approach cross-validates models, iteratively (1000 iterations) fitting TRFs on randomly mismatched pairings of speech envelopes/EEG responses and evaluating the models on matched data. This procedure was done separately for each trial, participant, and condition, and then grand averaged to get the average "null" TRF model, which served as a baseline (control).

4.2.11 Source Estimation

Forward modeling allowed us to investigate the TRFs and better understand how the information about the envelope of continuous stimuli is encoded in the brain. Specifically, we tested how low-level

(SNR) acoustic and high-level linguistic (Semantic) effects are distributed at sensor and source levels. Furthermore, we investigated whether and how the visual cortex is activated for neural tracking of the speech envelope in blindfolded individuals when competing retinal input is absent.

We performed source localization in Brainstorm software (Tadel et al., 2011) together with custom MATLAB scripts and the pipeline for EEG source estimation introduced by Stropahl and colleagues (2018; see also Bottari, Bednaya, Dormal, Villwock, Dzhelyova, Grin, Pietrini, Ricciardi, Rossion, & Roder, 2020) that we adapted to the TRF data. Specifically, source localization was performed using dynamical Statistical Parametric Mapping (dSPM, Dale et al., 2000). A Boundary Element Model (BEM) was computed for each participant using default parameters to calculate the forward solution and constrain source locations to the cortical surface. We used a standard electrode layout together with a standard anatomy template (ICBM152) for all participants. The model resulted in a single dipole oriented perpendicularly to the cortical surface for each vertex since dipole orientations were constrained to the cortical surface. We did not perform individual noise modeling since TRF has no clear nor true baseline period. Instead, we used an identity matrix as a noise covariance matrix, with the assumption of equal unit variance of noise on every sensor.

We created visual regions of interest (ROIs) based on predefined scouts from the Destrieux atlas (Destrieux et al., 2010) implemented in FreeSurfer (Fischl, 2012) and available in Brainstorm. Visual ROIs were selected for the left and right hemispheres and included primary (V1; Calcarine sulcus) and secondary (V2, Lingual gyrus) visual cortex, defined as the '*S_calcarine*' and the '*G_oc-tem_med-Lingual*' scouts in the atlas, correspondingly. These visual ROIs were selected based on recently reported evidence of their involvement in speech processing not only in blind but also sighted individuals, albeit to a lower extent (Martinelli et al., 2020; Petro, Paton, & Muckli, 2017; Seydell-Greenwald, Wang, Newport, Bi, & Striem-Amit, 2021; Van Ackeren, Barbero, Mattioni, Bottini, & Collignon, 2018; Vetter et al., 2020; Vetter, Smith, & Muckli, 2014). Upon the ROIs creation, their time-series were extracted and submitted to the analysis.

4.2.12 Statistical Analysis

Participants' behavioral responses concerning comprehension of the story were computed as the average correct responses (in %) across all three parts of the story, resulting in nine scores per participant for each condition. Intelligibility rates from each participant were computed similarly, by averaging across all three parts of the story. Statistical analysis of behavioral responses to assess low-level acoustic (SNR) effect was conducted using one-way repeated measure ANOVA. Post-hoc comparisons were made with two-tailed paired t-tests. Statistical analysis of behavioral responses to assess high-level linguistic (semantic) effect was performed using two-tailed paired t-tests.

As a sanity check, we first performed comparisons between the TRFs of each condition with the null TRF through paired t-tests with the significance threshold set at $p < 0.05$ (one-tailed) and corrected for multiple comparisons with the false-discovery rate (FDR) at 0.05 (Benjamini & Hochberg, 1995) at two electrodes selected a priori on the midline frontocentral (Fz) and the occipital (Oz) scalp locations, over a range of post-stimulus time-lags between 0 and 600 ms

To access differences in spatiotemporal profile of averaged TRFs between conditions, we performed non-parametric cluster-based permutation tests (Maris & Oostenveld, 2007) in FieldTrip toolbox (Oostenveld, Fries, Maris, & Schoffelen, 2011b). A cluster was defined along *electrodes x time-lags* dimensions, with extension criteria set to at least two neighboring electrodes. The t-statistic for adjusted *electrode x time-lag* pairs exceeding a preset critical threshold of 5% (cluster alpha = 0.05) was summed, and the adjusted pairs formed the clusters. Then, two-tailed tests were performed at the whole brain level (across all electrodes and time-lags from 0 to 600 ms), using the Monte-Carlo method with 1000 permutations. The maximum of the summed t-statistic in the observed data was compared with a random partition formed by permuting the experimental condition labels, resulting in a critical p-value for each cluster. In case the cluster-based p-value was less than 0.025 (corresponding to a critical alpha level of 0.05 for two-tailed testing, accounting for both positive and negative clusters), we rejected our null hypothesis that there were no differences between TRFs for two conditions.

Finally, cluster-based statistics on sources at the whole-brain level was performed in Brainstorm, across all electrodes and time-lags from 0 to 600 ms, using Monte-Carlo method with 1000 permutations, alpha = 0.05, two-tailed (meaning, alpha = 0.025 per each tail), cluster alpha = 0.05, and neighboring criteria for electrodes set for 2. Analysis of visual ROIs time-series between conditions was performed using paired t-tests, with the significance threshold set at $p < 0.05$ (one-tailed) and correcting for multiple comparisons with the FDR-method at 0.05.

4.3 Results

4.3.1 Behavioral responses

To ensure that the participants successfully understood the content of the target stories, they were asked to answer three Yes/No questions at the end of each segment (after ~ 5 min). Moreover, participants were asked to self-rate the intelligibility of each part of the target story from 1 (absolutely non-intelligible) to 7 (very intelligible).

4.3.1.1 Low-level acoustic (SNR) effect

As expected, both comprehension scores and intelligibility rates gradually decreased with SNR (see Figure 4.1C). Comprehension scores, converted to percentage of correct responses, decreased as a function of noise (*Speech-in-Quiet* mean \pm SE: $82.22 \pm 3.72\%$; *Speech-in-Noise at SNR1* mean \pm SE: $61.48 \pm 4.58\%$; *Speech-in-Noise at SNR2* mean \pm SE: $53.33 \pm 4.09\%$). A repeated measures ANOVA with a correction confirmed that listening condition significantly affected participants' comprehension ($F(2, 28) = 16.14$, $p = 0.00002$, Huynh-Feldt-corrected). Post-hoc comparisons showed that correct responses for *Speech-in-Quiet* were significantly higher than for *Speech-in-Noise at SNR1* ($t(14) = 4.40$, $p = 0.0006$) and *Speech-in-Noise at SNR2* ($t(14) = 5.46$, $p = 0.0001$), but no significant difference emerged between *Speech-in-Noise at SNR1* and *Speech-in-Noise at SNR2* ($t(14) = 1.43$, $p = 0.17$).

Intelligibility rates were in line with comprehension scores, dramatically dropping from *Speech-in-Quiet* (rated 7 by all participants, and thus reaching a ceiling which prevented comparisons with other conditions; see Liu & Wang, 2021; Šimkovic & Träuble, 2019) to *Speech-in-Noise at SNR1* (mean \pm SE: 3.53 ± 0.22) and further significantly

dropping at *Speech-in-Noise at SNR2* (mean \pm SE: 2.40 ± 0.19 ; *Speech-in-Noise at SNR1* vs. *Speech-in-Noise at SNR2*: $t(14) = 5.90$, $p < 0.0001$).

4.3.1.2 High-level linguistic (Semantic) effect

We found no difference in correct responses and intelligibility rates between *Speech-in-Noise at SNR1* and *Jabberwocky-in-Noise at SNR1* (all p -values > 0.05 ; correct responses, mean \pm SE: *Speech-in-Noise at SNR1*: $61.48 \pm 4.58\%$; *Jabberwocky-in-Noise at SNR1*: $62.22 \pm 3.03\%$; intelligibility rates, mean \pm SE: *Speech-in-Noise at SNR1*: 3.53 ± 0.22 ; *Jabberwocky-in-Noise at SNR1*: 3.84 ± 0.32). Results indicated that participants were able to equally attend target stories embedded in noise (SNR1), regardless of semantic information.

4.3.2 Neural tracking

4.3.2.1 Low-level acoustic (SNR) effect at the sensor level

First, we examined the temporal profile of SNR effect at preselected representative electrodes: frontal (Fz) and occipital (Oz; see Figure 4.2A). The TRFs for *Speech-in-Quiet* and *Speech-in-Noise at SNR2* significantly different from the null TRF ($p < 0.05$, one-tailed, FDR-corrected), suggesting that TRFs indeed reflected neural tracking of the speech envelope (Supplementary Figure C.1).

To access the effect of SNR on neural tracking of the speech envelope, we compared the TRFs of *Speech-in-Quiet* and *Speech-in-Noise at SNR2* (the most challenging) conditions (see Figure 4.2). The Cluster-based permutation test revealed significant differences between the TRFs for the two conditions ($p < 0.025$; cluster-corrected). A positive ($p = 0.002$, corrected) and a negative ($p = 0.002$, corrected) clusters were identified at time-lags interval 150-250 ms. Other pair of positive ($p = 0.001$, corrected) and negative clusters ($p = 0.002$, corrected) were also found at time-lags interval 290-410 ms (see Figure 4.2C). Both effects extended over fronto-central and over parieto-occipital electrodes. Results showed that TRF to *Speech-in-Noise at SNR2* was delayed and increased in magnitude compared to *Speech-in-Quiet* condition (see Figure 4.2A, B, C).

4.3.2.2 Low-level acoustic (SNR) effect at the source level

The cluster-based permutation test, performed at the whole brain level, contrasting TRFs for *Speech-in-Quiet* vs. *Speech-in-Noise at SNR2*,

revealed that SNR effect was localized at in both hemispheres (see Figure 4.2D): a significant cluster was found in the left hemisphere ($p = 0.008$, corrected), lasting from ~ 0 to ~ 484 ms, and another one in the right hemisphere ($p = 0.028$, corrected), lasting from ~ 141 to ~ 312 ms (see Supplementary Figure C.2). The effect was observed mostly over bilateral temporal cortex and also included parts of the bilateral parietal cortex, insular cortex, visual cortex, and left prefrontal cortex.

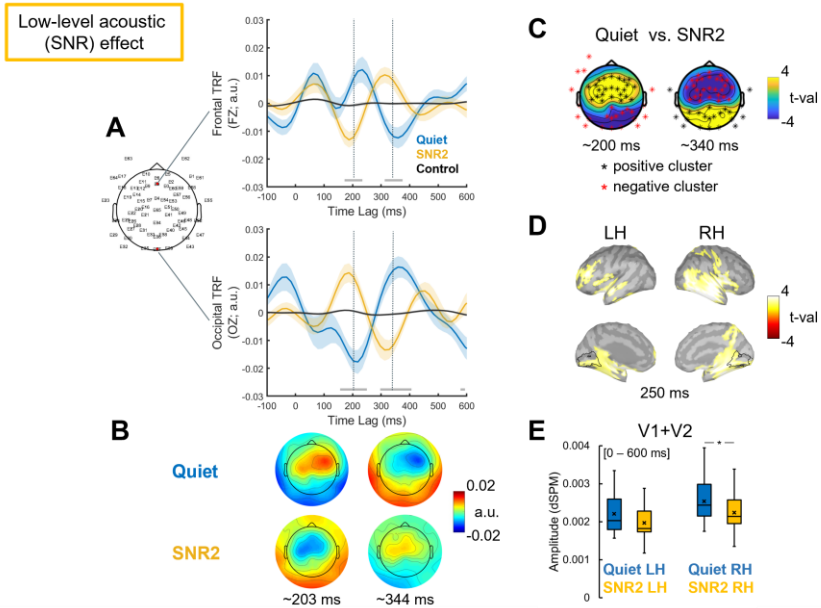


Figure 4.2: Low-level acoustic (SNR) effect. (A) Grand averaged temporal response functions (TRFs) for *Speech-in-Quiet* (Quiet, blue), *Speech-in-Noise at SNR2* (SNR2, yellow), and null TRF (Control, black). TRFs displayed over time-lags at frontal Fz and occipital Oz electrodes, marked with red on the electrode layout. Shaded areas represent the standard error of the mean (SE) across participants. Grey horizontal bars above the x-axis indicate time-lags at which TRFs for *Speech-in-Quiet* and *Speech-in-Noise at SNR2* differed significantly at these representative electrodes (series of paired two-tailed t-tests, $p < 0.05$, FDR-corrected). Grey dotted vertical lines indicate time-lags with the maximal difference between TRFs for *Speech-in-Quiet* and *Speech-in-Noise at SNR2*. (B) Topographic representations of TRFs, displayed at time-lags marked by grey dotted vertical lines on A. (C) The results of the cluster-based permutation test contrasting TRFs for *Speech-in-Quiet* vs. *Speech-in-Noise at SNR2*, displayed

around time-lags marked by grey dotted vertical lines on **A**. Significant ($p < 0.05$, corrected for two tails, $p < 0.025$ for each tail) positive and negative clusters comprised the electrodes marked in black and in red asterisks, respectively. **(D)** Differences at the source level, contrasting TRFs for *Speech-in-Quiet* vs. *Speech-in-Noise at SNR2* at the whole-brain level ($p < 0.05$, corrected for two tails). Lateral and medial views of the left (LH) and right (RH) hemispheres, displayed at the time-lag corresponding to the peak in the temporal profile (i.e., 250 ms). Bright yellow (positive t-values) indicates greater activation for Quiet over SNR2. Black contours indicate the ROIs borders (V1 and V2) in both hemispheres based on the Destrieux cortical atlas. **(E)** Activations obtained at the source space, in visual ROIs. Boxplots display source activation for each condition. The activation is *averaged* over the ROIs (V1 + V2) and across the 0 to 600 ms time window, in the left (LH) and right (RH) hemispheres, respectively. The line through the boxplot indicates median, × marker indicates the mean, lines indicate pairwise statistical comparisons (* $p < 0.05$, one-tailed).

4.3.2.3 Visual cortex ROIs

To test whether and how the visual cortex is taking part in neural tracking of speech and speech comprehension in blindfolded individuals, we performed source analysis on TRFs, using predefined ROIs in the visual cortex comprising V1 and V2.

The contrast *Speech-in-Quiet* vs. *Speech-in-Noise at SNR2* survived cluster-correction for multiple-comparisons in the left ($p = 0.008$, corrected) and right hemispheres ($p = 0.028$, corrected; Supplementary Figure C.3). Extracted time-series from V1 and V2 showed a similar pattern, with the magnitude of source activation for TRF in *Speech-in-Quiet* being larger than for TRF in *Speech-in-Noise at SNR2* at multiple time points (see Supplementary Figure C.3 reporting uncorrected results). Averaged activation across time points in combined ROIs (V1 + V2) was significantly larger for TRF in *Speech-in-Quiet* than for TRF in *Speech-in-Noise at SNR2* in the right hemisphere ($p = 0.04$, one-tailed), but not in the left hemisphere ($p = 0.08$, one-tailed) (see Figure 4.2E). These results suggest the dampening of visual cortex activity in case of challenging auditory inputs.

4.3.2.4 Higher-level linguistic (Semantic) effect at the sensor level

At the two electrodes of interest (The TRFs for *Speech-in-Noise at SNR1* and *Jabberwocky-in-Noise at SNR1* significantly differed from the

null TRF ($p < 0.05$, one-tailed, FDR-corrected), suggesting that estimated TRFs indeed reflected neural tracking of the speech envelope (Supplementary Figure C.1).

To access the effect of semantic information on neural tracking, we compared the TRFs of *Speech-in-Noise at SNR1* and *Jabberwocky-in-Noise at SNR1* conditions (see Figure 4.3). Cluster-based permutation test on TRFs revealed statistically significant differences between two conditions ($p < 0.025$; corrected). Three pairs of positive and negative clusters were identified at time-lags intervals of 70 – 165 ms (positive: $p = 0.001$, corrected; negative: $p = 0.01$, corrected), 200 – 290 ms (positive: $p = 0.001$, corrected; negative: $p = 0.001$, corrected), and 310 – 430 ms (positive: $p = 0.003$, corrected; negative: $p = 0.01$, corrected), comprising fronto-central electrodes and parieto-occipital electrodes (see Figure 4.3C). Results revealed that the TRFs of *Speech-in-Noise at SNR1* was higher and delayed compared to the TRF of *Jabberwocky-in-Noise at SNR1* (see Figure 4.3A, B and C).

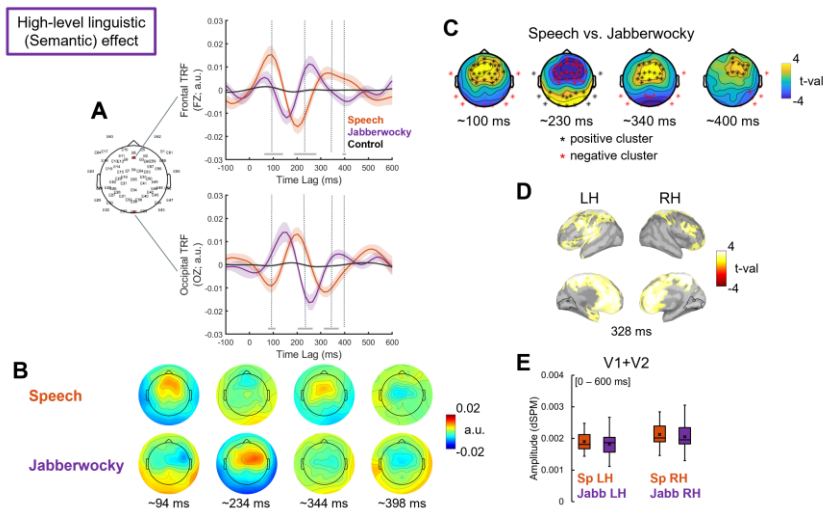


Figure 4.3: High-level (Semantic) effect. (A) Grand averaged temporal response functions (TRFs) for *Speech-in-Noise at SNR1* (Speech, red), for *Jabberwocky-in-Noise at SNR1* (Jabberwocky, purple), and null TRF (Control, black). TRFs displayed over time-lags at frontal Fz and occipital Oz electrodes, marked with red on the electrode layout. Shaded areas represent the standard error of the mean (SE) across participants. Grey horizontal bars above the x-axis indicate

time-lags at which TRFs for *Speech-in-Noise at SNR1* and *Jabberwocky-in-Noise at SNR1* differed significantly (running paired two-tailed t-tests, $p < 0.05$, FDR-corrected). Grey dotted vertical lines indicate time-lags with the maximal difference between TRFs for *Speech-in-Noise at SNR1* and *Jabberwocky-in-Noise at SNR1*. **(B)** Topographic representations of TRFs, displayed at time-lags marked by grey dotted vertical lines on **A**. **(C)** The results of the cluster-based permutation test contrasting TRFs for *Speech-in-Noise at SNR1* and *Jabberwocky-in-Noise at SNR1*, displayed around time-lags marked by grey dotted vertical lines on **A**. Significant ($p < 0.05$, cluster-corrected for two tails, $p < 0.025$ each tail) positive and negative clusters comprised the electrodes marked in black and in red asterisks, respectively. **(D)** Differences at the source level, contrasting TRFs for *Speech-in-Noise at SNR1* and *Jabberwocky-in-Noise at SNR1* at the whole brain level ($p < 0.05$, cluster-corrected for two tails). Lateral and medial views of the left (LH) and right (RH) hemispheres, displayed at the time-lag corresponding to the peaks in the temporal profile. Bright yellow (positive t-values) indicates greater activation for Speech over Jabberwocky. Black contours indicate the ROIs borders (union of V1 and V2) in both hemispheres based on the Destrieux cortical atlas. **(E)** Activations obtained at the source space, in visual ROIs. Boxplots display source activation for each condition. The activation is *averaged* over the ROIs (V1 + V2) and across the 0 to 600 ms time window, in the left (LH) and right (RH) hemispheres, respectively. The line through the boxplot indicates median, × marker indicates the mean.

4.3.2.5 Higher-level linguistic (Semantic) effect at the source level

Cluster-based permutation test, contrasting TRFs for *Speech-in-Noise at SNR1* and *Jabberwocky-in-Noise at SNR1* at the whole-brain level, revealed two clusters in both hemispheres: one in the left hemisphere ($p = 0.002$, corrected), extending over all time points, and one in the right hemisphere ($p = 0.006$, corrected), lasting from ~ 0 to ~ 531 ms (see Supplementary Figure C.2), with maximum activation ~ 330 ms (see Figure 4.3D). The effect extended primarily over the left auditory cortex and a large portion of bilateral fronto-parietal network at earlier time points and extended to the anterior temporal lobe (ATL) at later time points (see Supplementary Figure C.2).

4.3.2.6 Visual cortex ROIs

In the visual ROI the semantic effect did not survive cluster-correction for multiple-comparisons ($p > 0.05$, corrected for two tails) and extracted time-series from ROIs did not differ between source TRFs

for *Speech-in-Noise at SNR1* and *Jabberwocky-in-Noise at SNR1* ($p > 0.05$) (see Supplementary Figure C.3 and Figure 4.2E).

4.4 Discussion

We used a hierarchical model to investigate entrainment to continuous speech envelope in blindfolded individuals, assessing (1) the effects of low-level acoustic and high-level linguistic information on neural tracking and (2) testing how these effects are distributed at the source level, with the focus on the visual cortex. To address the role of low-level acoustic, we compared the entrainment to target stories presented in quiet or multi-talker babble noise. Results revealed that TRF was delayed and higher in magnitude at latencies between 100 and 300 ms when SNR decreases. This finding suggests that neural tracking requires greater resources in case of concurrent masking noise. Next, we also addressed the role of high (semantic) level of speech processing on neural entrainment by comparing TRFs to meaningful and meaningless stories. Results indicated delayed and higher TRFs when semantic information is present. Source modeling suggested that entrainment to continuous speech in noise engaged spread activation networks beyond the auditory cortex, including linguistic and attentional networks. Finally, in the absence of retinal input, we found evidence that the visual cortex entrained to the speech envelope. However, the magnitude of such entrainment was degraded with concurrent background noise, suggesting a suppressing mechanism helping to focus auditory attention in challenging listening conditions.

4.4.1 Effects of low-level acoustic (SNR) processing on neural tracking of speech envelope

We demonstrated that speech envelope tracking in noise, compared to quiet, was characterized by larger amplitude and delayed latency of the TRF responses and by the reversed polarity of the TRFs topography distributions over fronto-central parieto-occipital electrodes (see Figure 4.2A, B).

The TRF time-courses were consistent with previous studies reporting amplitudes and latencies being affected by concurrent noise (Brodbeck, Jiao, Hong, & Simon, 2020; Ding & Simon, 2013; Fiedler,

Wöstmann, Herbst, & Obleser, 2019; Gustafson, Billings, Hornsby, & Key, 2019; Zendel, West, Belleville, & Peretz, 2019) as well as enhanced N1 and N2 amplitudes in noise compared to quiet (Papesh, Billings, & Baltzell, 2015).

Increased frontal negativity around 100 ms (N1) is associated with attention-dependent processes in response to auditory changes (Hansen & Hillyard, 1980; Näätänen, 1982). The enhanced envelope tracking observed here for the N1-like response to speech in noise compared to quiet may reflect the use of more resources for the encoding of acoustic variations at earlier stages of speech processing when intelligibility gets degraded by noise (Alain, Quan, McDonald, & Van Roon, 2009; Näätänen & Picton, 1987; Parbery-Clark, Marmel, Bair, & Kraus, 2011).

Additional differences were observed around the second negative peak, corresponding to the N2 component. For speech in noise, the TRF peak around this component was smaller and delayed than for speech in quiet. Delayed N2 response is associated with attentive speech processing in challenging acoustic conditions (Balkenhol, Wallhäusser-Franke, Rotter, & Servais, 2020; Billings, Tremblay, Stecker, & Tolin, 2009; Finke, Büchner, Ruigendijk, Meyer, & Sandmann, 2016). Again, differences in this time-range (between 100 and 300 ms after stimulus onset) possibly reflect changes in the degree of attention required to encode incoming stimuli effectively. Particularly, delayed TRF peak response may reflect participants' effort in keeping track of meaningful information over time in the degraded signal. Compensatory mechanisms may be involved in segregating speech from noise. Previous evidence reported stronger envelope tracking of attended speech with increased background noise in hearing-impaired and elderly individuals compared to hearing younger adults (Brodbeck, Presacco, Anderson, & Simon, 2018; Decruy, Vanthornhout, & Francart, 2020; Presacco, Simon, & Anderson, 2016). Both internal (hearing loss) and external (background noise) factors can produce acoustic distortion, which can result in increased listening effort (Van Engen & Peelle, 2014) and enhanced envelope tracking.

There is a debate whether envelope tracking is enhanced (Ding et al., 2014; Ding & Simon, 2013; Fuglsang, Dau, & Hjortkjær, 2017; Presacco et al., 2016) or reduced (Desai et al., 2021; Ding & Simon, 2013; Kurthen et al., 2021; Vanthornhout, Decruy, Wouters, Simon, & Francart, 2018; L.

Wang, Wu, & Chen, 2020) with decreasing SNR. Our behavioral results showed that comprehension scores and intelligibility rates were directly proportional to SNR levels. Our results on TRFs also add to the findings that envelope tracking increases with noise and when listening becomes more challenging.

4.4.2 Effects of high-level linguistic (Semantic) processing on neural tracking of speech envelope

Topographical distributions of the TRFs suggest the involvement of distinct neural generators when semantic content is present or absent (see Figure 4.3B). Moreover, the temporal dynamics of TRFs for meaningful story was characterized by a more prominent P1 peak and generally delayed P1-N1-P2-N2 complex, as compared to meaningless story (see Figure 4.3A).

At a relatively early processing stage (~ 100 ms), we observed stronger neural tracking of the speech envelope for meaningful story than for meaningless story over fronto-central electrodes (see Figure 4.3A, B). This finding could seem surprising since auditory P1 is often associated with pre-attentive processes such as onset detection and sensory gating (Huotilainen et al., 1998; S. E. Miller, Graham, & Schafer, 2021; Thoma et al., 2003; Waldo et al., 1992). Predictive models of speech processing provide a plausible explanation for this result. Semantic content generates expectations about upcoming stimuli and limits the degree of uncertainty about what was heard (Poeppel, Idsardi, & van Wassenhove, 2008), affecting early auditory encoding (Broderick et al., 2019) and neural tracking of the speech envelope (Di Liberto et al., 2018; Kaufeld et al., 2020). Meaningful information may provide regularities in meaningful story, making it more predictable than meaningless story.

Moreover, it is possible that envelope tracking of meaningless story may not be affected by the background noise as much as meaningful story due to the difference in the degree of informational masking. It is possible that meaningless, jabberwocky story could "pop-out" from the background multi-talker babble noise due to lower informational masking compared to meaningful story. Under the linguistic similarity hypothesis (Van Engen & Bradlow, 2007), informational masking is more efficient when background babble noise has more linguistic similarity with the target speech stream (e.g., same spoken language, known accent) compared to a different or unknown language, accent and

semantically anomalous speech (Brouwer, Van Engen, Calandruccio, & Bradlow, 2012; Brungart, 2001; Calandruccio, Van Engen, Dhar, & Bradlow, 2010; Cooke, Garcia Lecumberri, & Barker, 2008; Garcia Lecumberri & Cooke, 2006; Van Engen, 2010; Van Engen & Bradlow, 2007). Therefore, it could have been easier for participants to segregate from the background noise meaningless story than meaningful story.

4.4.3 Two distributed networks are engaged in envelope tracking of continuous speech

Source analysis of TRFs highlighted temporal and fronto-parietal regions traditionally involved in speech and language comprehension (Hertrich, Dietrich, & Ackermann, 2020). Key regions for low-level acoustic effect tested here involved the bilateral temporal cortex, parts of the parietal, insular, and visual cortices bilaterally, and the left prefrontal cortex (see Figure 4.2D). Naturalistic speech stimuli are complex and resemble everyday listening conditions, thus leading to extended activations and involvement of higher-order cortical regions (Alexandrou et al., 2020; Hamilton & Huth, 2020). For example, narrative speech involves widely distributed bilateral neural activity that tracks hierarchically organized speech representations at multiple cortical sites and temporal windows (de Heer, Huth, Griffiths, Gallant, & Theunissen, 2017; Di Liberto et al., 2015; Huth, de Heer, Griffiths, Theunissen, & Gallant, 2016; Lerner, Honey, Silbert, & Hasson, 2011; Poeppel, 2003; Puschmann, Regev, Baillet, & Zatorre, 2021). Neuroimaging studies reported distributed cortical activations beyond the auditory cortex (comprising higher-order associative brain structures and attentional networks) during effortful listening (see Alain, Du, Bernstein, Barten, & Banai, 2018 for a meta-analysis).

Higher-level linguistic processing was assessed by contrasting meaningful and meaningless stories (Speech vs. Jabberwocky) and resulted in higher activation for meaningful story, mainly involving the left auditory cortex, a large portion of bilateral fronto-parietal network, and the left anterior temporal lobe later in time (see Figure 4.3D). Overall source modeling results of TRFs indicate that low-level acoustic effects mainly involved a bilateral temporo-parietal network, while higher-level (semantic) effects primarily affected a left dominant fronto-temporal network. These results support the notion that successful speech comprehension requires multiple extended networks beyond the

temporal lobe to process the acoustic signal at multiple and parallel hierarchical levels (Davis & Johnsrude, 2003, 2007; de Heer et al., 2017; Hickok & Poeppel, 2007; Peelle, 2012; Peelle, Johnsrude, & Davis, 2010)

4.4.4 Early visual cortex's entrainment to speech envelope in blindfolded individuals is reduced by background noise

We performed source analysis on the TRFs from preselected visual ROIs (V1 and V2) to assess whether the visual cortex contributes to neural envelope tracking in blindfolded individuals. While source estimates of EEG activity should be taken with caution, results suggested early visual cortex's involvement in envelope tracking, especially for low-level acoustic speech processing (Figure 4.3D, E).

A recent fMRI study showed that the visual cortex of blindfolded individuals displayed some degree of synchrony to audio tracks from movies and narratives, suggesting that auditory information can reach the visual cortices (Loiotile, Cusack, & Bedny, 2019). Overall, numerous fMRI findings supported the notion that the visual cortex is functionally engaged in processing non-visual stimuli in sighted individuals (Facchini & Aglioti, 2003; Merabet et al., 2008; Poirier et al., 2006; Qin & Yu, 2013; Ricciardi et al., 2011; Sathian, 2005; Seydell-Greenwald et al., 2021; Vetter et al., 2014; Zangaladze, Epstein, Grafton, & Sathian, 1999).

Interestingly, we observed a decrease in total signal magnitude for speech in noise compared to speech in quiet. This difference emerged in particular for the right visual cortex (although a trend also existed in the left hemisphere; see Figure 4.2E). Hemispheric asymmetry is not surprising, as previous evidence already showed the right hemisphere dominance for several aspects of natural speech processing, especially for tracking of slow temporal modulations within the delta-theta range (Alexandrou, Saarinen, Mäkelä, Kujala, & Salmelin, 2017; Poeppel, 2003). More importantly, this finding aligns with the evidence that the early visual cortex is sensitive to acoustic SNR effects (Bishop & Miller, 2009).

These results seem to suggest that the activity of the visual cortex could be modulated during continuous speech tracking. However, its activity gets suppressed in case the attentional network becomes more engaged in tracking relevant auditory information in challenging listening environment. Human neuroimaging studies reported crossmodal deactivation of the visual cortex by auditory stimuli during

active listening or passive stimulation (with the instructions to concentrate on the stimuli) and suggested that such suppression can be top-down modulated by attention as task demands increase (e.g., Hairston et al., 2008; Johnson & Zatorre, 2006; Laurienti et al., 2002). Several other studies found suppression effects of sound on visual perception. Such crossmodal suppression has been suggested to reduce the magnitude of the percept of a weaker or less relevant modality input considered as a perceptual noise (Hidaka & Ide, 2015).

Overall, our results align with recent evidence reporting that the visual cortex can contribute to auditory information processing in sighted individuals (Brang et al., 2022; Martinelli et al., 2020; Seydell-Greenwald et al., 2021; Vetter et al., 2014). Here, we observed that the visual cortex is more engaged in processing when speech signal is intelligible and clear (i.e., presented in quiet). Differences in mapping the speech envelope in the visual cortex for low-level acoustic representations exist and might reflect crossmodal visual cortex suppression. Such suppression could be top-down modulated and attributed to auditory attention (Cate et al., 2009), which plays an essential role in segregating relevant speech information in challenging listening conditions and congruent visual input is not available.

It could be argued that mental imagery mechanisms may drive the visual cortex's response to speech. Previous studies observed an overlap in neural representations in the occipital areas between perception and visual imagery, stemming from common top-down influences (see Dijkstra, Bosch, & Gerven, 2019 for a review). However, V1 has been shown to encode auditory information regardless of imageability (Martinelli et al., 2020; Seydell-Greenwald et al., 2021; Vetter et al., 2020, 2014). Thus, the role of the early visual cortex in auditory processing may not be merely ascribed to an imagery effect. If that was the case, when contrasting *Speech-in-Noise* and *Jabberwocky-in-Noise*, we could have observed higher visual cortex's responses in meaningful condition compared to meaningless one, since only the former contained visually imaginable information. However, no significant difference in the visual cortex's entrainment to the speech envelope was found between these conditions.

4.4.5 Limitations and future research perspectives

It is important to acknowledge the challenges of EEG based source modeling, as spatial resolution of EEG is generally known to be relatively poor, making it difficult to identify exact brain sources that generate the neuronal activity measured on the scalp. EEG based source modeling majorly suffers from an ill-posed inverse problem and can also result in misleading activity patterns due to, for instance, low SNR, unrealistic head models, invalid constraints, and so on. More accurate EEG source localization requires digitized electrode positions and individual anatomical scans of participants, which can diminish source estimation uncertainty (Shirazi and Huang, 2019; Michel and Brunet, 2019; Zorzos et al., 2021) but were not available in our study. Therefore, EEG source estimates should be interpreted with caution. However, it is worth noting that we used a validated pipeline for source modeling estimation (Stropahl et al., 2018; Bottari et al., 2020). Moreover, the same source modeling was performed across different conditions; thus, similar errors should be attributed to activations for each condition. While the exact location of the activity cannot be ensured with the present data, our results suggested that the activity of posterior cortices was modulated only by low-level and not high-level speech processing.

A further limitation pertains the input data we used for the encoding. We modeled neural tracking of the speech signal based on a single feature: the speech envelope comprising specific bandwidth frequencies (2-8 Hz). The envelope represents slow-variate temporal modulations of the speech signal. It contains multiple acoustic and linguistic cues important for continuous speech segmentation into smaller units, and therefore it has been hypothesized to be crucial for speech comprehension (Luo & Poeppel, 2007; Shannon, Zeng, Kamath, Wygonski, & Ekelid, 1995; Zoefel, 2018). However, it has also been argued that focusing on the envelope alone might not get the complete picture of the neural mechanism underlying speech comprehension (Oleser, Herrmann, & Henry, 2012). Recent studies reported that the inclusion of multiple speech features, such as spectrogram, phonemes, and phonetic features in the model sometimes result in a better model performance represented by a more robust neural tracking response (e.g., Brodbeck, Hong, et al., 2018; Di Liberto et al., 2015, 2018; Lesenfants, Vanthornhout, Verschueren, Decruy, & Francart, 2019). Future research may include multiple speech features to build a

multivariate model to assess neural speech tracking in the brain and how the visual cortex maps speech information when visual input is absent.

4.4.6 Conclusion

Overall, our results indicate low-level acoustic and high-level linguistic processes affecting envelope tracking of continuous speech. Envelope tracking may play a role in supporting active listening in challenging conditions and is enhanced when SNR decreases, and when segregation of target speech from the background noise becomes more difficult (i.e., due to linguistic similarity). Tracking speech signal embedded in noise requires spread networks of activation, including linguistic and attentional regions beyond the auditory cortex. In the absence of retinal input, the visual cortex might entrain to the speech envelope, however, the functional role of such activity remains to be ascertained. The magnitude of such entrainment is degraded by concurrent noise, suggesting a suppressing mechanism aimed at focusing resources within the auditory attention network in case of challenging listening conditions. Conversely, no clear impact of semantic content was found in the visual cortex, suggesting that the magnitude of such entrainment is more affected by low-level speech features.

Chapter 5

Conclusion

The findings reported in this dissertation expand the existing knowledge on the functional interplay between visual and auditory systems and on the neurophysiological mechanisms of experience-dependent plasticity in the human brain. Separate EEG studies were performed, considering modality (auditory/visual), hierarchy of the brain functional organization (low-level/high-level), and sensory deprivation (deprived/non-deprived cortices). We tested early sensory-deprived and neurotypical individuals, implementing different experimental paradigms together with various methods of the EEG data analysis. Therefore, several novel research questions were answered.

Theoretical implications. In the first study (Chapter 2), we provide the first-time evidence in humans that the absence of auditory experience selectively alters induced oscillatory activity during low-level visual processing. While the effect of early deafness on induced oscillatory activity in humans had not been previously reported, evidence in this direction emerged in studies employing congenitally deaf cats (Yusuf, Hubka, Tillein, & Kral, 2017). Our findings extend to humans and beyond the auditory cortices (specifically, to visual cortices) the common observation coming from animal models of auditory deprivation (Berger et al., 2017; Kral & Sharma, 2012; Yusuf et al., 2017; see Kral et al., 2019 for a review) that changes in sensory processing may reflect altered feedback processes rather than feedforward processes.

In the second study (Chapter 3), using EEG frequency-tagging approach, we were able to decompose which of the low- and high-level face processes are experience-dependent and whether these distinct face processing functions encounter distinct neural adaptations to altered sensory experience. Our findings suggest that the experience dependence of compensatory changes (both intramodal and crossmodal) may vary with different aspects of the face processing system in congenitally deaf signers. Our study is in agreement with and expands previous fMRI studies reporting divergent neural correlates of face processing in deaf signers compared to hearing non-signers (Benetti et al., 2017; McCullough, Emmorey, & Sereno, 2005).

In sum, Chapters 2 and 3 provide compelling evidence for selective experience-dependent functional changes in congenital and early deaf individuals associated with low-level and high-level visual processing. Furthermore, these chapters add novel insights into the corresponding neural mechanisms that may underlie specific superior visual processing in deafness.

The third study (Chapter 4) investigated to what extent the visual cortex plays a role in neural speech tracking in case of typical development. The results demonstrate both low- and high-level effects on the entrainment to the envelope of continuous speech signal embedded in multi-talker babble noise. Moreover, the results show that such entrainment requires broad networks of activation, including linguistic and attentional regions beyond the auditory cortex. Our findings suggest that entrainment to speech envelope may play a role in supporting active listening in babble noise when SNR degrades and segregation of target speech from the concurrent noise becomes more difficult due to linguistic similarity. Furthermore, Chapter 4 provides important evidence of a functional role of the visual cortex in the entrainment to the envelope of continuous speech and suggests a crossmodal suppression mechanism of the early visual cortex in challenging listening conditions when visual input is absent.

Thus, the research contribution of Chapter 4 is two-fold. First, it provides novel knowledge on the envelope tracking of continuous naturalistic speech without visual input, revealing the effects of low-level acoustic and high-level linguistic processes and how these effects are distributed at the source level. Second, it adds to the evidence coming from fMRI studies that the early visual cortex is actively engaged in speech processing, encoding temporal modulations of incoming sounds (i.e., envelope) in the absence of retinal input (Martinelli et al., 2020; Vetter et al., 2014). Chapter 4 extends these previous findings to continuous naturalistic speech processing and suggests neural mechanisms underlying such crossmodal effects.

Theoretical implications outlined above provide new insights into how the brain functions in general and on the brain's potential to adapt to sensory deprivation. Furthermore, the results reported here have translational implications.

Translational implications. We believe that our results may contribute to the development of effective sensory restoration and rehabilitation strategies for typically and non-typically developing individuals (Collignon, Champoux, Voss, & Lepore, 2011; Heimler, Weisz, & Collignon, 2014; Heimler & Amedi, 2020; Merabet & Pascual-Leone, 2010). Specifically, our results may inform the development of new generation tools for sensory restoration and rehabilitation that include visual-to-auditory sensory substitution devices (SSDs) for the blind, retinal implants for visually impaired individuals, mobile hearing enhancement devices (so-called hearables) for the deaf, as well as assisting listening devices (ALDs) for hearing aid (HA) and cochlear implant (CI) users.

It is also worth acknowledging some principal limitations.

Limitations. In the first study (Chapter 2), while we showed selective experience-dependent modulations of induced frontal theta activity during repeated visual stimuli processing in early deaf individuals (RS-theta effect), we were not able to completely disentangle low-level sensory processing (i.e., stimulus-specific physical properties) and higher-level cognitive processing (i.e., cognitive control of stimuli repetitions) that could both play a role in such effects.

The second study (Chapter 3) demonstrated increased left hemisphere involvement for face processing in congenitally deaf native signers. However, a caveat of this study is that we did not test an additional group of hearing native signers. Therefore, we could not entirely disentangle the effects caused by deafness and those by early sign language exposure.

The main limitation of the third study (Chapter 4) is that we modeled neural tracking of the speech signal using only a single feature, envelope, comprising frequencies in a specific range (2-8 Hz). Recent evidence suggests that the inclusion of multiple speech features carrying both acoustic and linguistic information (spectrogram, phonemes, phonetic features, word onsets) into the model may result in better model performance, thus, in a more robust neural tracking (e.g., Brodbeck, Hong, et al., 2018; Di Liberto et al., 2015; Lesenfants et al., 2019; Di Liberto et al., 2018).

The role of visual imagery also cannot be *completely* ruled out in our study (Chapter 4). It could be argued that visual mental imagery

mechanisms may drive the responses to speech in the visual cortex, since there is an overlap in neural representations in the occipital areas between perception and visual imagery (see Dijkstra et al., 2019 for a review). However, if that were the case, we could have observed a stronger response in V1-V2 for the meaningful condition (Speech-in-Noise) compared to the meaningless one (Jabberwocky-in-Noise), as only the former contained visually imaginable information.

Futures directions. The present dissertation outlines several directions for future research.

First, future works should address the main limitations of the studies described in Chapters 2-4. For example, for Chapter 2, future studies should explore how sensory and cognitive processes affect repetition suppression and its neural correlates in the deaf. For Chapter 3, future studies should include a group of hearing native signers to address the specific impact of facial expressions, used in a sign language at all levels of linguistic structure (Elliott & Jacobs, 2013), on the neural representation of face processing. For Chapter 4, it would be worth building a multivariate model (by including multiple speech features) to assess neural speech tracking in the brain and how the visual cortex maps speech information when visual input is absent.

Second, future research may also look at envelope tracking below 2 Hz or analyze envelope tracking in the delta and theta bands separately. Speech envelope tracking in the theta band has been argued to primarily reflect acoustic properties, capturing events mainly at the scale of syllables, whereas tracking in the delta band has been argued to reflect prosodic information and linguistic representations, capturing events at the scale of phrases and sentences (Ding & Simon, 2014; Ghitza, Giraud, & Poeppel, 2013; Giraud & Poeppel, 2012; Kösem & van Wassenhove, 2017). Furthermore, recent MEG findings suggest that envelope tracking in delta-band, but not in theta-band, could be speech-specific (Molinaro & Lizarazu, 2018). To date, an increasing number of studies have attempted to disambiguate the contributions of delta-band tracking and theta-band tracking to speech processing (e.g., Bröhl & Kayser, 2021; Ding et al., 2014; Etard & Reichenbach, 2019; Keshavarzi, Kegler, Kadir, & Reichenbach, 2020; Mai, Minett, & Wang, 2016; Molinaro & Lizarazu, 2018), however specific functional roles of theta- and delta- entrainment in speech perception and comprehension remain widely debated.

Another direction for further research lies in extending the findings reported in the third study (Chapter 4) to blind individuals. We used the blindfolded (for the short periods) brain of sighted individuals as a model to investigate mechanisms of neural speech tracking without interfering visual input. Testing blind participants using continuous naturalistic speech stimuli would further augment understanding the role of lifelong visual experience in functional specialization of the early visual cortex. That is, why and how the early visual cortex is involved in speech processing in the sighted and blind, and whether there are any shared mechanisms.

Altogether, the dissertation investigates the functional interplay between visual and auditory systems and its degree of experience-dependent plasticity. The data reported here add to the current knowledge on the role of early sensory experience in shaping the human brain and provide new insights into understanding which neurophysiological mechanisms may guide experience-dependent plasticity. The results demonstrate the impact of the permanent lack of early auditory experience, along with a sign language exposure, on shaping (via intra- and crossmodal plasticity) the brain organization at various hierarchical levels of visual processing (Chapters 2 and 3). The results also support the idea that some crossmodal responses in the brain (i.e., responses in the early visual cortex to speech) are nonspecific to sensory loss, emerging even in case of typical development and indicating a functional role of the early visual cortex in continuous naturalistic speech processing (Chapter 4). This work demonstrates the utility of various experimental paradigms and methods of analysis of the EEG data, including time-frequency analysis, frequency-tagging approach, and temporal-response function estimation (or forward modeling) to study low- and high-level interdependencies between visual and auditory systems and experience-dependent plasticity in both sensory-typical and lifelong sensory-deprived populations. Furthermore, we believe that our results may also contribute to the development of new generation sensory restoration tools and rehabilitation strategies for typically and non-typically developing individuals.

Appendix A

Supplementary Material for Chapter 2

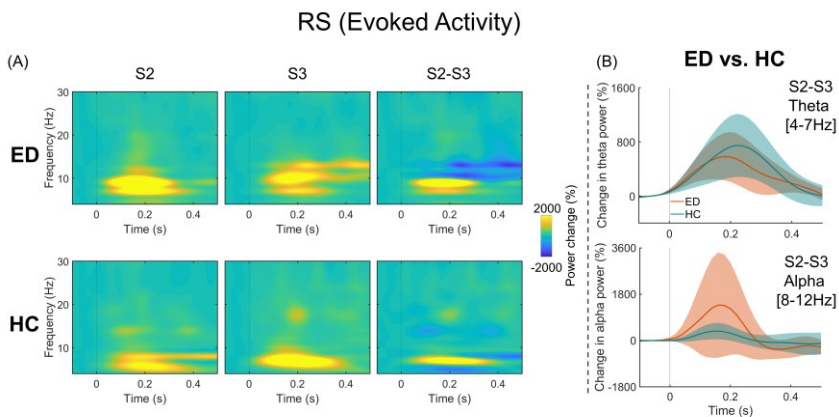


Figure A.1: Repetition Suppression (RS; Evoked Activity) in early deaf individuals and hearing controls. (A) Relative changes of evoked spectral power for each stimulus (S2, S3) and across stimulus repetition (S2-S3) as a function of time and frequency, for the early deaf individuals (ED) and hearing controls (HC); time-frequency plots display data averaged across posterior electrodes (Pz-P7-P3-PO3-O1-P8-P4-PO4-O2). (B) Relative changes of evoked power in the theta [4-7 Hz] and alpha [8-12 Hz] range upon stimulus repetition (S2-S3), displayed for each group and averaged across posterior electrodes (Pz-P7-P3-PO3-O1-P8-P4-PO4-O2); shaded areas represent the standard error of the mean.

ND (Evoked Activity)

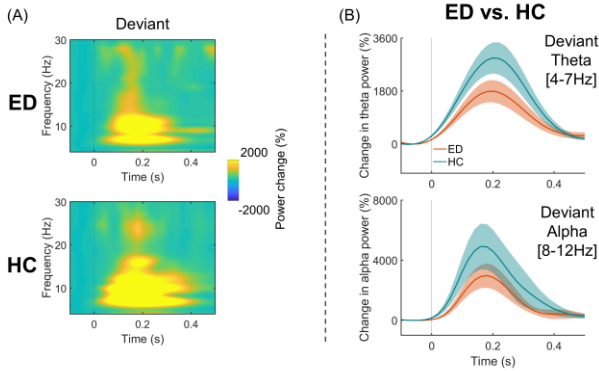


Figure A.2: Novelty Detection (ND; Evoked Activity) in early deaf individuals and hearing controls. (A) Relative changes of evoked spectral power in response to a novel stimulus (Deviant) as a function of time and frequency, in early deaf (ED) and hearing controls (HC); time-frequency plots display data averaged across posterior electrodes (Pz-P7-P3-PO3-O1-P8-P4-PO4-O2). **(B)** Relative changes of evoked power in the theta [4-7 Hz] and alpha [8-12 Hz] range for a novel stimulus (Deviant), displayed for each group and averaged across posterior electrodes (Pz-P7-P3-PO3-O1-P8-P4-PO4-O2); shaded areas represent the standard error of the mean.

Appendix B

Supplementary Material for Chapter 3

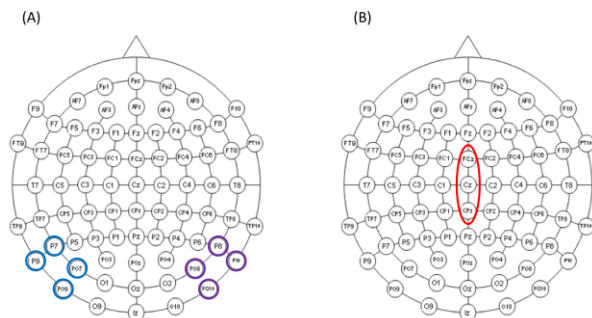


Figure B.1: Electrode cap montage and electrodes of interest. (A) Blue and violet circles highlight the posterior electrodes which were used for statistical analysis for all experiments (P7-8, PO7-8, P9-10, PO9-10). These electrodes captured the highest baseline-corrected amplitudes in each experiment. **(B)** An additional cluster of interest (red ellipse) including midline vertex electrodes used for statistical analysis to assess possible cross-modal responses in each experiment.

Auditory ROIs

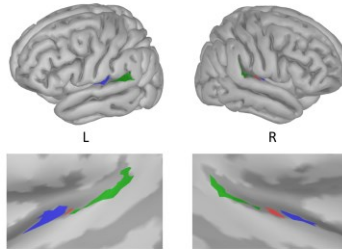


Figure B.2: Auditory ROI. Top: Location of the Auditory ROI in the folded brain. Bottom enlarged view of the Auditory ROI on the unfolded brain. The three-colour coding depict three small regions which were combined to get a close approximation to Brodmann areas 41 and 42 (Destrieux: *G_temp_sup-G_T_transv*, *S_temporal_transverse* and *G_temp_sup-Plan_tempo*).

Harmonic (N)	Frequency (Hz)	Periodic (z-scores)
1	1.2	17.61
2	2.4	44.97
3	3.6	28.34
4	4.8	30.78
6	7.2	25.73
7	8.4	31.42
8	9.6	15.46
9	10.8	11.92
11	13.2	11.51
12	14.4	8.22
13	15.6	5.156
14	16.8	3.77
16	19.2	2.50
17	20.4	2.41

Table B.1: Face-Object Categorization experiment. Consecutively significant harmonics at the oddball frequency 1.2 Hz (averaged across groups and all channels). Only consecutive harmonics with z-scores > 1.64 ($p < 0.05$) are reported.

Harmonic (N)	Frequency (Hz)	Periodic (z-scores)
1	1.2	3.64
2	2.4	12.85
3	3.6	20.51
4	4.8	20.31
6	7.2	21.53
7	8.4	9.54
8	9.6	6.55
9	10.8	3.41
11	13.2	2.98
12	14.4	10.60
13	15.6	4.37
14	16.8	4.27
16	19.2	3.09
17	20.4	3.40
18	21.6	3.63
19	22.8	2.02
21	25.2	2.07
22	26.4	2.88

Table B.2: Emotional Facial Expression Discrimination experiment. Consecutively significant harmonics of the oddball frequency 1.2 Hz (averaged across groups, emotions, condition, and all channels). Only consecutive harmonics with z-scores > 1.64 ($p < 0.05$) are shown here.

Harmonic (N)	Frequency (Hz)	Periodic (z-scores)
1	1.2	6.52
2	2.4	13.51
3	3.6	20.75
4	4.8	16.81
6	7.2	7.44
7	8.4	2.49

Table B.3: Individual Face Discrimination experiment. Consecutively significant harmonics at the oddball frequency 1.2 Hz (averaged across groups, condition, and all channels). Only consecutive harmonics with z-scores > 1.64 ($p < 0.05$) are reported.

B.1 Time-course of EEG data for each experiment

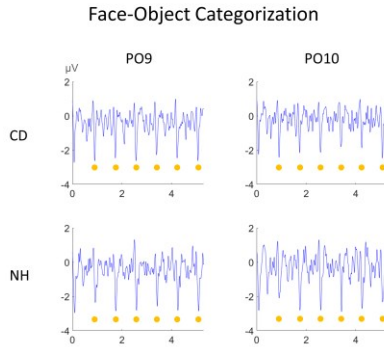


Figure B.3: Time-course of the grand averaged data at the posterior electrodes PO9 and PO10 for the Face-Object categorization experiment. Averages across segments between 0 and 5.6 s are displayed. Each 5.6 s segment included 6 repetitions of the AAAAB sequence. Yellow dots highlight the response to faces.

Emotional Facial Expression Discrimination

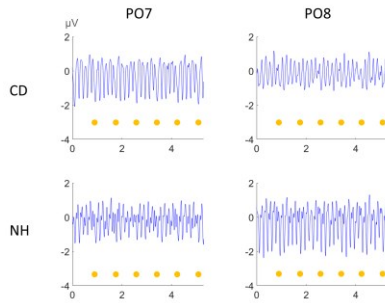


Figure B.4: Time-course of the grand averaged data for the upright condition, at the posterior electrodes PO7 and PO8 for the Emotional Facial Expression Discrimination experiment. Data across emotional facial expressions were collapsed. Averages across segments between 0 and 5.6 s are displayed. Each 5.6 s comprised 6 repetitions of the AAAAB sequence. Yellow dots highlight the response to emotional expressive faces.

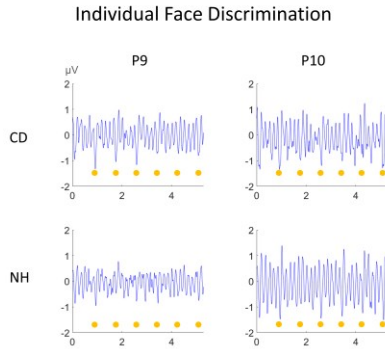


Figure B.5: Time-course of the grand averaged data for the upright condition at the posterior electrodes P9 and P10 for the Individual Face Discrimination experiment. Averages across segments between 0 and 5.6 s are displayed. Each 5.6 s included 6 repetitions of the AAAAB sequence. Yellow dots highlight the response to new face identities.

Statistical analyses in the frequency domain performed using a more conservative threshold of z -scores > 3.29 (corresponding to a $p < 0.001$, two-tailed) for the identification of significant harmonics.

In the FO experiment (experiment 1), 12 consecutive harmonics (i.e., 1.2 Hz to 16.8 Hz) were significant. In the EM experiment (experiment 2) 8 consecutive harmonics (i.e., 1.2 Hz to 10.8 Hz) were significant. The summed oddball response across emotional facial-expressions was calculated by averaging the summed oddball response calculated at the level of single Emotional Facial-Expressions in each group. Finally, for in the ID experiment, the significant summed oddball response was composed by the average first 5 harmonics (i.e., 1.2 Hz to 7.2 Hz).

B.1.1 Face-selective response

An ANOVA with Hemisphere (left and right) as within-participants factors and Group (CD and HC) as between-participants factor revealed a different pattern of lateralization of the response for the CD and HC groups. The interaction between the factors Hemisphere and Group was

significant ($F(1,22) = 4.3$, $p < 0.05$, $\eta_p^2 = 0.16$). Post-hoc pairwise comparisons did not reveal a greater response in the left hemisphere for the CD group as compared to the HC group, nor a greater response in the right hemisphere for the HC group as compared to the CD group (all p -values > 0.6 , corrected). Moreover, post-hoc pairwise comparisons did not reveal a greater response in the left hemisphere vs. the right hemisphere for the CD group, nor a greater response in the right hemisphere as compared to the left hemisphere for the HC group (all p -values > 0.1 , corrected). No between Group differences emerged at the vertex (see Methods section; $p > 0.7$). All results confirm the finding using a less conservative threshold (z -score > 1.64 , corresponding to a $p < 0.05$, one-tailed).

B.1.2 Response to facial expression change

The mixed-design ANOVA with Condition (upright and inverted) and Hemisphere (left and right) as within-participants factors, and Group (CD and HC) did not reveal significant effects neither for Hemisphere and Group interaction nor for the Hemisphere, Condition and Group interaction (all p -values > 0.1). Planned pairwise comparisons revealed that the HC group had a bilateral response for both upright and inverted conditions (left vs. right hemisphere comparison for upright: $F(1,22) = 0.16$, $p > 0.9$, $\eta_p^2 = 0.01$, corrected; inverted: $F(1,22) = 0.16$, $p > 0.6$, $\eta_p^2 = 0.01$, corrected). Conversely, a tendency toward a left hemispheric dominance was found in the CD group selectively for the upright conditions (left vs. right hemisphere comparison for upright: $F(1,22) = 4.2$, $p = 0.05$, $\eta_p^2 = 0.16$, corrected; inverted: $F(1,22) = 0.17$, $p > 0.6$, $\eta_p^2 = 0.01$, corrected). Finally, no significant interaction between the factors Condition and Group emerged at the vertex (all p -values > 0.7). All results confirm the finding using a less conservative threshold (z -score > 1.64 , corresponding to a $p < 0.05$, one-tailed).

B.1.3 Identity discrimination response

The mixed ANOVA with Condition (upright and inverted), Hemisphere (left and right) as within-participants factors, and Group (CD and HC) as between-participants factor did not reveal significant pre-selected interactions involving the factors Hemisphere and Group (all, $ps > 0.5$). Planned pairwise comparisons revealed that for both the HC group (HC left vs. right hemisphere, upright: $F(1,22) = 1.4$, $p > 0.2$,

$\eta_p^2 = 0.06$, corrected; inverted: $F(1,22) = 2.7$, $p > 0.1$, $\eta_p^2 = 0.11$; corrected) and the CD group (CD left vs. right hemisphere, upright: $F(1,22) = 0.3$, $p > 0.6$, $\eta_p^2 = 0.01$, corrected, inverted: $F(1,22) = 1.8$, $p > 0.1$, $\eta_p^2 = 0.08$, corrected) the response in the left and right hemispheres did not differ. Conversely, a significant interaction between the factors Condition and Group emerged at the vertex ($F(1,22) = 4.9$, $p < 0.04$, $\eta_p^2 = 0.18$). Post-hoc pairwise comparisons showed that both groups had a greater response for the upright as compared to inverted Condition ($p < 0.001$, corrected). Moreover, post-hoc pairwise comparisons did not reveal a between group effect neither for the upright nor for the inverted Condition (all p -values > 0.1 , corrected). All results confirm the finding using a less conservative threshold (z-score > 1.64 , corresponding to a $p < 0.05$, one-tailed).

B.2 Source analysis, within group results

B.2.1 Face-Object Categorization experiment

FO experiment (faces vs. objects). We compared in the Auditory ROIs, separately for each hemisphere, the source estimates in response to faces and to objects within the 200-300 ms time window. Two-sided t -tests for dependent samples were performed at each time-point within pre-selected time windows. False discovery rate (FDR; Genovese et al., 2002) was used to correct for multiple comparisons. FDR bound (q -value) was set at 0.05.

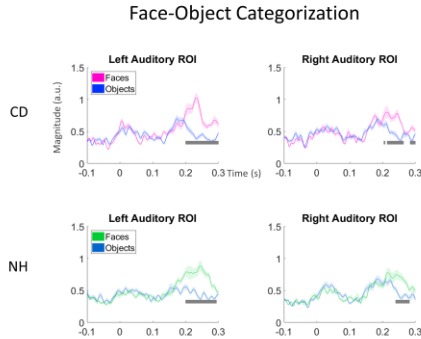


Figure B.6: Source analysis performed in the time domain for the Face-Object categorization experiment. Activity is shown in response to faces and objects. From left to right: time course of activity measured for each group at left and right Auditory ROIs. Top CD group, bottom HC group. Grey boxes highlight significant within-group differences within the 200-300 ms time window between the activity in response to Faces and Objects.

B.2.2 Individual Face Discrimination experiment

ID experiment (faces vs. objects): We compared in the Auditory ROIs, separately for each hemisphere, the source estimates in response to same and different face identities within the 300-400 ms time window. Two-sided t-tests for dependent samples were performed at each time-point within pre-selected time windows. False discovery rate (FDR; Genovese et al., 2002) was used to correct for multiple comparisons. FDR bound (q -value) was set at 0.05.

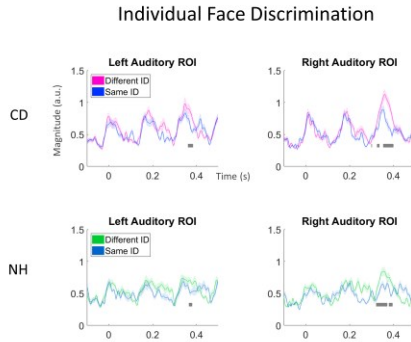


Figure B 7: Source analysis performed in the time domain for the Individual Face Discrimination experiment. Activity is shown in response to same and different face identities. From left to right: time course of activity measured for each group at left and right Auditory ROIs. Top CD group, bottom HC group. Grey boxes highlight significant (FDR-corrected) within-group differences within the 300-400 ms time window for the activity in response to same and different face identities.

Appendix C

Supplementary Material for Chapter 4

C.1 Questionnaire

Speech-in-Quiet Condition

Part 1 (First 5 minutes)

- 1) Polissena ha 13 anni? **(NO)**
- 2) Polissena faceva lezioni di Storia? **(YES)**
- 3) La zia di Polissena puzzava di tabacco? **(YES)**

Part 2 (Second 5 minutes)

- 1) I nastri delle scarpette di Polissena sono di seta? **(YES)**
- 2) Serafina è figlia di un dentista? **(NO)**
- 3) Polissena aveva il naso come quello della madre? **(NO)**

Part 3 (Third 5 minutes)

- 1) Agnese era in salotto? **(NO)**
- 2) Polissena aspettava fuori dal cancello? **(NO)**
- 3) Serafina ha 12 anni? **(YES)**

Speech-in-Noise at SNR 1 Condition

Part 1 (First 5 minutes)

- 1) Suor Zelinda porta a Polissena una tazza di tè fumante? **(NO)**
- 2) Polissena udì il suono di un tamburello? **(YES)**
- 3) Il cane di Lucrezia è un San Bernardo? **(YES)**

Part 2 (Second 5 minutes)

- 1) Il vecchio Giraldi è morto cadendo da un palazzo? **(NO)**
- 2) Tra gli animali di Lucrezia c'è anche un'oca? **(YES)**
- 3) I genitori di Lucrezia sono morti di peste? **(YES)**

Part 3 (Third 5 minutes)

- 1) Polissena aveva già stretto amicizia con Lucrezia? **(NO)**
- 2) Lucrezia affida il porcello allo scimpanzé? **(YES)**
- 3) Nello scrigno c'era un pesciolino di cristallo? **(NO)**

Speech-in-Noise at SNR 2 Condition

Part 1 (First 5 minutes)

- 1) A Cepaluna c'era una fontana? **(YES)**
- 2) L'unico edificio rimasto intatto a Paludis era la scuola? **(NO)**
- 3) La famiglia di Lucrezia si chiamava Ramusio? **(YES)**

Part 2 (Second 5 minutes)

- 1) Uno dei nomi di Lucrezia è Maria? **(YES)**
- 2) Lo sguardo del padre di Lucrezia era ironico? **(YES)**
- 3) La madre di Lucrezia era mora? **(NO)**

Part 3 (Third 5 minutes)

- 1) Dopo sei giorni di cammino, le ragazze raggiungono un'osteria? **(NO)**
- 2) Lucrezia era spaventata dai briganti? **(NO)**
- 3) Polissena veniva chiamata "Ludovico il ragno"? **(YES)**

Jabberwocky-in-Noise at SNR1 Condition

Part 1 (First 5 minutes)

- 1) Il vecchio Giraldi è morto cadendo da un palazzo? **(NO)**
- 2) Tra gli animali di Lucrezia c'è anche un'oca? **(YES)**
- 3) I genitori di Lucrezia sono morti di peste? **(YES)**

Part 2 (Second 5 minutes)

- 1) La pia farfalla è protagonista di una poesia? **(NO)**
- 2) A Sdrenfano si chiede di cancellare il mondo? **(YES)**
- 3) Le macchine sono piene di cronicaglie? **(NO)**

Part 3 (Third 5 minutes)

- 1) Il bullo si butta dal bulldozer? (**YES**)
- 2) I lonferi devono essere gettati nel fuoco piripigno? (**YES**)
- 3) Dio è giovane? (**NO**)

C.2 Choice of SNR level

The range of SNR levels was based on the results of our pilot experiments, with the idea of being capable to considerably affect participant's intelligibility rather than severely disrupting it. To select SNR levels, we behaviorally tested six other participants who did not take part in the main study. They listened short (~ 1 min) speech fragments embedded in noise at a range of fixed SNR levels ($\{-3.52$ dB, -1.74 dB, 0 dB, $+1.74$ dB, $+3.52$ dB}), with randomly drawn parts of the babble noise on the background to prevent participants' adaptation to a particular babble. As a result, we identified two SNR levels: $+3.52$ dB (SNR1, as an easier level for participants to comprehend) and $+1.74$ dB (SNR2, as a harder level for participants to comprehend).

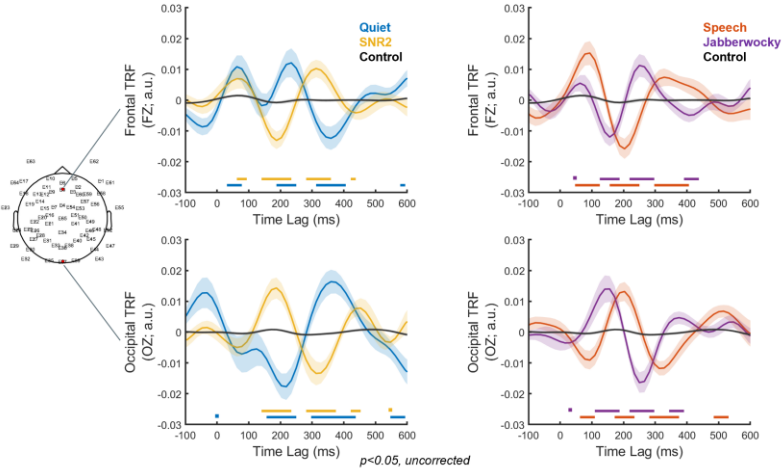


Figure C.1: TRF models' performance. Grand averaged temporal response functions (TRFs) for four experimental conditions: *Speech-in-Quiet* (Quiet, blue), *Speech-in-Noise at SNR2* (SNR2, yellow), *Speech-in-Noise at SNR1* (Speech, red), *Jabberwocky-in-Noise at SNR1* (Jabberwocky, purple); and null-distributed TRF model (Control, black). TRFs displayed over time-lags at frontal Fz and occipital Oz electrodes, marked with red on the electrode layout. Shaded areas represent the standard error of the mean (SE) across participants. Colored horizontal bars above the x-axis indicate time-lags at which TRFs of experimental conditions differed from the null TRF ($p < 0.05$, uncorrected).

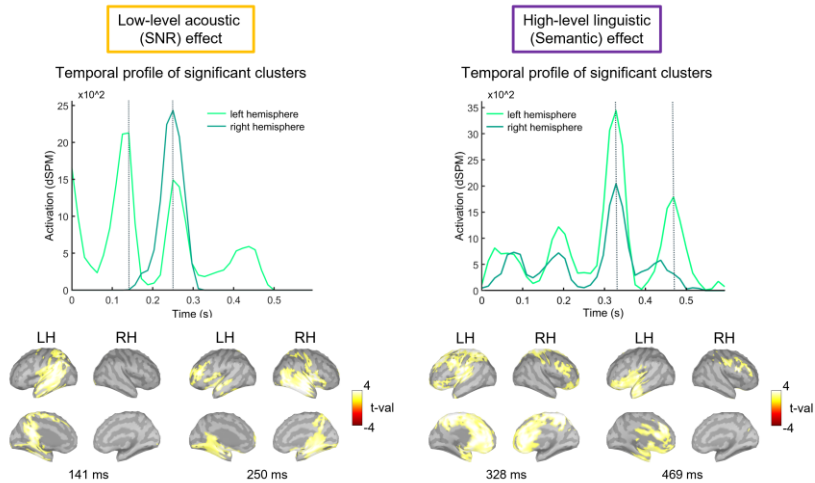


Figure C.2: Source analysis, whole-brain level. Grand averaged TRF source-localization results, corrected for multiple comparisons using a cluster-based permutation test across all electrodes and time-lags from 0 to 600 ms. Top panel: Temporal extent profile for each of the identified significant clusters in the left (light green) and right (dark green) hemispheres. Grey vertical lines mark time-lags corresponding to visually salient peaks in the temporal profile, in the left and right hemisphere, respectively. Bottom panel: Significant differences between TRFs at the source space ($p < 0.05$, cluster-corrected); lateral and medial views of the left (LH) and right (RH) hemispheres, displayed at the time-lags marked on the Top panel. Bright yellow (positive t -values) indicates greater activation for Quiet vs. SNR2 and for Speech vs. Jabberwocky, respectively.

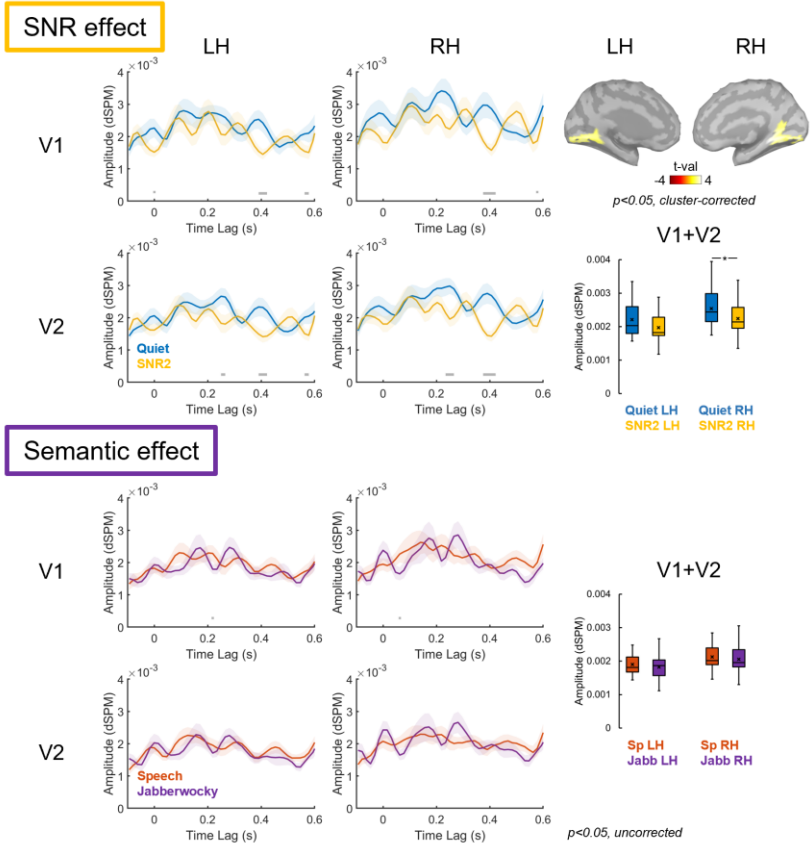


Figure C.3: Source analysis, visual ROIs. Grand averaged time series of the activation extracted for visual ROIs (V1 and V2), for the left (LH) and right (RH) hemispheres. Activation is displayed unitless and in absolute values, as provided by the normalization within the dSPM algorithm. Shaded areas indicate the standard error of the mean (SE). Grey horizontal bars above the x-axis indicate time-lags at which two conditions significantly differed ($p < 0.05$, uncorrected). Statistical map projected on the brain surface to highlight differences between conditions (Quiet vs. SNR2; $p < 0.05$, cluster-corrected) in ROIs, identified at the whole-brain level, and displayed for the left (LH) and right (RH) hemispheres at around 250 ms (corresponding to the peaks in the temporal profile); bright yellow (positive t-values) indicates greater activation for Quiet over SNR2. Boxplots show source activation for each condition, *averaged* over the ROIs (V1 + V2) and across all relevant time-points (from 0 to 600 ms

regarding speech envelope onset), in the left and right hemispheres, respectively. The line through the box indicates median, × marker indicates the mean, lines indicate pairwise statistical comparisons (* $p < 0.05$).

C.3 Effect of Speech Rate, Intensity and Modulation Depth

Neural tracking could be affected by speech rate (Müller, Wendt, Kollmeier, Debener, & Brand, 2019) and intensity of the stimuli (Drennan & Lalor, 2019). Thus, it could be argued that our results could also be driven by such differences. However, the target speaker was the same in all conditions, and RMS amplitude of the stimuli was normalized to a constant value, allowing to control for both speech rate and intensity.

Speech presented in quiet varies in amplitude modulation depth because of silent gaps, whereas speech presented in noise has homogenous amplitude. If amplitude modulation depth would have an effect, we should have observed clear between-condition differences in the early peak (P1), that has been suggested to reflect early, pre-perceptual sound processing (Ceponienė et al., 2005), which was not the case.

Bibliography

- Ahissar, E., Nagarajan, S., Ahissar, M., Protopapas, A., Mahncke, H., & Merzenich, M. M. (2001). Speech comprehension is correlated with temporal response patterns recorded from auditory cortex. *Proceedings of the National Academy of Sciences*, *98*(23), 13367–13372. doi: [10.1073/pnas.201400998](https://doi.org/10.1073/pnas.201400998)
- Alain, C., Du, Y., Bernstein, L. J., Barten, T., & Banai, K. (2018). Listening under difficult conditions: An activation likelihood estimation meta-analysis. *Human Brain Mapping*, *39*(7), 2695–2709. doi: [10.1002/hbm.24031](https://doi.org/10.1002/hbm.24031)
- Alain, C., Quan, J., McDonald, K., & Van Roon, P. (2009). Noise-induced increase in human auditory evoked neuromagnetic fields. *European Journal of Neuroscience*, *30*(1), 132–142. doi: [10.1111/j.1460-9568.2009.06792.x](https://doi.org/10.1111/j.1460-9568.2009.06792.x)
- Alday, P. M. (2019). M/EEG analysis of naturalistic stories: A review from speech to language processing. *Language, Cognition and Neuroscience*, *34*(4), 457–473. doi: [10.1080/23273798.2018.1546882](https://doi.org/10.1080/23273798.2018.1546882)
- Alexandrou, A. M., Saarinen, T., Kujala, J., & Salmelin, R. (2020). Cortical entrainment: What we can learn from studying naturalistic speech perception. *Language, Cognition and Neuroscience*, *35*(6), 681–693. doi: [10.1080/23273798.2018.1518534](https://doi.org/10.1080/23273798.2018.1518534)
- Alexandrou, A. M., Saarinen, T., Mäkelä, S., Kujala, J., & Salmelin, R. (2017). The right hemisphere is highlighted in connected natural speech production and perception. *NeuroImage*, *152*, 628–638. doi: [10.1016/j.neuroimage.2017.03.006](https://doi.org/10.1016/j.neuroimage.2017.03.006)
- Amadeo, M. B., Campus, C., Pavani, F., & Gori, M. (2019). Spatial Cues Influence Time Estimations in Deaf Individuals. *IScience*, *19*, 369–377. doi: [10.1016/j.isci.2019.07.042](https://doi.org/10.1016/j.isci.2019.07.042)
- Amaral, A. A., & Langers, D. R. M. (2013). The relevance of task-irrelevant sounds: Hemispheric lateralization and interactions with task-relevant streams. *Frontiers in Neuroscience*, *7*, 264. doi: [10.3389/fnins.2013.00264](https://doi.org/10.3389/fnins.2013.00264)
- Anzures, G., Quinn, P. C., Pascalis, O., Slater, A. M., Tanaka, J. W., & Lee, K. (2013). Developmental Origins of the Other-Race Effect. *Current Directions in Psychological Science*, *22*(3), 173–178. doi: [10.1177/0963721412474459](https://doi.org/10.1177/0963721412474459)
- Arnal, L. H., & Giraud, A.-L. (2012). Cortical oscillations and sensory predictions. *Trends in Cognitive Sciences*, *16*(7), 390–398. doi: [10.1016/j.tics.2012.05.003](https://doi.org/10.1016/j.tics.2012.05.003)
- Arnaud, L., Gracco, V., & Ménard, L. (2018). Enhanced Perception of Pitch Changes in Speech and Music in Early Blind Adults. *Neuropsychologia*, *117*, 261–270. doi: [10.1016/j.neuropsychologia.2018.06.009](https://doi.org/10.1016/j.neuropsychologia.2018.06.009)
- Auksztulewicz, R., & Friston, K. (2016). Repetition suppression and its contextual determinants in predictive coding. *Cortex*, *80*, 125–140. doi: [10.1016/j.cortex.2015.11.024](https://doi.org/10.1016/j.cortex.2015.11.024)
- Balkenhol, T., Wallhäusser-Franke, E., Rotter, N., & Servais, J. J. (2020). Changes in Speech-Related Brain Activity During Adaptation to Electro-Acoustic Hearing. *Frontiers in Neurology*, *11*:161. doi: [10.3389/fneur.2020.00161](https://doi.org/10.3389/fneur.2020.00161)

- Barbosa, L. S., & Kouider, S. (2018). Prior Expectation Modulates Repetition Suppression without Perceptual Awareness. *Scientific Reports*, *8*(1), 1–11. doi: [10.1038/s41598-018-23467-3](https://doi.org/10.1038/s41598-018-23467-3)
- Bastos, A. M., Vezoli, J., Bosman, C. A., Schoffelen, J.-M., Oostenveld, R., Dowdall, J. R., ... Fries, P. (2015). Visual Areas Exert Feedforward and Feedback Influences through Distinct Frequency Channels. *Neuron*, *85*(2), 390–401. doi: [10.1016/j.neuron.2014.12.018](https://doi.org/10.1016/j.neuron.2014.12.018)
- Bavelier, D., Dye, M. W. G., & Hauser, P. C. (2006). Do deaf individuals see better? *Trends in Cognitive Sciences*, *10*(11), 512–518. doi: [10.1016/j.tics.2006.09.006](https://doi.org/10.1016/j.tics.2006.09.006)
- Bavelier, D., & Neville, H. J. (2002). Cross-modal plasticity: Where and how? *Nature Reviews Neuroscience*, *3*(6), 443–452. doi: [10.1038/nrn848](https://doi.org/10.1038/nrn848)
- Bavelier, D., Tomann, A., Hutton, C., Mitchell, T., Corina, D., Liu, G., & Neville, H. (2000). Visual Attention to the Periphery Is Enhanced in Congenitally Deaf Individuals. *Journal of Neuroscience*, *20*(17), RC93–RC93. doi: [10.1523/JNEUROSCI.20-17-j0001.2000](https://doi.org/10.1523/JNEUROSCI.20-17-j0001.2000)
- Bavelier, D., Brozinsky, C., Tomann, A., Mitchell, T., Neville, H., & Liu, G. (2001). Impact of Early Deafness and Early Exposure to Sign Language on the Cerebral Organization for Motion Processing. *Journal of Neuroscience*, *21*(22), 8931–8942. doi: [10.1523/JNEUROSCI.21-22-08931.2001](https://doi.org/10.1523/JNEUROSCI.21-22-08931.2001)
- Bednaya, E., Pavani, F., Ricciardi, E., Pietrini, P., & Bottari, D. (2021). Oscillatory signatures of Repetition Suppression and Novelty Detection reveal altered induced visual responses in early deafness. *Cortex*, *142*, 138–153. doi: [10.1016/j.cortex.2021.05.017](https://doi.org/10.1016/j.cortex.2021.05.017)
- Bedny, M., Pascual-Leone, A., Dodell-Feder, D., Fedorenko, E., & Saxe, R. (2011). Language processing in the occipital cortex of congenitally blind adults. *Proceedings of the National Academy of Sciences*, *108*(11), 4429–4434. doi: [10.1073/pnas.1014818108](https://doi.org/10.1073/pnas.1014818108)
- Bedny, M., Richardson, H., & Saxe, R. (2015). “Visual” Cortex Responds to Spoken Language in Blind Children. *The Journal of Neuroscience*, *35*(33), 11674–11681. doi: [10.1523/JNEUROSCI.0634-15.2015](https://doi.org/10.1523/JNEUROSCI.0634-15.2015)
- Belin, P., & Zatorre, R. J. (2003). Adaptation to speaker’s voice in right anterior temporal lobe. *NeuroReport*, *14*(16), 2105–2109.
- Belin, P., Zatorre, R. J., Lafaille, P., Ahad, P., & Pike, B. (2000). Voice-selective areas in human auditory cortex. *Nature*, *403*(6767), 309–312. doi: [10.1038/35002078](https://doi.org/10.1038/35002078)
- Bell, A. J., & Sejnowski, T. J. (1995). An Information-Maximization Approach to Blind Separation and Blind Deconvolution. *Neural Computation*, *7*(6), 1129–1159. doi: [10.1162/neco.1995.7.6.1129](https://doi.org/10.1162/neco.1995.7.6.1129)
- Bell, L., Wagels, L., Neuschaefer-Rube, C., Fels, J., Gur, R. E., & Konrad, K. (2019). The Cross-Modal Effects of Sensory Deprivation on Spatial and Temporal Processes in Vision and Audition: A Systematic Review on Behavioral and Neuroimaging Research since 2000. *Neural Plasticity*, *2019*, 1–21. doi: [10.1155/2019/9603469](https://doi.org/10.1155/2019/9603469)
- Benetti, S., van Ackeren, M. J., Rabini, G., Zonca, J., Foa, V., Baruffaldi, F., ... Collignon, O. (2017). Functional selectivity for face processing in the temporal voice area of early deaf individuals. *Proceedings of the National Academy of Sciences*, *114*(31), E6437–E6446. doi: [10.1073/pnas.1618287114](https://doi.org/10.1073/pnas.1618287114)

- Benjamini, Y., Drai, D., Elmer, G., Kafkafi, N., & Golani, I. (2001). Controlling the false discovery rate in behavior genetics research. *Behavioural Brain Research*, *125*(1), 279–284. doi: [10.1016/S0166-4328\(01\)00297-2](https://doi.org/10.1016/S0166-4328(01)00297-2)
- Benjamini, Y., & Hochberg, Y. (1995). Controlling the False Discovery Rate: A Practical and Powerful Approach to Multiple Testing. *Journal of the Royal Statistical Society. Series B (Methodological)*, *57*(1), 289–300.
- Berger, C., Kühne, D., Scheper, V., & Kral, A. (2017). Congenital deafness affects deep layers in primary and secondary auditory cortex. *Journal of Comparative Neurology*, *525*(14), 3110–3125. doi: <https://doi.org/10.1002/cne.24267>
- Besle, J., Hussain, Z., Giard, M.-H., & Bertrand, O. (2013). The Representation of Audiovisual Regularities in the Human Brain. *Journal of Cognitive Neuroscience*, *25*(3), 365–373. doi: [10.1162/jocn_a_00334](https://doi.org/10.1162/jocn_a_00334)
- Bettger, J. G., Emmorey, K., McCullough, S. H., & Bellugi, U. (1997). Enhanced Facial Discrimination: Effects of Experience With American Sign Language. *The Journal of Deaf Studies and Deaf Education*, *2*(4), 223–233. doi: [10.1093/oxfordjournals.deafed.a014328](https://doi.org/10.1093/oxfordjournals.deafed.a014328)
- Billings, C. J., Tremblay, K. L., Stecker, G. C., & Tolin, W. M. (2009). Human evoked cortical activity to signal-to-noise ratio and absolute signal level. *Hearing Research*, *254*(1), 15–24. doi: [10.1016/j.heares.2009.04.002](https://doi.org/10.1016/j.heares.2009.04.002)
- Bishop, C. W., & Miller, L. M. (2009). A Multisensory Cortical Network for Understanding Speech in Noise. *Journal of Cognitive Neuroscience*, *21*(9), 1790–1804. doi: [10.1162/jocn.2009.21118](https://doi.org/10.1162/jocn.2009.21118)
- Bola, L., Zimmermann, M., Mostowski, P., Jednoróg, K., Marchewka, A., Rutkowski, P., & Szwed, M. (2017). Task-specific reorganization of the auditory cortex in deaf humans. *Proceedings of the National Academy of Sciences*, *114*(4), E600–E609. doi: [10.1073/pnas.1609000114](https://doi.org/10.1073/pnas.1609000114)
- Bosworth, R. G., & Dobkins, K. R. (2002). The Effects of Spatial Attention on Motion Processing in Deaf Signers, Hearing Signers, and Hearing Nonsigners. *Brain and Cognition*, *49*(1), 152–169. doi: [10.1006/brcg.2001.1497](https://doi.org/10.1006/brcg.2001.1497)
- Bottari, D., Bednaya, E., Dormal, G., Villwock, A., Dzhelyova, M., Grin, K., ... Röder, B. (2020). EEG frequency-tagging demonstrates increased left hemispheric involvement and crossmodal plasticity for face processing in congenitally deaf signers. *NeuroImage*, *223*, 117315. doi: [10.1016/j.neuroimage.2020.117315](https://doi.org/10.1016/j.neuroimage.2020.117315)
- Bottari, D., Caclin, A., Giard, M.-H., & Pavani, F. (2011). Changes in Early Cortical Visual Processing Predict Enhanced Reactivity in Deaf Individuals. *PLOS ONE*, *6*(9), e25607. doi: [10.1371/journal.pone.0025607](https://doi.org/10.1371/journal.pone.0025607)
- Bottari, D., Heimler, B., Caclin, A., Dalmolin, A., Giard, M.-H., & Pavani, F. (2014). Visual change detection recruits auditory cortices in early deafness. *NeuroImage*, *94*, 172–184. doi: [10.1016/j.neuroimage.2014.02.031](https://doi.org/10.1016/j.neuroimage.2014.02.031)
- Bottari, D., Nava, E., Ley, P., & Pavani, F. (2010). Enhanced reactivity to visual stimuli in deaf individuals. *Restorative Neurology and Neuroscience*, *28*(2), 167–179. doi: [10.3233/RNN-2010-0502](https://doi.org/10.3233/RNN-2010-0502)

- Bottari, D., Troje, N. F., Ley, P., Hense, M., Kekunnaya, R., & Röder, B. (2016). Sight restoration after congenital blindness does not reinstate alpha oscillatory activity in humans. *Scientific Reports*, *6*(1), 1–10. doi: [10.1038/srep24683](https://doi.org/10.1038/srep24683)
- Bourguignon, M., Baart, M., Kapnoula, E. C., & Molinaro, N. (2018). *Hearing through lip-reading: The brain synthesizes features of absent speech*. bioRxiv. doi: [10.1101/395483](https://doi.org/10.1101/395483)
- Bourguignon, M., Baart, M., Kapnoula, E. C., & Molinaro, N. (2020). Lip-Reading Enables the Brain to Synthesize Auditory Features of Unknown Silent Speech. *Journal of Neuroscience*, *40*(5), 1053–1065. doi: [10.1523/JNEUROSCI.1101-19.2019](https://doi.org/10.1523/JNEUROSCI.1101-19.2019)
- Brang, D., Plass, J., Sherman, A., Stacey, W. C., Wasade, V. S., Grabowecky, M., ... Suzuki, S. (2022). Visual cortex responds to sound onset and offset during passive listening. *Journal of Neurophysiology*, *127*(6), 1547–1563. <https://doi.org/10.1152/jn.00164.2021>
- Brodbeck, C., Hong, L. E., & Simon, J. Z. (2018). Rapid Transformation from Auditory to Linguistic Representations of Continuous Speech. *Current Biology*, *28*(24), 3976–3983.e5. doi: [10.1016/j.cub.2018.10.042](https://doi.org/10.1016/j.cub.2018.10.042)
- Brodbeck, C., Jiao, A., Hong, L. E., & Simon, J. Z. (2020). Neural speech restoration at the cocktail party: Auditory cortex recovers masked speech of both attended and ignored speakers. *PLoS Biology*, *18*(10), e3000883. doi: [10.1371/journal.pbio.3000883](https://doi.org/10.1371/journal.pbio.3000883)
- Brodbeck, C., Presacco, A., Anderson, S., & Simon, J. Z. (2018). Over-Representation of Speech in Older Adults Originates from Early Response in Higher Order Auditory Cortex. *Acta Acustica United with Acustica*, *104*(5), 774–777. doi: [10.3813/AAA.919221](https://doi.org/10.3813/AAA.919221)
- Brodbeck, C., & Simon, J. Z. (2020). Continuous speech processing. *Current Opinion in Physiology*, *18*, 25–31. doi: [10.1016/j.cophys.2020.07.014](https://doi.org/10.1016/j.cophys.2020.07.014)
- Broderick, M. P., Anderson, A. J., & Lalor, E. C. (2019). Semantic Context Enhances the Early Auditory Encoding of Natural Speech. *Journal of Neuroscience*, *39*(38), 7564–7575. doi: [10.1523/JNEUROSCI.0584-19.2019](https://doi.org/10.1523/JNEUROSCI.0584-19.2019)
- Broderick, M. P., Di Liberto, G. M., Anderson, A. J., Rofes, A., & Lalor, E. C. (2021). Dissociable electrophysiological measures of natural language processing reveal differences in speech comprehension strategy in healthy ageing. *Scientific Reports*, *11*(1), 4963. doi: [10.1038/s41598-021-84597-9](https://doi.org/10.1038/s41598-021-84597-9)
- Bröhl, F., & Kayser, C. (2021). Delta/theta band EEG differentially tracks low and high frequency speech-derived envelopes. *NeuroImage*, *233*, 117958. doi: [10.1016/j.neuroimage.2021.117958](https://doi.org/10.1016/j.neuroimage.2021.117958)
- Brouwer, S., Van Engen, K. J., Calandruccio, L., & Bradlow, A. R. (2012). Linguistic contributions to speech-on-speech masking for native and non-native listeners: Language familiarity and semantic content. *The Journal of the Acoustical Society of America*, *131*(2), 1449–1464. doi: [10.1121/1.3675943](https://doi.org/10.1121/1.3675943)
- Brozinsky, C. J., & Bavelier, D. (2004). Motion velocity thresholds in deaf signers: Changes in lateralization but not in overall sensitivity. *Cognitive Brain Research*, *21*(1), 1–10. doi: [10.1016/j.cogbrainres.2004.05.002](https://doi.org/10.1016/j.cogbrainres.2004.05.002)
- Brungart, D. S. (2001). Informational and energetic masking effects in the perception of two simultaneous talkers. *The Journal of the Acoustical Society of America*, *109*(3), 1101–1109.

doi: [10.1121/1.1345696](https://doi.org/10.1121/1.1345696)

Burton, H., Snyder, A. Z., Conturo, T. E., Akbudak, E., Ollinger, J. M., & Raichle, M. E. (2002). Adaptive Changes in Early and Late Blind: A fMRI Study of Braille Reading. *Journal of Neurophysiology*, *87*(1), 589–607. doi: [10.1152/jn.00285.2001](https://doi.org/10.1152/jn.00285.2001)

Busch, N., Debener, S., Kranczioch, C., Engel, A., & Herrmann, C. S. (2004). Size matters: Effects of stimulus size, duration and eccentricity on the visual gamma-band response. *Clinical Neurophysiology*, *115*(8), 1810–1820. doi: [10.1016/j.clinph.2004.03.015](https://doi.org/10.1016/j.clinph.2004.03.015)

Calandruccio, L., Van Engen, K., Dhar, S., & Bradlow, A. R. (2010). The Effectiveness of Clear Speech as a Masker. *Journal of Speech, Language, and Hearing Research: JSLHR*, *53*(6), 1458–1471. doi: [10.1044/1092-4388\(2010/09-0210\)](https://doi.org/10.1044/1092-4388(2010/09-0210))

Calder, A. J., Rhodes, G., Johnson, M. H., & Haxby, J. V. (2011). Oxford Handbook of Face Perception. In *Oxford Handbook of Face Perception*. Oxford University Press. doi: [10.1093/oxfordhb/9780199559053.001.0001](https://doi.org/10.1093/oxfordhb/9780199559053.001.0001)

Callaway, E. M. (1998). Local circuits in primary visual cortex of the macaque monkey. *Annual Review of Neuroscience*, *21*(1), 47–74. doi: [10.1146/annurev.neuro.21.1.47](https://doi.org/10.1146/annurev.neuro.21.1.47)

Campos Viola, F., Thorne, J., Edmonds, B., Schneider, T., Eichele, T., & Debener, S. (2009). Semi-automatic identification of independent components representing EEG artifact. *Clinical Neurophysiology*, *120*(5), 868–877. doi: [10.1016/j.clinph.2009.01.015](https://doi.org/10.1016/j.clinph.2009.01.015)

Cantlon, J. F., Pineda, P., Dehaene, S., & Pelphrey, K. A. (2011). Cortical Representations of Symbols, Objects, and Faces Are Pruned Back during Early Childhood. *Cerebral Cortex*, *21*(1), 191–199. doi: [10.1093/cercor/bhq078](https://doi.org/10.1093/cercor/bhq078)

Cardin, V., Grin, K., Vinogradova, V., & Manini, B. (2020). Crossmodal reorganisation in deafness: Mechanisms for functional preservation and functional change. *Neuroscience & Biobehavioral Reviews*, *113*, 227–237. doi: [10.1016/j.neubiorev.2020.03.019](https://doi.org/10.1016/j.neubiorev.2020.03.019)

Cardin, V., Orfanidou, E., Rönnerberg, J., Capek, C. M., Rudner, M., & Woll, B. (2013). Dissociating cognitive and sensory neural plasticity in human superior temporal cortex. *Nature Communications*, *4*(1), 1473. doi: [10.1038/ncomms2463](https://doi.org/10.1038/ncomms2463)

Cate, A. D., Herron, T. J., Yund, E. W., Stecker, G. C., Rinne, T., Kang, X., ... Woods, D. L. (2009). Auditory Attention Activates Peripheral Visual Cortex. *PLOS ONE*, *4*(2), e4645. doi: [10.1371/journal.pone.0004645](https://doi.org/10.1371/journal.pone.0004645)

Cavanagh, J. F., & Frank, M. J. (2014). Frontal theta as a mechanism for cognitive control. *Trends in Cognitive Sciences*, *18*(8), 414–421. doi: [10.1016/j.tics.2014.04.012](https://doi.org/10.1016/j.tics.2014.04.012)

Cavanagh, J. F., Frank, M. J., Klein, T. J., & Allen, J. J. B. (2010). Frontal theta links prediction errors to behavioral adaptation in reinforcement learning. *NeuroImage*, *49*(4), 3198–3209. doi: [10.1016/j.neuroimage.2009.11.080](https://doi.org/10.1016/j.neuroimage.2009.11.080)

Ceponienė, R., Alku, P., Westerfield, M., Torki, M., & Townsend, J. (2005). ERPs differentiate syllable and nonphonetic sound processing in children and adults. *Psychophysiology*, *42*(4), 391–406. doi: [10.1111/j.1469-8986.2005.00305.x](https://doi.org/10.1111/j.1469-8986.2005.00305.x)

Chang, Y. (2014). Reorganization and plastic changes of the human brain associated with skill learning and expertise. *Frontiers in Human Neuroscience*, *8*, 35. doi:

[10.3389/fnhum.2014.00035](https://doi.org/10.3389/fnhum.2014.00035)

Chen, C.-C., Kiebel, S. J., Kilner, J. M., Ward, N. S., Stephan, K. E., Wang, W.-J., & Friston, K. J. (2012). A dynamic causal model for evoked and induced responses. *NeuroImage*, *59*(1), 340–348. doi: [10.1016/j.neuroimage.2011.07.066](https://doi.org/10.1016/j.neuroimage.2011.07.066)

Chen, L.-C., Stropahl, M., Schönwiesner, M., & Debener, S. (2017). Enhanced visual adaptation in cochlear implant users revealed by concurrent EEG-fNIRS. *NeuroImage*, *146*, 600–608. doi: [10.1016/j.neuroimage.2016.09.033](https://doi.org/10.1016/j.neuroimage.2016.09.033)

Cherry, E. C. (1953). Some Experiments on the Recognition of Speech, with One and with Two Ears. *The Journal of the Acoustical Society of America*, *25*(5), 975–979. doi: [10.1121/1.1907229](https://doi.org/10.1121/1.1907229)

Clayton, M. S., Yeung, N., & Cohen Kadosh, R. (2018). The many characters of visual alpha oscillations. *The European Journal of Neuroscience*, *48*(7), 2498–2508. doi: [10.1111/ejn.13747](https://doi.org/10.1111/ejn.13747)

Cohen, M. X., & Donner, T. H. (2013). Midfrontal conflict-related theta-band power reflects neural oscillations that predict behavior. *Journal of Neurophysiology*, *110*(12), 2752–2763. doi: [10.1152/jn.00479.2013](https://doi.org/10.1152/jn.00479.2013)

Collignon, O., Vandewalle, G., Voss, P., Albouy, G., Charbonneau, G., Lassonde, M., & Lepore, F. (2011). Functional specialization for auditory-spatial processing in the occipital cortex of congenitally blind humans. *Proceedings of the National Academy of Sciences*, *108*(11), 4435–4440. doi: [10.1073/pnas.1013928108](https://doi.org/10.1073/pnas.1013928108)

Collignon, O., Voss, P., Lassonde, M., & Lepore, F. (2009). Cross-modal plasticity for the spatial processing of sounds in visually deprived subjects. *Experimental Brain Research*, *192*(3), 343–358. doi: [10.1007/s00221-008-1553-z](https://doi.org/10.1007/s00221-008-1553-z)

Collignon, O., Champoux, F., Voss, P., & Lepore, F. (2011). Sensory rehabilitation in the plastic brain. In *Progress in Brain Research* (Vol. 191, pp. 211–231). Elsevier. doi: [10.1016/B978-0-444-53752-2.00003-5](https://doi.org/10.1016/B978-0-444-53752-2.00003-5)

Combrisson, E., & Jerbi, K. (2015). Exceeding chance level by chance: The caveat of theoretical chance levels in brain signal classification and statistical assessment of decoding accuracy. *Journal of Neuroscience Methods*, *250*, 126–136. doi: [10.1016/j.jneumeth.2015.01.010](https://doi.org/10.1016/j.jneumeth.2015.01.010)

Cooke, M., Garcia Lecumberri, M. L., & Barker, J. (2008). The foreign language cocktail party problem: Energetic and informational masking effects in non-native speech perception. *The Journal of the Acoustical Society of America*, *123*(1), 414–427. doi: [10.1121/1.2804952](https://doi.org/10.1121/1.2804952)

Cramer, A. O. J., van Ravenzwaaij, D., Matzke, D., Steingroever, H., Wetzels, R., Grasman, R. P. P., ... Wagenmakers, E.-J. (2016). Hidden multiplicity in exploratory multiway ANOVA: Prevalence and remedies. *Psychonomic Bulletin & Review*, *23*, 640–647. doi: [10.3758/s13423-015-0913-5](https://doi.org/10.3758/s13423-015-0913-5)

Crosse, M. J., Di Liberto, G. M., Bednar, A., & Lalor, E. C. (2016). The Multivariate Temporal Response Function (mTRF) Toolbox: A MATLAB Toolbox for Relating Neural Signals to Continuous Stimuli. *Frontiers in Human Neuroscience*, *10*. doi: [10.3389/fnhum.2016.00604](https://doi.org/10.3389/fnhum.2016.00604)

- Crosse, M. J., Zuk, N. J., Di Liberto, G. M., Nidiffer, A. R., Molholm, S., & Lalor, E. C. (2021). Linear Modeling of Neurophysiological Responses to Speech and Other Continuous Stimuli: Methodological Considerations for Applied Research. *Frontiers in Neuroscience*, *15*, 1350. doi: [10.3389/fnins.2021.705621](https://doi.org/10.3389/fnins.2021.705621)
- Dale, A. M., Liu, A. K., Fischl, B. R., Buckner, R. L., Belliveau, J. W., Lewine, J. D., & Halgren, E. (2000). Dynamic Statistical Parametric Mapping: Combining fMRI and MEG for High-Resolution Imaging of Cortical Activity. *Neuron*, *26*(1), 55–67. doi: [10.1016/S0896-6273\(00\)81138-1](https://doi.org/10.1016/S0896-6273(00)81138-1)
- David, O., Kilner, J., & Friston, K. (2006). Mechanisms of evoked and induced responses in MEG/EEG. *NeuroImage*, *31*, 1580–1591. doi: [10.1016/j.neuroimage.2006.02.034](https://doi.org/10.1016/j.neuroimage.2006.02.034)
- Davis, M. H., & Johnsrude, I. S. (2003). Hierarchical Processing in Spoken Language Comprehension. *Journal of Neuroscience*, *23*(8), 3423–3431. doi: [10.1523/JNEUROSCI.23-08-03423.2003](https://doi.org/10.1523/JNEUROSCI.23-08-03423.2003)
- Davis, M. H., & Johnsrude, I. S. (2007). Hearing speech sounds: Top-down influences on the interface between audition and speech perception. *Hearing Research*, *229*(1–2), 132–147. doi: [10.1016/j.heares.2007.01.014](https://doi.org/10.1016/j.heares.2007.01.014)
- de Heer, W. A., Huth, A. G., Griffiths, T. L., Gallant, J. L., & Theunissen, F. E. (2017). The Hierarchical Cortical Organization of Human Speech Processing. *The Journal of Neuroscience*, *37*(27), 6539–6557. doi: [10.1523/JNEUROSCI.3267-16.2017](https://doi.org/10.1523/JNEUROSCI.3267-16.2017)
- de Heering, A., Aljuhanay, A., Rossion, B., & Pascalis, O. (2012). Early Deafness Increases the Face Inversion Effect but Does Not Modulate the Composite Face Effect. *Frontiers in Psychology*, *3*. doi: [10.3389/fpsyg.2012.00124](https://doi.org/10.3389/fpsyg.2012.00124)
- de Heering, A., & Rossion, B. (2015). Rapid categorization of natural face images in the infant right hemisphere. *ELife*, *4*, e06564. doi: [10.7554/eLife.06564](https://doi.org/10.7554/eLife.06564)
- Decruy, L., Vanthornhout, J., & Francart, T. (2019). Evidence for enhanced neural tracking of the speech envelope underlying age-related speech-in-noise difficulties. *Journal of Neurophysiology*, *122*(2), 601–615. doi: [10.1152/jn.00687.2018](https://doi.org/10.1152/jn.00687.2018)
- Decruy, L., Vanthornhout, J., & Francart, T. (2020). Hearing impairment is associated with enhanced neural tracking of the speech envelope. *Hearing Research*, *393*, 107961. doi: [10.1016/j.heares.2020.107961](https://doi.org/10.1016/j.heares.2020.107961)
- Dehaene, S., Cohen, L., Morais, J., & Kolinsky, R. (2015). Illiterate to literate: Behavioural and cerebral changes induced by reading acquisition. *Nature Reviews Neuroscience*, *16*(4), 234–244. doi: [10.1038/nrn3924](https://doi.org/10.1038/nrn3924)
- Dehaene, S., Pegado, F., Braga, L. W., Ventura, P., Filho, G. N., Jobert, A., ... Cohen, L. (2010). How Learning to Read Changes the Cortical Networks for Vision and Language. *Science*, *330*(6009), 1359–1364. doi: [10.1126/science.1194140](https://doi.org/10.1126/science.1194140)
- Delorme, A., & Makeig, S. (2004). EEGLAB: An open source toolbox for analysis of single-trial EEG dynamics including independent component analysis. *Journal of Neuroscience Methods*, *134*(1), 9–21. doi: [10.1016/j.jneumeth.2003.10.009](https://doi.org/10.1016/j.jneumeth.2003.10.009)
- Delorme, A., Sejnowski, T., & Makeig, S. (2007). Enhanced detection of artifacts in EEG data using higher-order statistics and independent component analysis. *NeuroImage*,

34(4), 1443–1449. doi: [10.1016/j.neuroimage.2006.11.004](https://doi.org/10.1016/j.neuroimage.2006.11.004)

Desai, M., Holder, J., Villarreal, C., Clark, N., Hoang, B., & Hamilton, L. S. (2021). Generalizable EEG Encoding Models with Naturalistic Audiovisual Stimuli. *Journal of Neuroscience*, 41(43), 8946–8962. doi: [10.1523/JNEUROSCI.2891-20.2021](https://doi.org/10.1523/JNEUROSCI.2891-20.2021)

Destrieux, C., Fischl, B., Dale, A., & Halgren, E. (2010). Automatic parcellation of human cortical gyri and sulci using standard anatomical nomenclature. *NeuroImage*, 53(1), 1–15. doi: [10.1016/j.neuroimage.2010.06.010](https://doi.org/10.1016/j.neuroimage.2010.06.010)

Di Liberto, G. M., O’Sullivan, J. A., & Lalor, E. C. (2015). Low-Frequency Cortical Entrainment to Speech Reflects Phoneme-Level Processing. *Current Biology*, 25(19), 2457–2465. doi: [10.1016/j.cub.2015.08.030](https://doi.org/10.1016/j.cub.2015.08.030)

Di Liberto, G. M., Peter, V., Kalashnikova, M., Goswami, U., Burnham, D., & Lalor, E. C. (2018). Atypical cortical entrainment to speech in the right hemisphere underpins phonemic deficits in dyslexia. *NeuroImage*, 175, 70–79. doi: [10.1016/j.neuroimage.2018.03.072](https://doi.org/10.1016/j.neuroimage.2018.03.072)

Dietrich, S., Hertrich, I., & Ackermann, H. (2013). Ultra-fast speech comprehension in blind subjects engages primary visual cortex, fusiform gyrus, and pulvinar – a functional magnetic resonance imaging (fMRI) study. *BMC Neuroscience*, 14(1), 74. doi: [10.1186/1471-2202-14-74](https://doi.org/10.1186/1471-2202-14-74)

Dijkstra, N., Bosch, S. E., & Gerven, M. A. J. van. (2019). Shared Neural Mechanisms of Visual Perception and Imagery. *Trends in Cognitive Sciences*, 23(5), 423–434. doi: [10.1016/j.tics.2019.02.004](https://doi.org/10.1016/j.tics.2019.02.004)

Ding, N., Chatterjee, M., & Simon, J. Z. (2014). Robust cortical entrainment to the speech envelope relies on the spectro-temporal fine structure. *NeuroImage*, 88, 41–46. doi: [10.1016/j.neuroimage.2013.10.054](https://doi.org/10.1016/j.neuroimage.2013.10.054)

Ding, N., Melloni, L., Zhang, H., Tian, X., & Poeppel, D. (2016). Cortical tracking of hierarchical linguistic structures in connected speech. *Nature Neuroscience*, 19(1), 158–164. doi: [10.1038/nn.4186](https://doi.org/10.1038/nn.4186)

Ding, N., & Simon, J. Z. (2012). Neural coding of continuous speech in auditory cortex during monaural and dichotic listening. *Journal of Neurophysiology*, 107(1), 78–89. doi: [10.1152/jn.00297.2011](https://doi.org/10.1152/jn.00297.2011)

Ding, N., & Simon, J. Z. (2013). Adaptive Temporal Encoding Leads to a Background-Insensitive Cortical Representation of Speech. *Journal of Neuroscience*, 33(13), 5728–5735. doi: [10.1523/JNEUROSCI.5297-12.2013](https://doi.org/10.1523/JNEUROSCI.5297-12.2013)

Ding, N., & Simon, J. Z. (2014). Cortical entrainment to continuous speech: Functional roles and interpretations. *Frontiers in Human Neuroscience*, 8. doi: [10.3389/fnhum.2014.00311](https://doi.org/10.3389/fnhum.2014.00311)

Dole, M., Méary, D., & Pascalis, O. (2017). Modifications of Visual Field Asymmetries for Face Categorization in Early Deaf Adults: A Study With Chimeric Faces. *Frontiers in Psychology*, 8. doi: [10.3389/fpsyg.2017.00030](https://doi.org/10.3389/fpsyg.2017.00030)

Doucet, M. E., Bergeron, F., Lassonde, M., Ferron, P., & Lepore, F. (2006). Cross-modal reorganization and speech perception in cochlear implant users. *Brain*, 129(12), 3376–3383. doi: [10.1093/brain/awl264](https://doi.org/10.1093/brain/awl264)

- Drennan, D. P., & Lalor, E. C. (2019). Cortical Tracking of Complex Sound Envelopes: Modeling the Changes in Response with Intensity. *ENeuro*, *6*(3). doi: [10.1523/ENEURO.0082-19.2019](https://doi.org/10.1523/ENEURO.0082-19.2019)
- Duchaine, B., & Yovel, G. (2015). A Revised Neural Framework for Face Processing. *Annual Review of Vision Science*, *1*(1), 393–416. doi: [10.1146/annurev-vision-082114-035518](https://doi.org/10.1146/annurev-vision-082114-035518)
- Dundas, E. M., Plaut, D. C., & Behrmann, M. (2015). Variable Left-hemisphere Language and Orthographic Lateralization Reduces Right-hemisphere Face Lateralization. *Journal of Cognitive Neuroscience*, *27*(5), 913–925. doi: [10.1162/jocn_a_00757](https://doi.org/10.1162/jocn_a_00757)
- Duprez, J., Gulbinaite, R., & Cohen, M. X. (2020). Midfrontal theta phase coordinates behaviorally relevant brain computations during cognitive control. *NeuroImage*, *207*, 116340. doi: [10.1016/j.neuroimage.2019.116340](https://doi.org/10.1016/j.neuroimage.2019.116340)
- Dye, M. W. G., Baril, D. E., & Bavelier, D. (2007). Which aspects of visual attention are changed by deafness? The case of the Attentional Network Test. *Neuropsychologia*, *45*(8), 1801–1811. doi: [10.1016/j.neuropsychologia.2006.12.019](https://doi.org/10.1016/j.neuropsychologia.2006.12.019)
- Dye, M. W. G., Hauser, P. C., & Bavelier, D. (2008). Visual Skills and Cross-Modal Plasticity in Deaf Readers. *Annals of the New York Academy of Sciences*, *1145*, 71–82. doi: [10.1196/annals.1416.013](https://doi.org/10.1196/annals.1416.013)
- Dye, M. W. G., Hauser, P. C., & Bavelier, D. (2009). Is Visual Selective Attention in Deaf Individuals Enhanced or Deficient? The Case of the Useful Field of View. *PLoS ONE*, *4*(5), e5640. doi: [10.1371/journal.pone.0005640](https://doi.org/10.1371/journal.pone.0005640)
- Dzhelyova, M., Jacques, C., & Rossion, B. (2017). At a Single Glance: Fast Periodic Visual Stimulation Uncovers the Spatio-Temporal Dynamics of Brief Facial Expression Changes in the Human Brain. *Cerebral Cortex*, *27*(8), 4106–4123. doi: [10.1093/cercor/bhw223](https://doi.org/10.1093/cercor/bhw223)
- Dzhelyova, M., & Rossion, B. (2014a). Supra-additive contribution of shape and surface information to individual face discrimination as revealed by fast periodic visual stimulation. *Journal of Vision*, *14*(14), 15. doi: [10.1167/14.14.15](https://doi.org/10.1167/14.14.15)
- Dzhelyova, M., & Rossion, B. (2014b). The effect of parametric stimulus size variation on individual face discrimination indexed by fast periodic visual stimulation. *BMC Neuroscience*, *15*(1), 87. doi: [10.1186/1471-2202-15-87](https://doi.org/10.1186/1471-2202-15-87)
- Elbert, T., Flor, H., Birbaumer, N., Knecht, S., Hampson, S., Larbig, W., & Taub, E. (1994). Extensive reorganization of the somatosensory cortex in adult humans after nervous system injury. *Neuroreport*, *5*(18), 2593–2597. doi: [10.1097/00001756-199412000-00047](https://doi.org/10.1097/00001756-199412000-00047)
- Elbert, Thomas, Sterr, A., Rockstroh, B., Pantev, C., Müller, M. M., & Taub, E. (2002). Expansion of the Tonotopic Area in the Auditory Cortex of the Blind. *Journal of Neuroscience*, *22*(22), 9941–9944. doi: [10.1523/JNEUROSCI.22-22-09941.2002](https://doi.org/10.1523/JNEUROSCI.22-22-09941.2002)
- Elliott, E. A., & Jacobs, A. M. (2013). Facial Expressions, Emotions, and Sign Languages. *Frontiers in Psychology*, *4*, 115. doi: [10.3389/fpsyg.2013.00115](https://doi.org/10.3389/fpsyg.2013.00115)
- Emmorey, K., & McCullough, S. (2009). The bimodal bilingual brain: Effects of sign language experience. *Brain and Language*, *109*(2), 124–132. doi: [10.1016/j.bandl.2008.03.005](https://doi.org/10.1016/j.bandl.2008.03.005)

- Emmorey, K., Midgley, K. J., Kohen, C. B., Sehyr, Z. S., & Holcomb, P. J. (2017). The N170 ERP component differs in laterality, distribution, and association with continuous reading measures for deaf and hearing readers. *Neuropsychologia*, *106*, 298–309. doi: [10.1016/j.neuropsychologia.2017.10.001](https://doi.org/10.1016/j.neuropsychologia.2017.10.001)
- Emmorey, K., Weisberg, J., McCullough, S., & Petrich, J. A. F. (2013). Mapping the reading circuitry for skilled deaf readers: An fMRI study of semantic and phonological processing. *Brain and Language*, *126*(2), 169–180. doi: [10.1016/j.bandl.2013.05.001](https://doi.org/10.1016/j.bandl.2013.05.001)
- Engel, A. K., Fries, P., & Singer, W. (2001). Dynamic predictions: Oscillations and synchrony in top-down processing. *Nature Reviews Neuroscience*, *2*(10), 704–716. doi: [10.1038/35094565](https://doi.org/10.1038/35094565)
- Engell, A. D., & McCarthy, G. (2014). Repetition suppression of face-selective evoked and induced EEG recorded from human cortex. *Human Brain Mapping*, *35*(8), 4155–4162. doi: [10.1002/hbm.22467](https://doi.org/10.1002/hbm.22467)
- Etard, O., & Reichenbach, T. (2019). Neural speech tracking in the theta and in the delta frequency band differentially encode clarity and comprehension of speech in noise. *The Journal of Neuroscience*, 1828–18. doi: [10.1523/JNEUROSCI.1828-18.2019](https://doi.org/10.1523/JNEUROSCI.1828-18.2019)
- Facchini, S., & Aglioti, S. M. (2003). Short term light deprivation increases tactile spatial acuity in humans. *Neurology*, *60*(12), 1998–1999. doi: [10.1212/01.wnl.0000068026.15208.d0](https://doi.org/10.1212/01.wnl.0000068026.15208.d0)
- Fiedler, L., Wöstmann, M., Herbst, S. K., & Obleser, J. (2019). Late cortical tracking of ignored speech facilitates neural selectivity in acoustically challenging conditions. *NeuroImage*, *186*, 33–42. doi: [10.1016/j.neuroimage.2018.10.057](https://doi.org/10.1016/j.neuroimage.2018.10.057)
- File, D., & Czigler, I. (2019). Automatic detection of violations of statistical regularities in the periphery is affected by the focus of spatial attention: A visual mismatch negativity study. *European Journal of Neuroscience*, *49*(10), 1348–1356. doi: [10.1111/ejn.14306](https://doi.org/10.1111/ejn.14306)
- Finke, M., Büchner, A., Ruigendijk, E., Meyer, M., & Sandmann, P. (2016). On the relationship between auditory cognition and speech intelligibility in cochlear implant users: An ERP study. *Neuropsychologia*, *87*, 169–181. doi: [10.1016/j.neuropsychologia.2016.05.019](https://doi.org/10.1016/j.neuropsychologia.2016.05.019)
- Finney, E. M., Clementz, B. A., Hickok, G., & Dobkins, K. R. (2003). Visual stimuli activate auditory cortex in deaf subjects: Evidence from MEG. *NeuroReport*, *14*(11), 1425–1427.
- Finney, E. M., Fine, I., & Dobkins, K. R. (2001). Visual stimuli activate auditory cortex in the deaf. *Nature Neuroscience*, *4*(12), 1171–1173. doi: [10.1038/nn763](https://doi.org/10.1038/nn763)
- Fischl, B. (2012). FreeSurfer. *NeuroImage*, *62*(2), 774–781. doi: [10.1016/j.neuroimage.2012.01.021](https://doi.org/10.1016/j.neuroimage.2012.01.021)
- Foster, J. J., & Awh, E. (2019). The role of alpha oscillations in spatial attention: Limited evidence for a suppression account. *Current Opinion in Psychology*, *29*, 34–40. doi: [10.1016/j.copsyc.2018.11.001](https://doi.org/10.1016/j.copsyc.2018.11.001)
- Foxe, J., & Snyder, A. (2011). The Role of Alpha-Band Brain Oscillations as a Sensory Suppression Mechanism during Selective Attention. *Frontiers in Psychology*, *2*, 154. doi: [10.3389/fpsyg.2011.00154](https://doi.org/10.3389/fpsyg.2011.00154)

- Friston, K. (2005). A theory of cortical responses. *Philosophical Transactions of the Royal Society B: Biological Sciences*, 360, 815–836. doi: [10.1098/rstb.2005.1622](https://doi.org/10.1098/rstb.2005.1622)
- Fründ, I., Busch, N., Körner, U., Schadow, J., & Herrmann, C. S. (2007). EEG oscillations in the gamma and alpha range respond differently to spatial frequency. *Vision Research*, 47(15), 2086–2098. doi: [10.1016/j.visres.2007.03.022](https://doi.org/10.1016/j.visres.2007.03.022)
- Fuglsang, S. A., Dau, T., & Hjortkjaer, J. (2017). Noise-robust cortical tracking of attended speech in real-world acoustic scenes. *NeuroImage*, 156, 435–444. doi: [10.1016/j.neuroimage.2017.04.026](https://doi.org/10.1016/j.neuroimage.2017.04.026)
- Gainotti, G., & Marra, C. (2011). Differential Contribution of Right and Left Temporo-Occipital and Anterior Temporal Lesions to Face Recognition Disorders. *Frontiers in Human Neuroscience*, 5:55. doi: [10.3389/fnhum.2011.00055](https://doi.org/10.3389/fnhum.2011.00055)
- Galaburda, A. M., & Pandya, D. N. (1983). The intrinsic architectonic and connective organization of the superior temporal region of the rhesus monkey. *Journal of Comparative Neurology*, 221(2), 169–184. doi: <https://doi.org/10.1002/cne.902210206>
- Garcia Lecumberri, M. L., & Cooke, M. (2006). Effect of masker type on native and non-native consonant perception in noise. *The Journal of the Acoustical Society of America*, 119(4), 2445–2454. doi: [10.1121/1.2180210](https://doi.org/10.1121/1.2180210)
- Garrido, M. I., Kilner, J. M., Stephan, K. E., & Friston, K. J. (2009). The mismatch negativity: A review of underlying mechanisms. *Clinical Neurophysiology*, 120(3), 453–463. doi: [10.1016/j.clinph.2008.11.029](https://doi.org/10.1016/j.clinph.2008.11.029)
- Genovese, C. R., Lazar, N. A., & Nichols, T. (2002). Thresholding of Statistical Maps in Functional Neuroimaging Using the False Discovery Rate. *NeuroImage*, 15(4), 870–878. doi: [10.1006/nimg.2001.1037](https://doi.org/10.1006/nimg.2001.1037)
- Ghitza, O., Giraud, A.-L., & Poeppel, D. (2013). Neuronal oscillations and speech perception: Critical-band temporal envelopes are the essence. *Frontiers in Human Neuroscience*, 6:340. doi: [10.3389/fnhum.2012.00340](https://doi.org/10.3389/fnhum.2012.00340)
- Giard, M. H., & Peronnet, F. (1999). Auditory-Visual Integration during Multimodal Object Recognition in Humans: A Behavioral and Electrophysiological Study. *Journal of Cognitive Neuroscience*, 11(5), 473–490. doi: [10.1162/08992999563544](https://doi.org/10.1162/08992999563544)
- Giraud, A.-L., & Poeppel, D. (2012). Cortical oscillations and speech processing: Emerging computational principles and operations. *Nature Neuroscience*, 15(4), 511–517. doi: [10.1038/nn.3063](https://doi.org/10.1038/nn.3063)
- Gotts, S. J., Chow, C. C., & Martin, A. (2012). Repetition priming and repetition suppression: A case for enhanced efficiency through neural synchronization. *Cognitive Neuroscience*, 3(3–4), 227–237. doi: [10.1080/17588928.2012.670617](https://doi.org/10.1080/17588928.2012.670617)
- Gougoux, F., Belin, P., Voss, P., Lepore, F., Lassonde, M., & Zatorre, R. J. (2009). Voice perception in blind persons: A functional magnetic resonance imaging study. *Neuropsychologia*, 47(13), 2967–2974. doi: [10.1016/j.neuropsychologia.2009.06.027](https://doi.org/10.1016/j.neuropsychologia.2009.06.027)
- Gougoux, F., Zatorre, R. J., Lassonde, M., Voss, P., & Lepore, F. (2005). A Functional Neuroimaging Study of Sound Localization: Visual Cortex Activity Predicts Performance in Early-Blind Individuals. *PLoS Biology*, 3(2), e27. doi: [10.1371/journal.pbio.0030027](https://doi.org/10.1371/journal.pbio.0030027)

- Gramfort, A., Papadopoulos, T., Olivi, E., & Clerc, M. (2010). OpenMEEG: Opensource software for quasistatic bioelectromagnetics. *BioMedical Engineering OnLine*, *9*(1), 45. doi: [10.1186/1475-925X-9-45](https://doi.org/10.1186/1475-925X-9-45)
- Grill-Spector, K., Henson, R., & Martin, A. (2006). Repetition and the brain: Neural models of stimulus-specific effects. *Trends in Cognitive Sciences*, *10*(1), 14–23. doi: [10.1016/j.tics.2005.11.006](https://doi.org/10.1016/j.tics.2005.11.006)
- Grill-Spector, K., Weiner, K. S., Kay, K., & Gomez, J. (2017). The Functional Neuroanatomy of Human Face Perception. *Annual Review of Vision Science*, *3*(1), 167–196. doi: [10.1146/annurev-vision-102016-061214](https://doi.org/10.1146/annurev-vision-102016-061214)
- Gross, J., Hoogenboom, N., Thut, G., Schyns, P., Panzeri, S., Belin, P., & Garrod, S. (2013). Speech Rhythms and Multiplexed Oscillatory Sensory Coding in the Human Brain. *PLOS Biology*, *11*(12), e1001752. doi: [10.1371/journal.pbio.1001752](https://doi.org/10.1371/journal.pbio.1001752)
- Grotheer, M., & Kovács, G. (2016). Can predictive coding explain repetition suppression? *Cortex*, *80*, 113–124. doi: [10.1016/j.cortex.2015.11.027](https://doi.org/10.1016/j.cortex.2015.11.027)
- Gruber, T., Giabbiconi, C.-M., Trujillo-Barreto, N. J., & Müller, M. M. (2006). Repetition suppression of induced gamma band responses is eliminated by task switching. *European Journal of Neuroscience*, *24*(9), 2654–2660. doi: [10.1111/j.1460-9568.2006.05130.x](https://doi.org/10.1111/j.1460-9568.2006.05130.x)
- Gruber, T., Malinowski, P., & Müller, M. M. (2004). Modulation of oscillatory brain activity and evoked potentials in a repetition priming task in the human EEG: Oscillatory brain activity and repetition priming. *European Journal of Neuroscience*, *19*(4), 1073–1082. doi: [10.1111/j.0953-816X.2004.03176.x](https://doi.org/10.1111/j.0953-816X.2004.03176.x)
- Gustafson, S. J., Billings, C. J., Hornsby, B. W. Y., & Key, A. P. (2019). Effect of competing noise on cortical auditory evoked potentials elicited by speech sounds in 7- to 25-year-old listeners. *Hearing Research*, *373*, 103–112. doi: [10.1016/j.heares.2019.01.004](https://doi.org/10.1016/j.heares.2019.01.004)
- Háden, G. P., Németh, R., Török, M., & Winkler, I. (2016). Mismatch response (MMR) in neonates: Beyond refractoriness. *Biological Psychology*, *117*, 26–31. doi: [10.1016/j.biopsycho.2016.02.004](https://doi.org/10.1016/j.biopsycho.2016.02.004)
- Hairston, W. D., Hodges, D. A., Casanova, R., Hayasaka, S., Kraft, R., Maldjian, J. A., & Burdette, J. H. (2008). Closing the mind's eye: Deactivation of visual cortex related to auditory task difficulty. *NeuroReport*, *19*(2), 151–154. doi: [10.1097/WNR.0b013e3282f42509](https://doi.org/10.1097/WNR.0b013e3282f42509)
- Hamilton, L. S., & Huth, A. G. (2020). The revolution will not be controlled: Natural stimuli in speech neuroscience. *Language, Cognition and Neuroscience*, *35*(5), 573–582. doi: [10.1080/23273798.2018.1499946](https://doi.org/10.1080/23273798.2018.1499946)
- Hänel-Faulhaber, B., Skotara, N., Kügow, M., Salden, U., Bottari, D., & Röder, B. (2014). ERP correlates of German Sign Language processing in deaf native signers. *BMC Neuroscience*, *15*(1), 62. doi: [10.1186/1471-2202-15-62](https://doi.org/10.1186/1471-2202-15-62)
- Hansen, J. C., & Hillyard, S. A. (1980). Endogenous brain potentials associated with selective auditory attention. *Electroencephalography and Clinical Neurophysiology*, *49*(3–4), 277–290. doi: [10.1016/0013-4694\(80\)90222-9](https://doi.org/10.1016/0013-4694(80)90222-9)
- Hansen, P., Kringelbach, M., & Salmelin, R. (2010). *MEG: An Introduction to Methods*.

Oxford University Press. doi: [10.1093/acprof:oso/9780195307238.001.0001](https://doi.org/10.1093/acprof:oso/9780195307238.001.0001)

Haufe, S., Meinecke, F., Gorgen, K., Dhne, S., Haynes, J.-D., Blankertz, B., & Biemann, F. (2014). On the interpretation of weight vectors of linear models in multivariate neuroimaging. *NeuroImage*, *87*, 96–110. doi: [10.1016/j.neuroimage.2013.10.067](https://doi.org/10.1016/j.neuroimage.2013.10.067)

Hauser, P., Paludneviciene, R., Supalla, T., & Bavelier, D. (2008). American Sign Language - Sentence reproduction test: Development & implications. *Sign Languages: Spinning and Unraveling the Past, Present and Future*, 155–167.

Hausfeld, L., Riecke, L., Valente, G., & Formisano, E. (2018). Cortical tracking of multiple streams outside the focus of attention in naturalistic auditory scenes. *NeuroImage*, *181*, 617–626. doi: [10.1016/j.neuroimage.2018.07.052](https://doi.org/10.1016/j.neuroimage.2018.07.052)

Hauswald, A., Lithari, C., Collignon, O., Leonardelli, E., & Weisz, N. (2018). A Visual Cortical Network for Deriving Phonological Information from Intelligible Lip Movements. *Current Biology*, *28*(9), 1453–1459.e3. doi: [10.1016/j.cub.2018.03.044](https://doi.org/10.1016/j.cub.2018.03.044)

Hauthal, N., Sandmann, P., Debener, S., & Thorne, J. D. (2013). Visual movement perception in deaf and hearing individuals. *Advances in Cognitive Psychology*, *9*(2), 53–61. doi: [10.5709/acp-0131-z](https://doi.org/10.5709/acp-0131-z)

Hauthal, N., Thorne, J. D., Debener, S., & Sandmann, P. (2014). Source Localisation of Visual Evoked Potentials in Congenitally Deaf Individuals. *Brain Topography*, *27*(3), 412–424. doi: [10.1007/s10548-013-0341-7](https://doi.org/10.1007/s10548-013-0341-7)

Haxby, J. V., Hoffman, E. A., & Gobbini, M. I. (2000). The distributed human neural system for face perception. *Trends in Cognitive Sciences*, *4*(6), 223–233. doi: [10.1016/S1364-6613\(00\)01482-0](https://doi.org/10.1016/S1364-6613(00)01482-0)

Heimler, B., Weisz, N., & Collignon, O. (2014). Revisiting the adaptive and maladaptive effects of crossmodal plasticity. *Neuroscience*, *283*, 44–63. doi: [10.1016/j.neuroscience.2014.08.003](https://doi.org/10.1016/j.neuroscience.2014.08.003)

Heimler, B., & Amedi, A. (2020). Are critical periods reversible in the adult brain? Insights on cortical specializations based on sensory deprivation studies. *Neuroscience & Biobehavioral Reviews*, *116*, 494–507. doi: [10.1016/j.neubiorev.2020.06.034](https://doi.org/10.1016/j.neubiorev.2020.06.034)

Heinrich, S. P. (2009). Permutation-Based Significance Tests for Multiharmonic Steady-State Evoked Potentials. *IEEE Transactions on Biomedical Engineering*, *56*(2), 534–537. doi: [10.1109/TBME.2008.2006021](https://doi.org/10.1109/TBME.2008.2006021)

Herrmann, C. S., Grigutsch, M., & Busch, N. (2004). EEG Oscillations and Wavelet Analysis. In *T. C. Handy (Ed), Event-related potentials: A methods handbook*. (pp. 229–259). Cambridge, MA: MIT Press.

Herrmann, C. S., Rach, S., Vosskuhl, J., & Strber, D. (2014). Time–Frequency Analysis of Event-Related Potentials: A Brief Tutorial. *Brain Topography*, *27*(4), 438–450. doi: [10.1007/s10548-013-0327-5](https://doi.org/10.1007/s10548-013-0327-5)

Hertrich, I., Dietrich, S., & Ackermann, H. (2020). The Margins of the Language Network in the Brain. *Frontiers in Communication*, *5*:519955. doi: [10.3389/fcomm.2020.519955](https://doi.org/10.3389/fcomm.2020.519955)

Hesse, P. N., Schmitt, C., Klingenhoefer, S., & Bremmer, F. (2017). Preattentive Processing

- of Numerical Visual Information. *Frontiers in Human Neuroscience*, *11*, 70. doi: [10.3389/fnhum.2017.00070](https://doi.org/10.3389/fnhum.2017.00070)
- Hickok, G., & Poeppel, D. (2007). The cortical organization of speech processing. *Nature Reviews Neuroscience*, *8*(5), 393–402. doi: [10.1038/nrn2113](https://doi.org/10.1038/nrn2113)
- Hidaka, S., & Ide, M. (2015). Sound can suppress visual perception. *Scientific Reports*, *5*(1), 10483. doi: [10.1038/srep10483](https://doi.org/10.1038/srep10483)
- Holdgraf, C. R., Rieger, J. W., Micheli, C., Martin, S., Knight, R. T., & Theunissen, F. E. (2017). Encoding and Decoding Models in Cognitive Electrophysiology. *Frontiers in Systems Neuroscience*, *11*. doi: [10.3389/fnsys.2017.00061](https://doi.org/10.3389/fnsys.2017.00061)
- Hoover, A. E. N., Démonet, J.-F., & Steeves, J. K. E. (2010). Superior voice recognition in a patient with acquired prosopagnosia and object agnosia. *Neuropsychologia*, *48*(13), 3725–3732. doi: [10.1016/j.neuropsychologia.2010.09.008](https://doi.org/10.1016/j.neuropsychologia.2010.09.008)
- Howard, C. J., & Holcombe, A. O. (2010). Unexpected changes in direction of motion attract attention. *Attention, Perception, & Psychophysics*, *72*(8), 2087–2095. doi: [10.3758/BF03196685](https://doi.org/10.3758/BF03196685)
- Howard, M. F., & Poeppel, D. (2010). Discrimination of Speech Stimuli Based on Neuronal Response Phase Patterns Depends on Acoustics But Not Comprehension. *Journal of Neurophysiology*, *104*(5), 2500–2511. doi: [10.1152/jn.00251.2010](https://doi.org/10.1152/jn.00251.2010)
- Hsu, Y.-F., Hämäläinen, J. A., & Waszak, F. (2014). Repetition suppression comprises both attention-independent and attention-dependent processes. *NeuroImage*, *98*, 168–175. doi: [10.1016/j.neuroimage.2014.04.084](https://doi.org/10.1016/j.neuroimage.2014.04.084)
- Huber, E., Chang, K., Alvarez, I., Hundle, A., Bridge, H., & Fine, I. (2019). Early Blindness Shapes Cortical Representations of Auditory Frequency within Auditory Cortex. *Journal of Neuroscience*, *39*(26), 5143–5152. doi: [10.1523/JNEUROSCI.2896-18.2019](https://doi.org/10.1523/JNEUROSCI.2896-18.2019)
- Huotilainen, M., Winkler, I., Alho, K., Escera, C., Virtanen, J., Ilmoniemi, R. J., ... Näätänen, R. (1998). Combined mapping of human auditory EEG and MEG responses. *Electroencephalography and Clinical Neurophysiology*, *108*(4), 370–379. doi: [10.1016/s0168-5597\(98\)00017-3](https://doi.org/10.1016/s0168-5597(98)00017-3)
- Huth, A. G., de Heer, W. A., Griffiths, T. L., Theunissen, F. E., & Gallant, J. L. (2016). Natural speech reveals the semantic maps that tile human cerebral cortex. *Nature*, *532*(7600), 453–458. doi: [10.1038/nature17637](https://doi.org/10.1038/nature17637)
- Huth, A. G., Lee, T., Nishimoto, S., Bilenko, N. Y., Vu, A. T., & Gallant, J. L. (2016). Decoding the Semantic Content of Natural Movies from Human Brain Activity. *Frontiers in Systems Neuroscience*, *10*:81. doi: [10.3389/fnsys.2016.00081](https://doi.org/10.3389/fnsys.2016.00081)
- Huth, A. G., Nishimoto, S., Vu, A. T., & Gallant, J. L. (2012). A continuous semantic space describes the representation of thousands of object and action categories across the human brain. *Neuron*, *76*(6), 1210–1224. doi: [10.1016/j.neuron.2012.10.014](https://doi.org/10.1016/j.neuron.2012.10.014)
- Jääskeläinen, I. P., Sams, M., Glerean, E., & Ahveninen, J. (2021). Movies and narratives as naturalistic stimuli in neuroimaging. *NeuroImage*, *224*, 117445. doi: [10.1016/j.neuroimage.2020.117445](https://doi.org/10.1016/j.neuroimage.2020.117445)

- Jensen, O., Mathilde, B., Marshall, T., & Tiesinga, P. (2015). Oscillatory mechanisms of feedforward and feedback visual processing. *Trends in Neurosciences*, *38*(4), 192–194. doi: [10.1016/j.tins.2015.02.006](https://doi.org/10.1016/j.tins.2015.02.006)
- Jensen, O., & Mazaheri, A. (2010). Shaping Functional Architecture by Oscillatory Alpha Activity: Gating by Inhibition. *Frontiers in Human Neuroscience*, *4*, 186. doi: [10.3389/fnhum.2010.00186](https://doi.org/10.3389/fnhum.2010.00186)
- Jensen, O., Spaak, E., & Zumer, J. (2014). Human Brain Oscillations: From Physiological Mechanisms to Analysis and Cognition. In *Magnetoencephalography: From Signals to Dynamic Cortical Networks* (pp. 359–404). doi: [10.1007/978-3-642-33045-2_17](https://doi.org/10.1007/978-3-642-33045-2_17)
- Johnson, J. A., & Zatorre, R. J. (2006). Neural substrates for dividing and focusing attention between simultaneous auditory and visual events. *NeuroImage*, *31*(4), 1673–1681. doi: [10.1016/j.neuroimage.2006.02.026](https://doi.org/10.1016/j.neuroimage.2006.02.026)
- Jung, T.-P., Makeig, S., Humphries, C., Lee, T.-W., McKEOWN, M. J., Iragui, V., & Sejnowski, T. J. (2000). Removing electroencephalographic artifacts by blind source separation. *Psychophysiology*, *37*(2), 163–178. doi: [10.1111/1469-8986.3720163](https://doi.org/10.1111/1469-8986.3720163)
- Jung, T.-P., Makeig, S., Westerfield, M., Townsend, J., Courchesne, E., & Sejnowski, T. J. (2000). Removal of eye activity artifacts from visual event-related potentials in normal and clinical subjects. *Clinical Neurophysiology*, *111*(10), 1745–1758. doi: [10.1016/S1388-2457\(00\)00386-2](https://doi.org/10.1016/S1388-2457(00)00386-2)
- Kafkas, A., & Montaldi, D. (2018). How do memory systems detect and respond to novelty? *Neuroscience Letters*, *680*, 60–68. doi: [10.1016/j.neulet.2018.01.053](https://doi.org/10.1016/j.neulet.2018.01.053)
- Kaliukhovich, D. A., & Vogels, R. (2012). Stimulus repetition affects both strength and synchrony of macaque inferior temporal cortical activity. *Journal of Neurophysiology*, *107*(12), 3509–3527. doi: [10.1152/jn.00059.2012](https://doi.org/10.1152/jn.00059.2012)
- Karns, C. M., Dow, M. W., & Neville, H. J. (2012). Altered Cross-Modal Processing in the Primary Auditory Cortex of Congenitally Deaf Adults: A Visual-Somatosensory fMRI Study with a Double-Flash Illusion. *Journal of Neuroscience*, *32*(28), 9626–9638. doi: [10.1523/JNEUROSCI.6488-11.2012](https://doi.org/10.1523/JNEUROSCI.6488-11.2012)
- Kaufeld, G., Bosker, H. R., Oever, S. ten, Alday, P. M., Meyer, A. S., & Martin, A. E. (2020). Linguistic Structure and Meaning Organize Neural Oscillations into a Content-Specific Hierarchy. *Journal of Neuroscience*, *40*(49), 9467–9475. doi: [10.1523/JNEUROSCI.0302-20.2020](https://doi.org/10.1523/JNEUROSCI.0302-20.2020)
- Kerlin, J. R., Shahin, A. J., & Miller, L. M. (2010). Attentional Gain Control of Ongoing Cortical Speech Representations in a “Cocktail Party.” *The Journal of Neuroscience*, *30*(2), 620–628. doi: [10.1523/JNEUROSCI.3631-09.2010](https://doi.org/10.1523/JNEUROSCI.3631-09.2010)
- Keshavarzi, M., Kegler, M., Kadir, S., & Reichenbach, T. (2020). Transcranial alternating current stimulation in the theta band but not in the delta band modulates the comprehension of naturalistic speech in noise. *NeuroImage*, *210*, 116557. doi: [10.1016/j.neuroimage.2020.116557](https://doi.org/10.1016/j.neuroimage.2020.116557)
- Kienitz, R., Cox, M. A., Dougherty, K., Saunders, R. C., Schmiedt, J. T., Leopold, D. A., ... Schmid, M. C. (2021). Theta, but Not Gamma Oscillations in Area V4 Depend on Input

from Primary Visual Cortex. *Current Biology*, 31(3), 635–642.e3. doi: [10.1016/j.cub.2020.10.091](https://doi.org/10.1016/j.cub.2020.10.091)

Kimura, M., Ohira, H., & Schröger, E. (2010). Localizing sensory and cognitive systems for pre-attentive visual deviance detection: An sLORETA analysis of the data of Kimura et al. (2009). *Neuroscience Letters*, 485(3), 198–203. doi: [10.1016/j.neulet.2010.09.011](https://doi.org/10.1016/j.neulet.2010.09.011)

Klimesch, W. (2012). Alpha-band oscillations, attention, and controlled access to stored information. *Trends in Cognitive Sciences*, 16(12), 606–617. doi: [10.1016/j.tics.2012.10.007](https://doi.org/10.1016/j.tics.2012.10.007)

Klimesch, W. (2018). The frequency architecture of brain and brain body oscillations: An analysis. *European Journal of Neuroscience*, 48(7), 2431–2453. doi: [10.1111/ejn.14192](https://doi.org/10.1111/ejn.14192)

Klimesch, W., Fellinger, R., & Freunberger, R. (2011). Alpha Oscillations and Early Stages of Visual Encoding. *Front. Psychology*. doi: [10.3389/fpsyg.2011.00118](https://doi.org/10.3389/fpsyg.2011.00118)

Klimesch, W., Sauseng, P., & Hanslmayr, S. (2007). EEG alpha oscillations: The inhibition–timing hypothesis. *Brain Research Reviews*, 53(1), 63–88. doi: [10.1016/j.brainresrev.2006.06.003](https://doi.org/10.1016/j.brainresrev.2006.06.003)

Kohn, A. (2007). Visual Adaptation: Physiology, Mechanisms, and Functional Benefits. *Journal of Neurophysiology*, 97(5), 3155–3164. doi: [10.1152/jn.00086.2007](https://doi.org/10.1152/jn.00086.2007)

Kösem, A., & van Wassenhove, V. (2017). Distinct contributions of low- and high-frequency neural oscillations to speech comprehension. *Language, Cognition and Neuroscience*, 32(5), 536–544. doi: [10.1080/23273798.2016.1238495](https://doi.org/10.1080/23273798.2016.1238495)

Kral, A. (2013). Auditory critical periods: A review from system’s perspective. *Neuroscience*, 247, 117–133. doi: [10.1016/j.neuroscience.2013.05.021](https://doi.org/10.1016/j.neuroscience.2013.05.021)

Kral, A., Dorman, M. F., & Wilson, B. S. (2019). Neuronal Development of Hearing and Language: Cochlear Implants and Critical Periods. *Annual Review of Neuroscience*, 42(1), 47–65. doi: [10.1146/annurev-neuro-080317-061513](https://doi.org/10.1146/annurev-neuro-080317-061513)

Kral, A., & Eggermont, J. J. (2007). What’s to lose and what’s to learn: Development under auditory deprivation, cochlear implants and limits of cortical plasticity. *Brain Research Reviews*, 56(1), 259–269. doi: [10.1016/j.brainresrev.2007.07.021](https://doi.org/10.1016/j.brainresrev.2007.07.021)

Kral, A., Kronenberger, W. G., Pisoni, D. B., & O’Donoghue, G. M. (2016). Neurocognitive factors in sensory restoration of early deafness: A connectome model. *The Lancet Neurology*, 15(6), 610–621. doi: [10.1016/S1474-4422\(16\)00034-X](https://doi.org/10.1016/S1474-4422(16)00034-X)

Kral, A., & Sharma, A. (2012). Developmental neuroplasticity after cochlear implantation. *Trends in Neurosciences*, 35(2), 111–122. doi: [10.1016/j.tins.2011.09.004](https://doi.org/10.1016/j.tins.2011.09.004)

Kral, A., Yusuf, P. A., & Land, R. (2017). Higher-order auditory areas in congenital deafness: Top-down interactions and corticocortical decoupling. *Hearing Research*, 343, 50–63. doi: [10.1016/j.heares.2016.08.017](https://doi.org/10.1016/j.heares.2016.08.017)

Kupers, R., & Ptito, M. (2014). Compensatory plasticity and cross-modal reorganization following early visual deprivation. *Neuroscience & Biobehavioral Reviews*, 41, 36–52. doi: [10.1016/j.neubiorev.2013.08.001](https://doi.org/10.1016/j.neubiorev.2013.08.001)

Kurthen, I., Galbier, J., Jagoda, L., Neuschwander, P., Giroud, N., & Meyer, M. (2021). Selective attention modulates neural envelope tracking of informationally masked speech

- in healthy older adults. *Human Brain Mapping*, 42(10), 3042–3057. doi: [10.1002/hbm.25415](https://doi.org/10.1002/hbm.25415)
- Kushnerenko, E., Ceponiene, R., Balan, P., Fellman, V., & Näätänen, R. (2002). Maturation of the auditory change detection response in infants: A longitudinal ERP study. *NeuroReport*, 13(15), 1843–1848. doi: <https://doi.org/10.1097/00001756-200210280-00002>
- Lakatos, P., Gross, J., & Thut, G. (2019). A New Unifying Account of the Roles of Neuronal Entrainment. *Current Biology*, 29(18), R890–R905. doi: [10.1016/j.cub.2019.07.075](https://doi.org/10.1016/j.cub.2019.07.075)
- Lakatos, P., O’Connell, M. N., Barczak, A., Mills, A., Javitt, D. C., & Schroeder, C. E. (2009). The Leading Sense: Supramodal Control of Neurophysiological Context by Attention. *Neuron*, 64(3), 419–430. doi: [10.1016/j.neuron.2009.10.014](https://doi.org/10.1016/j.neuron.2009.10.014)
- Lalor, E. C., & Foxe, J. J. (2010). Neural responses to uninterrupted natural speech can be extracted with precise temporal resolution. *European Journal of Neuroscience*, 31(1), 189–193. doi: [10.1111/j.1460-9568.2009.07055.x](https://doi.org/10.1111/j.1460-9568.2009.07055.x)
- Lalor, E. C., Pearlmutter, B. A., Reilly, R. B., McDarby, G., & Foxe, J. J. (2006). The VESPA: A method for the rapid estimation of a visual evoked potential. *NeuroImage*, 32(4), 1549–1561. doi: [10.1016/j.neuroimage.2006.05.054](https://doi.org/10.1016/j.neuroimage.2006.05.054)
- Lalor, E. C., Power, A. J., Reilly, R. B., & Foxe, J. J. (2009). Resolving Precise Temporal Processing Properties of the Auditory System Using Continuous Stimuli. *Journal of Neurophysiology*, 102(1), 349–359. doi: [10.1152/jn.90896.2008](https://doi.org/10.1152/jn.90896.2008)
- Land, R., Baumhoff, P., Tillein, J., Lomber, S. G., Hubka, P., & Kral, A. (2016). Cross-Modal Plasticity in Higher-Order Auditory Cortex of Congenitally Deaf Cats Does Not Limit Auditory Responsiveness to Cochlear Implants. *The Journal of Neuroscience*, 36(23), 6175–6185. doi: [10.1523/JNEUROSCI.0046-16.2016](https://doi.org/10.1523/JNEUROSCI.0046-16.2016)
- Land, R., Radecke, J.-O., & Kral, A. (2018). Congenital Deafness Reduces, But Does Not Eliminate Auditory Responsiveness in Cat Extrastriate Visual Cortex. *Neuroscience*, 375, 149–157. doi: [10.1016/j.neuroscience.2018.01.065](https://doi.org/10.1016/j.neuroscience.2018.01.065)
- Landry, S. P., Shiller, D. M., & Champoux, F. (2013). Short-term visual deprivation improves the perception of harmonicity. *Journal of Experimental Psychology: Human Perception and Performance*, 39(6), 1503–1507. doi: [10.1037/a0034015](https://doi.org/10.1037/a0034015)
- Lange, F., Seer, C., Finke, M., Dengler, R., & Kopp, B. (2015). Dual routes to cortical orienting responses: Novelty detection and uncertainty reduction. *Biological Psychology*, 105, 66–71. doi: [10.1016/j.biopsycho.2015.01.001](https://doi.org/10.1016/j.biopsycho.2015.01.001)
- Laurienti, P. J., Burdette, J. H., Wallace, M. T., Yen, Y.-F., Field, A. S., & Stein, B. E. (2002). Deactivation of Sensory-Specific Cortex by Cross-Modal Stimuli. *Journal of Cognitive Neuroscience*, 14(3), 420–429. doi: [10.1162/089892902317361930](https://doi.org/10.1162/089892902317361930)
- Lazzouni, L., Voss, P., & Lepore, F. (2012). Short-term crossmodal plasticity of the auditory steady-state response in blindfolded sighted individuals. *European Journal of Neuroscience*, 35(10), 1630–1636. doi: [10.1111/j.1460-9568.2012.08088.x](https://doi.org/10.1111/j.1460-9568.2012.08088.x)
- Lee, H.-K., & Whitt, J. (2015). Cross-modal synaptic plasticity in adult primary sensory cortices. *Current Opinion in Neurobiology*, 35, 119–126. doi: [10.1016/j.conb.2015.08.002](https://doi.org/10.1016/j.conb.2015.08.002)
- Legendre, G., Andrillon, T., Koroma, M., & Kouider, S. (2019). Sleepers track informative

speech in a multitalker environment. *Nature Human Behaviour*, 3(3), 274. doi: [10.1038/s41562-018-0502-5](https://doi.org/10.1038/s41562-018-0502-5)

Leleu, A., Dzhelyova, M., Rossion, B., Brochard, R., Durand, K., Schaal, B., & Baudouin, J.-Y. (2018). Tuning functions for automatic detection of brief changes of facial expression in the human brain. *NeuroImage*, 179, 235–251. doi: [10.1016/j.neuroimage.2018.06.048](https://doi.org/10.1016/j.neuroimage.2018.06.048)

Leonard, M. K., Ramirez, N. F., Torres, C., Travis, K. E., Hatrak, M., Mayberry, R. L., & Halgren, E. (2012). Signed Words in the Congenitally Deaf Evoke Typical Late Lexicosemantic Responses with No Early Visual Responses in Left Superior Temporal Cortex. *Journal of Neuroscience*, 32(28), 9700–9705. doi: [10.1523/JNEUROSCI.1002-12.2012](https://doi.org/10.1523/JNEUROSCI.1002-12.2012)

Lerner, Y., Honey, C. J., Silbert, L. J., & Hasson, U. (2011). Topographic Mapping of a Hierarchy of Temporal Receptive Windows Using a Narrated Story. *Journal of Neuroscience*, 31(8), 2906–2915. doi: [10.1523/JNEUROSCI.3684-10.2011](https://doi.org/10.1523/JNEUROSCI.3684-10.2011)

Lesenfants, D., Vanthornhout, J., Verschuere, E., Decruy, L., & Francart, T. (2019). Predicting individual speech intelligibility from the cortical tracking of acoustic- and phonetic-level speech representations. *Hearing Research*, 380, 1–9. doi: [10.1016/j.heares.2019.05.006](https://doi.org/10.1016/j.heares.2019.05.006)

Letourneau, S. M., & Mitchell, T. V. (2013). Visual field bias in hearing and deaf adults during judgments of facial expression and identity. *Frontiers in Psychology*, 4. doi: [10.3389/fpsyg.2013.00319](https://doi.org/10.3389/fpsyg.2013.00319)

Lin, F.-H., Witzel, T., Ahlfors, S. P., Stufflebeam, S. M., Belliveau, J. W., & Hämäläinen, M. S. (2006). Assessing and improving the spatial accuracy in MEG source localization by depth-weighted minimum-norm estimates. *NeuroImage*, 31(1), 160–171. doi: [10.1016/j.neuroimage.2005.11.054](https://doi.org/10.1016/j.neuroimage.2005.11.054)

Liu, Q., & Wang, L. (2021). T-Test and ANOVA for data with ceiling and/or floor effects. *Behavior Research Methods*, 53(1), 264–277. doi: [10.3758/s13428-020-01407-2](https://doi.org/10.3758/s13428-020-01407-2)

Liu-Shuang, J., Norcia, A. M., & Rossion, B. (2014). An objective index of individual face discrimination in the right occipito-temporal cortex by means of fast periodic oddball stimulation. *Neuropsychologia*, 52, 57–72. doi: [10.1016/j.neuropsychologia.2013.10.022](https://doi.org/10.1016/j.neuropsychologia.2013.10.022)

Lochy, A., de Heering, A., & Rossion, B. (2019). The non-linear development of the right hemispheric specialization for human face perception. *Neuropsychologia*, 126, 10–19. doi: [10.1016/j.neuropsychologia.2017.06.029](https://doi.org/10.1016/j.neuropsychologia.2017.06.029)

Liotile, R. E., Cusack, R., & Bedny, M. (2019). Naturalistic Audio-Movies and Narrative Synchronize “Visual” Cortices across Congenitally Blind But Not Sighted Individuals. *Journal of Neuroscience*, 39(45), 8940–8948. doi: [10.1523/JNEUROSCI.0298-19.2019](https://doi.org/10.1523/JNEUROSCI.0298-19.2019)

Lomber, S. G., Meredith, M. A., & Kral, A. (2010). Cross-modal plasticity in specific auditory cortices underlies visual compensations in the deaf. *Nature Neuroscience*, 13(11), 1421–1427. doi: [10.1038/nn.2653](https://doi.org/10.1038/nn.2653)

Lomber, S. G., Meredith, M. A., & Kral, A. (2011). Adaptive crossmodal plasticity in deaf auditory cortex. In *Progress in Brain Research* (Vol. 191, pp. 251–270). Elsevier. doi: [10.1016/B978-0-444-53752-2.00001-1](https://doi.org/10.1016/B978-0-444-53752-2.00001-1)

Lueschow, A., Miller, E. K., & Desimone, R. (1994). Inferior Temporal Mechanisms for

- Invariant Object Recognition. *Cerebral Cortex*, 4(5), 523–531. doi: [10.1093/cercor/4.5.523](https://doi.org/10.1093/cercor/4.5.523)
- Lundqvist, D., Flykt, A., & Öhman, A. (1998). The Karolinska Directed Emotional Faces - KDEF, CD ROM from Department of Clinical Neuroscience, Psychology section, Karolinska Institutet, ISBN 91-630-7164-9.
- Luo, H., & Poeppel, D. (2007). Phase Patterns of Neuronal Responses Reliably Discriminate Speech in Human Auditory Cortex. *Neuron*, 54(6), 1001–1010. doi: [10.1016/j.neuron.2007.06.004](https://doi.org/10.1016/j.neuron.2007.06.004)
- Macchi Cassia, V., Kuefner, D., Picozzi, M., & Vescovo, E. (2009). Early Experience Predicts Later Plasticity for Face Processing: Evidence for the Reactivation of Dormant Effects. *Psychological Science*, 20(7), 853–859. doi: [10.1111/j.1467-9280.2009.02376.x](https://doi.org/10.1111/j.1467-9280.2009.02376.x)
- Macchi Cassia, V., Turati, C., & Simion, F. (2004). Can a nonspecific bias toward top-heavy patterns explain newborns' face preference? *Psychological Science*, 15(6), 379–383. doi: [10.1111/j.0956-7976.2004.00688.x](https://doi.org/10.1111/j.0956-7976.2004.00688.x)
- MacSweeney, M., Woll, B., Campbell, R., McGuire, P. K., David, A. S., Williams, S. C. R., ... Brammer, M. J. (2002). Neural systems underlying British Sign Language and audio-visual English processing in native users. *Brain*, 125(7), 1583–1593. doi: [10.1093/brain/awf153](https://doi.org/10.1093/brain/awf153)
- Mai, G., Minett, J. W., & Wang, W. S.-Y. (2016). Delta, theta, beta, and gamma brain oscillations index levels of auditory sentence processing. *NeuroImage*, 133, 516–528. doi: [10.1016/j.neuroimage.2016.02.064](https://doi.org/10.1016/j.neuroimage.2016.02.064)
- Maraini, F. (2019). Gnòsi delle fânfole. La nave di Teseo.
- Maris, E., & Oostenveld, R. (2007). Nonparametric statistical testing of EEG- and MEG-data. *Journal of Neuroscience Methods*, 164(1), 177–190. doi: [10.1016/j.jneumeth.2007.03.024](https://doi.org/10.1016/j.jneumeth.2007.03.024)
- Martinelli, A., Handjaras, G., Betta, M., Leo, A., Cecchetti, L., Pietrini, P., ... Bottari, D. (2020). *Auditory features modelling demonstrates sound envelope representation in striate cortex*. bioRxiv. doi: [10.1101/2020.04.15.043174](https://doi.org/10.1101/2020.04.15.043174)
- McCarthy, C. (2014). The Road (M. Testa, Trans.). Einaudi. (Original work published 2006).
- Mazaheri, A., & Jensen, O. (2006). Posterior activity is not phase-reset by visual stimuli. *Proceedings of the National Academy of Sciences*, 103(8), 2948–2952. doi: [10.1073/pnas.0505785103](https://doi.org/10.1073/pnas.0505785103)
- McCullough, S., Emmorey, K., & Sereno, M. (2005). Neural organization for recognition of grammatical and emotional facial expressions in deaf ASL signers and hearing nonsigners. *Cognitive Brain Research*, 22(2), 193–203. doi: [10.1016/j.cogbrainres.2004.08.012](https://doi.org/10.1016/j.cogbrainres.2004.08.012)
- Merabet, L. B., Hamilton, R., Schlaug, G., Swisher, J. D., Kiriakopoulos, E. T., Pitskel, N. B., ... Pascual-Leone, A. (2008). Rapid and Reversible Recruitment of Early Visual Cortex for Touch. *PLOS ONE*, 3(8), e3046. doi: [10.1371/journal.pone.0003046](https://doi.org/10.1371/journal.pone.0003046)
- Merabet, L. B., & Pascual-Leone, A. (2010). Neural reorganization following sensory loss: The opportunity of change. *Nature Reviews Neuroscience*, 11(1), 44–52. doi: [10.1038/nrn2758](https://doi.org/10.1038/nrn2758)

- Michalareas, G., Vezoli, J., van Pelt, S., Schoffelen, J.-M., Kennedy, H., & Fries, P. (2016). Alpha-Beta and Gamma Rhythms Subserve Feedback and Feedforward Influences among Human Visual Cortical Areas. *Neuron*, *89*(2), 384–397. doi: [10.1016/j.neuron.2015.12.018](https://doi.org/10.1016/j.neuron.2015.12.018)
- Michel, C. M., & Brunet, D. (2019). EEG Source Imaging: A Practical Review of the Analysis Steps. *Frontiers in Neurology*, *10*. doi: [10.3389/fneur.2019.00325](https://doi.org/10.3389/fneur.2019.00325)
- Michel, C. M., Murray, M. M., Lantz, G., Gonzalez, S., Spinelli, L., & Grave de Peralta, R. (2004). EEG source imaging. *Clinical Neurophysiology*, *115*(10), 2195–2222. doi: [10.1016/j.clinph.2004.06.001](https://doi.org/10.1016/j.clinph.2004.06.001)
- Miller, E. K., Li, L., & Desimone, R. (1993). Activity of neurons in anterior inferior temporal cortex during a short-term memory task. *The Journal of Neuroscience*, *13*(4), 1460–1478. doi: [10.1523/JNEUROSCI.13-04-01460.1993](https://doi.org/10.1523/JNEUROSCI.13-04-01460.1993)
- Miller, S. E., Graham, J., & Schafer, E. (2021). Auditory Sensory Gating of Speech and Nonspeech Stimuli. *Journal of Speech, Language, and Hearing Research*, *64*(4), 1404–1412. doi: [10.1044/2020_JSLHR-20-00535](https://doi.org/10.1044/2020_JSLHR-20-00535)
- Mirkovic, B., Debener, S., Jaeger, M., & De Vos, M. (2015). Decoding the attended speech stream with multi-channel EEG: Implications for online, daily-life applications. *Journal of Neural Engineering*, *12*(4), 046007. doi: [10.1088/1741-2560/12/4/046007](https://doi.org/10.1088/1741-2560/12/4/046007)
- Molinaro, N., & Lizarazu, M. (2018). Delta (but not theta)-band cortical entrainment involves speech-specific processing. *European Journal of Neuroscience*, *48*(7), 2642–2650. doi: [10.1111/ejn.13811](https://doi.org/10.1111/ejn.13811)
- Morales, S., & Bowers, M. E. (2022). Time-frequency analysis methods and their application in developmental EEG data. *Developmental Cognitive Neuroscience*, *54*, 101067. doi: [10.1016/j.dcn.2022.101067](https://doi.org/10.1016/j.dcn.2022.101067)
- Morlet, D., & Fischer, C. (2014). MMN and Novelty P3 in Coma and Other Altered States of Consciousness: A Review. *Brain Topography*, *27*(4), 467–479. doi: [10.1007/s10548-013-0335-5](https://doi.org/10.1007/s10548-013-0335-5)
- Mouraux, A., & Iannetti, G. D. (2008). Across-trial averaging of event-related EEG responses and beyond. *Magnetic Resonance Imaging*, *26*(7), 1041–1054. doi: [10.1016/j.mri.2008.01.011](https://doi.org/10.1016/j.mri.2008.01.011)
- Muchnik, C., Efrati, M., Nemeth, E., Malin, M., & Hildesheimer, M. (1991). Central Auditory Skills in Blind and Sighted Subjects. *Scandinavian Audiology*, *20*(1), 19–23. doi: [10.3109/01050399109070785](https://doi.org/10.3109/01050399109070785)
- Müller, J. A., Wendt, D., Kollmeier, B., Debener, S., & Brand, T. (2019). Effect of Speech Rate on Neural Tracking of Speech. *Frontiers in Psychology*, *10*. doi: [10.3389/fpsyg.2019.00449](https://doi.org/10.3389/fpsyg.2019.00449)
- Münste, T. F., Altenmüller, E., & Jäncke, L. (2002). The musician's brain as a model of neuroplasticity. *Nature Reviews. Neuroscience*, *3*(6), 473–478. doi: [10.1038/nrn843](https://doi.org/10.1038/nrn843)
- Myers, B. R., Lense, M. D., & Gordon, R. L. (2019). Pushing the Envelope: Developments in Neural Entrainment to Speech and the Biological Underpinnings of Prosody Perception. *Brain Sciences*, *9*(3). doi: [10.3390/brainsci9030070](https://doi.org/10.3390/brainsci9030070)
- Näätänen, R. (1982). Processing negativity: An evoked-potential reflection of selective

- attention. *Psychological Bulletin*, 92(3), 605–640. doi: [10.1037/0033-2909.92.3.605](https://doi.org/10.1037/0033-2909.92.3.605)
- Näätänen, R., Kujala, T., Escera, C., Baldeweg, T., Kreegipuu, K., Carlson, S., & Ponton, C. (2012). The mismatch negativity (MMN) – A unique window to disturbed central auditory processing in ageing and different clinical conditions. *Clinical Neurophysiology*, 123(3), 424–458. doi: [10.1016/j.clinph.2011.09.020](https://doi.org/10.1016/j.clinph.2011.09.020)
- Näätänen, R., Paavilainen, P., Rinne, T., & Alho, K. (2007). The mismatch negativity (MMN) in basic research of central auditory processing: A review. *Clinical Neurophysiology*, 118(12), 2544–2590. doi: [10.1016/j.clinph.2007.04.026](https://doi.org/10.1016/j.clinph.2007.04.026)
- Näätänen, R., & Picton, T. (1987). The N1 wave of the human electric and magnetic response to sound: A review and an analysis of the component structure. *Psychophysiology*, 24(4), 375–425. doi: [10.1111/j.1469-8986.1987.tb00311.x](https://doi.org/10.1111/j.1469-8986.1987.tb00311.x)
- Näätänen, R., Tervaniemi, M., Sussman, E., Paavilainen, P., & Winkler, I. (2001). 'Primitive intelligence' in the auditory cortex. *Trends in Neurosciences*, 24(5), 283–288. doi: [10.1016/S0166-2236\(00\)01790-2](https://doi.org/10.1016/S0166-2236(00)01790-2)
- Nava, E., Bottari, D., Zampini, M., & Pavani, F. (2008). Visual temporal order judgment in profoundly deaf individuals. *Experimental Brain Research*, 190(2), 179–188. doi: [10.1007/s00221-008-1459-9](https://doi.org/10.1007/s00221-008-1459-9)
- Neville, H. J., & Bavelier, D. (1998). Neural organization and plasticity of language. *Current Opinion in Neurobiology*, 8(2), 254–258. doi: [10.1016/S0959-4388\(98\)80148-7](https://doi.org/10.1016/S0959-4388(98)80148-7)
- Neville, H. J., Bavelier, D., Corina, D., Rauschecker, J., Karni, A., Lalwani, A., ... Turner, R. (1998). Cerebral organization for language in deaf and hearing subjects: Biological constraints and effects of experience. *Proceedings of the National Academy of Sciences*, 95(3), 922–929. doi: [10.1073/pnas.95.3.922](https://doi.org/10.1073/pnas.95.3.922)
- Neville, H. J., & Lawson, D. (1987a). Attention to central and peripheral visual space in a movement detection task: An event-related potential and behavioral study. I. Normal hearing adults. *Brain Research*, 405(2), 253–267. doi: [10.1016/0006-8993\(87\)90295-2](https://doi.org/10.1016/0006-8993(87)90295-2)
- Neville, H. J., & Lawson, D. (1987b). Attention to central and peripheral visual space in a movement detection task: An event-related potential and behavioral study. II. Congenitally deaf adults. *Brain Research*, 405(2), 268–283. doi: [10.1016/0006-8993\(87\)90296-4](https://doi.org/10.1016/0006-8993(87)90296-4)
- Neville, H. J., & Lawson, D. (1987c). Attention to central and peripheral visual space in a movement detection task. III. Separate effects of auditory deprivation and acquisition of a visual language. *Brain Research*, 405(2), 284–294. doi: [10.1016/0006-8993\(87\)90297-6](https://doi.org/10.1016/0006-8993(87)90297-6)
- Niemeyer, W., & Starlinger, I. (1981). Do the blind hear better? Investigations on auditory processing in congenital or early acquired blindness II. Central functions. *Audiology: Official Organ of the International Society of Audiology*, 20(6), 510–515. doi: [10.3109/00206098109072719](https://doi.org/10.3109/00206098109072719)
- Nilsson, M. E., & Schenkman, B. N. (2016). Blind people are more sensitive than sighted people to binaural sound-location cues, particularly inter-aural level differences. *Hearing Research*, 332, 223–232. doi: [10.1016/j.heares.2015.09.012](https://doi.org/10.1016/j.heares.2015.09.012)
- Norcia, A. M., Appelbaum, L. G., Ales, J. M., Cottareau, B. R., & Rossion, B. (2015). The

steady-state visual evoked potential in vision research: A review. *Journal of Vision*, 15(6), 4–4. doi: [10.1167/15.6.4](https://doi.org/10.1167/15.6.4)

Obleser, J., Herrmann, B., & Henry, M. (2012). Neural Oscillations in Speech: Don't be Enslaved by the Envelope. *Frontiers in Human Neuroscience*, 6:250. doi: [10.3389/fnhum.2012.00250](https://doi.org/10.3389/fnhum.2012.00250)

Obleser, J., & Kayser, C. (2019). Neural Entrainment and Attentional Selection in the Listening Brain. *Trends in Cognitive Sciences*. doi: [10.1016/j.tics.2019.08.004](https://doi.org/10.1016/j.tics.2019.08.004)

Oostenveld, R., Fries, P., Maris, E., & Schoffelen, J.-M. (2011). FieldTrip: Open source software for advanced analysis of MEG, EEG, and invasive electrophysiological data. *Computational Intelligence and Neuroscience*, 2011, 156869. doi: [10.1155/2011/156869](https://doi.org/10.1155/2011/156869)

O'Sullivan, A. E., Crosse, M. J., Liberto, G. M. D., Cheveigné, A. de, & Lalor, E. C. (2021). Neurophysiological Indices of Audiovisual Speech Processing Reveal a Hierarchy of Multisensory Integration Effects. *Journal of Neuroscience*, 41(23), 4991–5003. doi: [10.1523/JNEUROSCI.0906-20.2021](https://doi.org/10.1523/JNEUROSCI.0906-20.2021)

O'Sullivan, J. A., Power, A. J., Mesgarani, N., Rajaram, S., Foxe, J. J., Shinn-Cunningham, B. G., ... Lalor, E. C. (2015). Attentional Selection in a Cocktail Party Environment Can Be Decoded from Single-Trial EEG. *Cerebral Cortex*, 25(7), 1697–1706. doi: [10.1093/cercor/bht355](https://doi.org/10.1093/cercor/bht355)

Palva, S., & Palva, J. M. (2011). Functional Roles of Alpha-Band Phase Synchronization in Local and Large-Scale Cortical Networks. *Frontiers in Psychology*, 2, 204. doi: [10.3389/fpsyg.2011.00204](https://doi.org/10.3389/fpsyg.2011.00204)

Papesh, M. A., Billings, C. J., & Baltzell, L. S. (2015). Background noise can enhance cortical auditory evoked potentials under certain conditions. *Clinical Neurophysiology: Official Journal of the International Federation of Clinical Neurophysiology*, 126(7), 1319–1330. doi: [10.1016/j.clinph.2014.10.017](https://doi.org/10.1016/j.clinph.2014.10.017)

Parbery-Clark, A., Marmel, F., Bair, J., & Kraus, N. (2011). What subcortical–cortical relationships tell us about processing speech in noise. *European Journal of Neuroscience*, 33(3), 549–557. doi: [10.1111/j.1460-9568.2010.07546.x](https://doi.org/10.1111/j.1460-9568.2010.07546.x)

Park, H., Kayser, C., Thut, G., & Gross, J. (2016). Lip movements entrain the observers' low-frequency brain oscillations to facilitate speech intelligibility. *ELife*, 5. doi: [10.7554/eLife.14521](https://doi.org/10.7554/eLife.14521)

Pascual-Leone, A., & Torres, F. (1993). Plasticity of the sensorimotor cortex representation of the reading finger in Braille readers. *Brain: A Journal of Neurology*, 116 (Pt 1), 39–52. doi: [10.1093/brain/116.1.39](https://doi.org/10.1093/brain/116.1.39)

Pascual-Leone, A., Wassermann, E. M., Sadato, N., & Hallett, M. (1995). The role of reading activity on the modulation of motor cortical outputs to the reading hand in Braille readers. *Annals of Neurology*, 38(6), 910–915. doi: [10.1002/ana.410380611](https://doi.org/10.1002/ana.410380611)

Pascual-Leone, A., & Hamilton, R. (2001). Chapter 27 The metamodal organization of the brain. In *Progress in Brain Research* (Vol. 134, pp. 427–445). Elsevier. doi: [10.1016/S0079-6123\(01\)34028-1](https://doi.org/10.1016/S0079-6123(01)34028-1)

Pavani, F., & Bottari, D. (2012). Visual Abilities in Individuals with Profound Deafness A

- Critical Review. In *M. M. Murray & M. Wallace (Eds), The Neural Bases of Multisensory Processes* (pp. 423–448). Boca Raton, FL: CRC Press.
- Pavani, F., & Röder, B. (2012). Crossmodal plasticity as a consequence of sensory loss: Insights from blindness and deafness. In *B. E. Stein (Ed), The New Handbook of Multisensory Processes* (pp. 737–759). Cambridge, MA: MIT Press.
- Peelle, J. E. (2012). The hemispheric lateralization of speech processing depends on what “speech” is: A hierarchical perspective. *Frontiers in Human Neuroscience*, *6*, 309. doi: [10.3389/fnhum.2012.00309](https://doi.org/10.3389/fnhum.2012.00309)
- Peelle, J. E., Gross, J., & Davis, M. H. (2013). Phase-Locked Responses to Speech in Human Auditory Cortex are Enhanced During Comprehension. *Cerebral Cortex*, *23*(6), 1378–1387. doi: [10.1093/cercor/bhs118](https://doi.org/10.1093/cercor/bhs118)
- Peelle, J. E., Johnsrude, I., & Davis, M. H. (2010). Hierarchical processing for speech in human auditory cortex and beyond. *Frontiers in Human Neuroscience*, *4*. doi: [10.3389/fnhum.2010.00051](https://doi.org/10.3389/fnhum.2010.00051)
- Petro, L. S., Paton, A. T., & Muckli, L. (2017). Contextual modulation of primary visual cortex by auditory signals. *Philosophical Transactions of the Royal Society B: Biological Sciences*, *372*(1714), 20160104. doi: [10.1098/rstb.2016.0104](https://doi.org/10.1098/rstb.2016.0104)
- Petrus, E., Isaiiah, A., Jones, A. P., Li, D., Wang, H., Lee, H.-K., & Kanold, P. O. (2014). Cross-modal induction of thalamocortical potentiation leads to enhanced information processing in the auditory cortex. *Neuron*, *81*(3), 664–673. doi: [10.1016/j.neuron.2013.11.023](https://doi.org/10.1016/j.neuron.2013.11.023)
- Petrus, E., Rodriguez, G., Patterson, R., Connor, B., Kanold, P. O., & Lee, H.-K. (2015). Vision Loss Shifts the Balance of Feedforward and Intracortical Circuits in Opposite Directions in Mouse Primary Auditory and Visual Cortices. *The Journal of Neuroscience*, *35*(23), 8790–8801. doi: [10.1523/JNEUROSCI.4975-14.2015](https://doi.org/10.1523/JNEUROSCI.4975-14.2015)
- Pitzorno, B. (1993). Polissena del Porcello [Polissena and her Pig]. Mondadori.
- Plass, J., Brang, D., Suzuki, S., & Grabowecky, M. (2020). Vision perceptually restores auditory spectral dynamics in speech. *Proceedings of the National Academy of Sciences*, *117*(29), 16920–16927. doi: [10.1073/pnas.2002887117](https://doi.org/10.1073/pnas.2002887117)
- Poeppl, D. (2003). The analysis of speech in different temporal integration windows: Cerebral lateralization as ‘asymmetric sampling in time.’ *Speech Communication*, *41*(1), 245–255. doi: [10.1016/S0167-6393\(02\)00107-3](https://doi.org/10.1016/S0167-6393(02)00107-3)
- Poeppl, D., & Assaneo, M. F. (2020). Speech rhythms and their neural foundations. *Nature Reviews Neuroscience*, *21*(6), 322–334. doi: [10.1038/s41583-020-0304-4](https://doi.org/10.1038/s41583-020-0304-4)
- Poeppl, D., Idsardi, W. J., & van Wassenhove, V. (2008). Speech perception at the interface of neurobiology and linguistics. *Philosophical Transactions of the Royal Society of London. Series B, Biological Sciences*, *363*(1493), 1071–1086. doi: [10.1098/rstb.2007.2160](https://doi.org/10.1098/rstb.2007.2160)
- Poirier, C., Collignon, O., Scheiber, C., Renier, L., Vanlierde, A., Tranduy, D., ... De Volder, A. G. (2006). Auditory motion perception activates visual motion areas in early blind subjects. *NeuroImage*, *31*(1), 279–285. doi: [10.1016/j.neuroimage.2005.11.036](https://doi.org/10.1016/j.neuroimage.2005.11.036)
- Presacco, A., Simon, J. Z., & Anderson, S. (2016). Evidence of degraded representation of

- speech in noise, in the aging midbrain and cortex. *Journal of Neurophysiology*, *116*(5), 2346–2355. doi: [10.1152/jn.00372.2016](https://doi.org/10.1152/jn.00372.2016)
- Proksch, J., & Bavelier, D. (2002). Changes in the Spatial Distribution of Visual Attention after Early Deafness. *Journal of Cognitive Neuroscience*, *14*(5), 687–701. doi: [10.1162/08989290260138591](https://doi.org/10.1162/08989290260138591)
- Puschmann, S., Regev, M., Baillet, S., & Zatorre, R. J. (2021). MEG Intersubject Phase Locking of Stimulus-Driven Activity during Naturalistic Speech Listening Correlates with Musical Training. *Journal of Neuroscience*, *41*(12), 2713–2722. doi: [10.1523/JNEUROSCI.0932-20.2020](https://doi.org/10.1523/JNEUROSCI.0932-20.2020)
- Qin, W., & Yu, C. (2013). Neural Pathways Conveying Novisual Information to the Visual Cortex. *Neural Plasticity*, *2013*, 864920. doi: [10.1155/2013/864920](https://doi.org/10.1155/2013/864920)
- Queneau, R. (1983). Exercices de style (U. Eco, Trans.). Einaudi. (Original work published 1947).
- Ranganath, C., & Rainer, G. (2003). Neural mechanisms for detecting and remembering novel events. *Nature Reviews Neuroscience*, *4*(3), 193–202. doi: [10.1038/nrn1052](https://doi.org/10.1038/nrn1052)
- Rauschecker, J. P. (1995). Developmental plasticity and memory. *Behavioural Brain Research*, *66*(1), 7–12. doi: [10.1016/0166-4328\(94\)00117-X](https://doi.org/10.1016/0166-4328(94)00117-X)
- Rauschecker, J. P. (2002). Cortical map plasticity in animals and humans. In *Plasticity in the Adult Brain: From Genes to Neurotherapy. Vol. 138. Progress in Brain Research* (pp. 73–88). Elsevier. doi: [10.1016/S0079-6123\(02\)38072-5](https://doi.org/10.1016/S0079-6123(02)38072-5)
- Recanzone, G. H., Merzenich, M. M., Jenkins, W. M., Grajski, K. A., & Dinse, H. R. (1992). Topographic reorganization of the hand representation in cortical area 3b owl monkeys trained in a frequency-discrimination task. *Journal of Neurophysiology*, *67*(5), 1031–1056. doi: [10.1152/jn.1992.67.5.1031](https://doi.org/10.1152/jn.1992.67.5.1031)
- Retter, T. L., Jiang, F., Webster, M. A., & Rossion, B. (2020). All-or-none face categorization in the human brain. *NeuroImage*, *213*, 116685. doi: [10.1016/j.neuroimage.2020.116685](https://doi.org/10.1016/j.neuroimage.2020.116685)
- Retter, T. L., & Rossion, B. (2016). Uncovering the neural magnitude and spatio-temporal dynamics of natural image categorization in a fast visual stream. *Neuropsychologia*, *91*, 9–28. doi: [10.1016/j.neuropsychologia.2016.07.028](https://doi.org/10.1016/j.neuropsychologia.2016.07.028)
- Ricciardi, E., Basso, D., Sani, L., Bonino, D., Vecchi, T., Pietrini, P., & Miniussi, C. (2011). Functional inhibition of the human middle temporal cortex affects non-visual motion perception: A repetitive transcranial magnetic stimulation study during tactile speed discrimination. *Experimental Biology and Medicine*, *236*(2), 138–144. doi: [10.1258/ebm.2010.010230](https://doi.org/10.1258/ebm.2010.010230)
- Ricciardi, E., Bonino, D., Pellegrini, S., & Pietrini, P. (2014). Mind the blind brain to understand the sighted one! Is there a supramodal cortical functional architecture? *Neuroscience & Biobehavioral Reviews*, *41*, 64–77. doi: [10.1016/j.neubiorev.2013.10.006](https://doi.org/10.1016/j.neubiorev.2013.10.006)
- Ricciardi, E., Bottari, D., Pfitz, M., Röder, B., & Pietrini, P. (2020). The sensory-deprived brain as a unique tool to understand brain development and function. *Neuroscience & Biobehavioral Reviews*, *108*, 78–82. doi: [10.1016/j.neubiorev.2019.10.017](https://doi.org/10.1016/j.neubiorev.2019.10.017)

- Ricciardi, E., & Pietrini, P. (2011). New light from the dark: What blindness can teach us about brain function. *Current Opinion in Neurology*, 24(4), 357–363. doi: [10.1097/WCO.0b013e328348bdf](https://doi.org/10.1097/WCO.0b013e328348bdf)
- Ricciardi, E., Vanello, N., Sani, L., Gentili, C., Scilingo, E. P., Landini, L., ... Pietrini, P. (2007). The Effect of Visual Experience on the Development of Functional Architecture in hMT+. *Cerebral Cortex*, 17(12), 2933–2939. doi: [10.1093/cercor/bhm018](https://doi.org/10.1093/cercor/bhm018)
- Richter, C. G., Coppola, R., & Bressler, S. L. (2018). Top-down beta oscillatory signaling conveys behavioral context in early visual cortex. *Scientific Reports*, 8(1), 6991. doi: [10.1038/s41598-018-25267-1](https://doi.org/10.1038/s41598-018-25267-1)
- Riecke, L., Formisano, E., Sorger, B., Ba kent, D., & Gaudrain, E. (2018). Neural Entrainment to Speech Modulates Speech Intelligibility. *Current Biology*, 28(2), 161–169.e5. doi: [10.1016/j.cub.2017.11.033](https://doi.org/10.1016/j.cub.2017.11.033)
- Rigoulot, S., Knoth, I. S., Lafontaine, M.-P., Vannasing, P., Major, P., Jacquemont, S., ... Lippé, S. (2017). Altered visual repetition suppression in Fragile X Syndrome: New evidence from ERPs and oscillatory activity. *International Journal of Developmental Neuroscience*, 59(1), 52–59. doi: <https://doi.org/10.1016/j.ijdevneu.2017.03.008>
- Roach, B. J., & Mathalon, D. H. (2008). Event-Related EEG Time-Frequency Analysis: An Overview of Measures and An Analysis of Early Gamma Band Phase Locking in Schizophrenia. *Schizophrenia Bulletin*, 34(5), 907–926. doi: [10.1093/schbul/sbn093](https://doi.org/10.1093/schbul/sbn093)
- Röder, B., & Neville, H. J. (2003). Developmental plasticity. In *J. Grafman & I.H. Robertson (Eds), Handbook of neuropsychology* (2nd ed., Vol. 9, pp. 231–270). Amsterdam: Elsevier Science.
- Röder, B., Rösler, F., Hennighausen, E., & Näcker, F. (1996). Event-related potentials during auditory and somatosensory discrimination in sighted and blind human subjects. *Cognitive Brain Research*, 4(2), 77–93. doi: [10.1016/0926-6410\(96\)00024-9](https://doi.org/10.1016/0926-6410(96)00024-9)
- Röder, B., Teder-Sälejärvi, W., Sterr, A., Rösler, F., Hillyard, S. A., & Neville, H. J. (1999). Improved auditory spatial tuning in blind humans. *Nature*, 400(6740), 162–166. doi: [10.1038/22106](https://doi.org/10.1038/22106)
- Röder, B., Rösler, F., & Neville, H. J. (1999). Effects of interstimulus interval on auditory event-related potentials in congenitally blind and normally sighted humans. *Neuroscience Letters*, 264(1), 53–56. doi: [10.1016/S0304-3940\(99\)00182-2](https://doi.org/10.1016/S0304-3940(99)00182-2)
- Röder, B., Stock, O., Bien, S., Neville, H., & Rösler, F. (2002). Speech processing activates visual cortex in congenitally blind humans: Plasticity of language functions in blind adults. *European Journal of Neuroscience*, 16(5), 930–936. doi: [10.1046/j.1460-9568.2002.02147.x](https://doi.org/10.1046/j.1460-9568.2002.02147.x)
- Rossion, B. (2014). Understanding individual face discrimination by means of fast periodic visual stimulation. *Experimental Brain Research*, 232(6), 1599–1621. doi: [10.1007/s00221-014-3934-9](https://doi.org/10.1007/s00221-014-3934-9)
- Rossion, B., Jacques, C., & Jonas, J. (2018). Mapping face categorization in the human ventral occipitotemporal cortex with direct neural intracranial recordings. *Annals of the New York Academy of Sciences*, 1426(1), 5–24. doi: [10.1111/nyas.13596](https://doi.org/10.1111/nyas.13596)
- Rossion, B., Retter, T. L., & Liu-Shuang, J. (2020). Understanding human individuation of

- unfamiliar faces with oddball fast periodic visual stimulation and electroencephalography. *European Journal of Neuroscience*, 52(10), 4283–4344. doi: [10.1111/ejn.14865](https://doi.org/10.1111/ejn.14865)
- Rossion, B., Torfs, K., Jacques, C., & Liu-Shuang, J. (2015). Fast periodic presentation of natural images reveals a robust face-selective electrophysiological response in the human brain. *Journal of Vision*, 18.
- Sadaghiani, S., & Kleinschmidt, A. (2016). Brain Networks and -Oscillations: Structural and Functional Foundations of Cognitive Control. *Trends in Cognitive Sciences*, 20(11), 805–817. doi: [10.1016/j.tics.2016.09.004](https://doi.org/10.1016/j.tics.2016.09.004)
- Sadato, N., Pascual-Leone, A., Grafman, J., Ibañez, V., Deiber, M.-P., Dold, G., & Hallett, M. (1996). Activation of the primary visual cortex by Braille reading in blind subjects. *Nature*, 380(6574), 526–528. doi: [10.1038/380526a0](https://doi.org/10.1038/380526a0)
- Sandmann, P., Dillier, N., Eichele, T., Meyer, M., Kegel, A., Pascual-Marqui, R. D., ... Debener, S. (2012). Visual activation of auditory cortex reflects maladaptive plasticity in cochlear implant users. *Brain*, 135(2), 555–568. doi: [10.1093/brain/awr329](https://doi.org/10.1093/brain/awr329)
- Sathian, K. (2005). Visual cortical activity during tactile perception in the sighted and the visually deprived. *Developmental Psychobiology*, 46(3), 279–286. doi: [10.1002/dev.20056](https://doi.org/10.1002/dev.20056)
- Schneider, W., Eschman, A., & Zuccolotto, A. (2002). E-Prime Reference Guide. Pittsburgue, PA: Psychology Software Tools.
- Schneider, T. R., Lorenz, S., Senkowski, D., & Engel, A. K. (2011). Gamma-Band Activity as a Signature for Cross-Modal Priming of Auditory Object Recognition by Active Haptic Exploration. *Journal of Neuroscience*, 31(7), 2502–2510. doi: [10.1523/JNEUROSCI.6447-09.2011](https://doi.org/10.1523/JNEUROSCI.6447-09.2011)
- Schomaker, J., & Meeter, M. (2014). Novelty detection is enhanced when attention is otherwise engaged: An event-related potential study. *Experimental Brain Research*, 232(3), 995–1011. doi: [10.1007/s00221-013-3811-y](https://doi.org/10.1007/s00221-013-3811-y)
- Seghier, M. L. (2008). Laterality index in functional MRI: Methodological issues. *Magnetic Resonance Imaging*, 26(5), 594–601. doi: [10.1016/j.mri.2007.10.010](https://doi.org/10.1016/j.mri.2007.10.010)
- Seydell-Greenwald, A., Wang, X., Newport, E., Bi, Y., & Striem-Amit, E. (2021). Primary visual cortex is activated by spoken language comprehension. *Journal of Vision*, 21(9), 2256. doi: [10.1167/jov.21.9.2256](https://doi.org/10.1167/jov.21.9.2256)
- Shannon, R. V., Zeng, F.-G., Kamath, V., Wygonski, J., & Ekelid, M. (1995). Speech Recognition with Primarily Temporal Cues. *Science*, 270(5234), 303–304. doi: [10.1126/science.270.5234.303](https://doi.org/10.1126/science.270.5234.303)
- Sharma, A., Campbell, J., & Cardon, G. (2015). Developmental and cross-modal plasticity in deafness: Evidence from the P1 and N1 event related potentials in cochlear implanted children. *International Journal of Psychophysiology*, 95(2), 135–144. doi: [10.1016/j.ijpsycho.2014.04.007](https://doi.org/10.1016/j.ijpsycho.2014.04.007)
- Sheehan, M. J., & Nachman, M. W. (2014). Morphological and population genomic evidence that human faces have evolved to signal individual identity. *Nature Communications*, 5(1), 4800. doi: [10.1038/ncomms5800](https://doi.org/10.1038/ncomms5800)

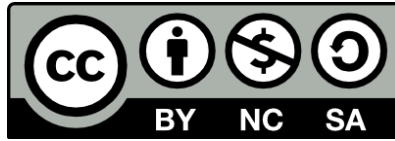
- Shirazi, S. Y., & Huang, H. J. (2019). More Reliable EEG Electrode Digitizing Methods Can Reduce Source Estimation Uncertainty, but Current Methods Already Accurately Identify Brodmann Areas. *Frontiers in Neuroscience*, *13*, 1159. doi: [10.3389/fnins.2019.01159](https://doi.org/10.3389/fnins.2019.01159)
- Siegel, M., Donner, T. H., & Engel, A. K. (2012). Spectral fingerprints of large-scale neuronal interactions. *Nature Reviews Neuroscience*, *13*(2), 121–134. doi: [10.1038/nrn3137](https://doi.org/10.1038/nrn3137)
- Simion, F., Regolin, L., & Bulf, H. (2008). A predisposition for biological motion in the newborn baby. *Proceedings of the National Academy of Sciences*, *105*(2), 809–813. doi: [10.1073/pnas.0707021105](https://doi.org/10.1073/pnas.0707021105)
- Šimkovic, M., & Träuble, B. (2019). Robustness of statistical methods when measure is affected by ceiling and/or floor effect. *PLOS ONE*, *14*(8), e0220889. doi: [10.1371/journal.pone.0220889](https://doi.org/10.1371/journal.pone.0220889)
- Skotara, N., Salden, U., Kügow, M., Hänel-Faulhaber, B., & Röder, B. (2012). The influence of language deprivation in early childhood on L2 processing: An ERP comparison of deaf native signers and deaf signers with a delayed language acquisition. *BMC Neuroscience*, *13*(1), 44. doi: [10.1186/1471-2202-13-44](https://doi.org/10.1186/1471-2202-13-44)
- Smittenaar, C. R., MacSweeney, M., Sereno, M. I., & Schwarzkopf, D. S. (2016). Does Congenital Deafness Affect the Structural and Functional Architecture of Primary Visual Cortex? *The Open Neuroimaging Journal*, *10*(1). doi: [10.2174/1874440001610010001](https://doi.org/10.2174/1874440001610010001)
- Snyder, K. A., & Keil, A. (2008). Repetition Suppression of Induced Gamma Activity Predicts Enhanced Orienting toward a Novel Stimulus in 6-month-old Infants. *Journal of Cognitive Neuroscience*, *20*(12), 2137–2152. doi: [10.1162/jocn.2008.20149](https://doi.org/10.1162/jocn.2008.20149)
- Sokolov, E. N. (1963). Higher Nervous Functions: The Orienting Reflex. *Annual Review of Physiology*, *25*(1), 545–580. doi: [10.1146/annurev.ph.25.030163.002553](https://doi.org/10.1146/annurev.ph.25.030163.002553)
- Sokolov, E. N. (1990). The orienting response, and future directions of its development. *The Pavlovian Journal of Biological Science*, *25*(3), 142–150. doi: [10.1007/BF02974268](https://doi.org/10.1007/BF02974268)
- Spyropoulos, G., Bosman, C. A., & Fries, P. (2018). A theta rhythm in macaque visual cortex and its attentional modulation. *Proceedings of the National Academy of Sciences*, *115*(24), E5614–E5623. doi: [10.1073/pnas.1719433115](https://doi.org/10.1073/pnas.1719433115)
- Stefanics, G., Kimura, M., & Czigler, I. (2011). Visual Mismatch Negativity Reveals Automatic Detection of Sequential Regularity Violation. *Frontiers in Human Neuroscience*, *5*, 46. doi: [10.3389/fnhum.2011.00046](https://doi.org/10.3389/fnhum.2011.00046)
- Stenroos, M., Hunold, A., & Haueisen, J. (2014). Comparison of three-shell and simplified volume conductor models in magnetoencephalography. *NeuroImage*, *94*, 337–348. doi: [10.1016/j.neuroimage.2014.01.006](https://doi.org/10.1016/j.neuroimage.2014.01.006)
- Stivalet, P., Moreno, Y., Richard, J., Barraud, P.-A., & Raphel, C. (1998). Differences in visual search tasks between congenitally deaf and normally hearing adults. *Cognitive Brain Research*, *6*(3), 227–232. doi: [10.1016/S0926-6410\(97\)00026-8](https://doi.org/10.1016/S0926-6410(97)00026-8)
- Stoll, C., Palluel-Germain, R., Caldara, R., Lao, J., Dye, M. W. G., Aptel, F., & Pascalis, O. (2018). Face Recognition is Shaped by the Use of Sign Language. *The Journal of Deaf Studies and Deaf Education*, *23*(1), 62–70. doi: [10.1093/deafed/enx034](https://doi.org/10.1093/deafed/enx034)

- Stothart, G., & Kazanina, N. (2013). Oscillatory characteristics of the visual mismatch negativity: What evoked potentials aren't telling us. *Frontiers in Human Neuroscience*, *7*, 426. doi: [10.3389/fnhum.2013.00426](https://doi.org/10.3389/fnhum.2013.00426)
- Stothart, G., Quadflieg, S., & Milton, A. (2017). A fast and implicit measure of semantic categorisation using steady state visual evoked potentials. *Neuropsychologia*, *102*, 11–18. doi: [10.1016/j.neuropsychologia.2017.05.025](https://doi.org/10.1016/j.neuropsychologia.2017.05.025)
- Striem-Amit, E., Bubic, A., & Amedi, A. (2012). Chapter 21 Neurophysiological Mechanisms Underlying Plastic Changes and Rehabilitation following Sensory Loss in Blindness and Deafness. In *M. M. Murray & M. T. Wallace (Eds.), The Neural Bases of Multisensory Processes*. Boca Raton, FL: CRC Press/Taylor & Francis.
- Striem-Amit, E., Dakwar, O., Reich, L., & Amedi, A. (2012). The large-scale organization of “visual” streams emerges without visual experience. *Cerebral Cortex*, *22*(7), 1698–1709. doi: [10.1093/cercor/bhr253](https://doi.org/10.1093/cercor/bhr253)
- Stropahl, M., Bauer, A.-K. R., Debener, S., & Bleichner, M. G. (2018). Source-Modeling Auditory Processes of EEG Data Using EEGLAB and Brainstorm. *Frontiers in Neuroscience*, *12*, 309. doi: [10.3389/fnins.2018.00309](https://doi.org/10.3389/fnins.2018.00309)
- Stropahl, M., Chen, L.-C., & Debener, S. (2017). Cortical reorganization in postlingually deaf cochlear implant users: Intra-modal and cross-modal considerations. *Hearing Research*, *343*, 128–137. doi: [10.1016/j.heares.2016.07.005](https://doi.org/10.1016/j.heares.2016.07.005)
- Stropahl, M., Plotz, K., Schönfeld, R., Lenarz, T., Sandmann, P., Yovel, G., ... Debener, S. (2015). Cross-modal reorganization in cochlear implant users: Auditory cortex contributes to visual face processing. *NeuroImage*, *121*, 159–170. doi: [10.1016/j.neuroimage.2015.07.062](https://doi.org/10.1016/j.neuroimage.2015.07.062)
- Summerfield, C., Trittschuh, E. H., Monti, J. M., Mesulam, M.-M., & Egner, T. (2008). Neural repetition suppression reflects fulfilled perceptual expectations. *Nature Neuroscience*, *11*(9), 1004–1006. doi: [10.1038/nn.2163](https://doi.org/10.1038/nn.2163)
- Summerfield, C., Wyart, V., Johnen, V. M., & de Gardelle, V. (2011). Human Scalp Electroencephalography Reveals that Repetition Suppression Varies with Expectation. *Frontiers in Human Neuroscience*, *5*. doi: [10.3389/fnhum.2011.00067](https://doi.org/10.3389/fnhum.2011.00067)
- Tadel, F., Baillet, S., Mosher, J. C., Pantazis, D., & Leahy, R. M. (2011). Brainstorm: A User-Friendly Application for MEG/EEG Analysis. *Computational Intelligence and Neuroscience*, *2011*, e879716. doi: [10.1155/2011/879716](https://doi.org/10.1155/2011/879716)
- Tallon-Baudry, C., & Bertrand, O. (1999). Oscillatory gamma activity in humans and its role in object representation. *Trends in Cognitive Sciences*, *3*(4), 151–162. doi: [10.1016/s1364-6613\(99\)01299-1](https://doi.org/10.1016/s1364-6613(99)01299-1)
- Tallon-Baudry, C., Bertrand, O., Delpuech, C., & Pernier, J. (1996). Stimulus Specificity of Phase-Locked and Non-Phase-Locked 40 Hz Visual Responses in Human. *Journal of Neuroscience*, *16*(13), 4240–4249. doi: [10.1523/JNEUROSCI.16-13-04240.1996](https://doi.org/10.1523/JNEUROSCI.16-13-04240.1996)
- Tallon-Baudry, C., Bertrand, O., Delpuech, C., & Pernier, J. (1997). Oscillatory γ -Band (30–70 Hz) Activity Induced by a Visual Search Task in Humans. *Journal of Neuroscience*, *17*(2), 722–734. doi: [10.1523/JNEUROSCI.17-02-00722.1997](https://doi.org/10.1523/JNEUROSCI.17-02-00722.1997)

- Thoma, R. J., Hanlon, F. M., Moses, S. N., Edgar, J. C., Huang, M., Weisend, M. P., ... Cañive, J. M. (2003). Lateralization of Auditory Sensory Gating and Neuropsychological Dysfunction in Schizophrenia. *American Journal of Psychiatry*, *160*(9), 1595–1605. doi: [10.1176/appi.ajp.160.9.1595](https://doi.org/10.1176/appi.ajp.160.9.1595)
- Van Ackeren, M. J., Barbero, F. M., Mattioni, S., Bottini, R., & Collignon, O. (2018). Neuronal populations in the occipital cortex of the blind synchronize to the temporal dynamics of speech. *ELife*, *7*, e31640. doi: [10.7554/eLife.31640](https://doi.org/10.7554/eLife.31640)
- Van Diepen, R. M., Foxe, J. J., & Mazaheri, A. (2019). The functional role of alpha-band activity in attentional processing: The current zeitgeist and future outlook. *Current Opinion in Psychology*, *29*, 229–238. doi: [10.1016/j.copsyc.2019.03.015](https://doi.org/10.1016/j.copsyc.2019.03.015)
- Van Diepen, R. M., & Mazaheri, A. (2018). The Caveats of observing Inter-Trial Phase-Coherence in Cognitive Neuroscience. *Scientific Reports*, *8*(1), 2990. doi: [10.1038/s41598-018-20423-z](https://doi.org/10.1038/s41598-018-20423-z)
- Van Engen, K. J. (2010). Similarity and familiarity: Second language sentence recognition in first- and second-language multi-talker babble. *Speech Communication*, *52*(11–12), 943–953. doi: [10.1016/j.specom.2010.05.002](https://doi.org/10.1016/j.specom.2010.05.002)
- Van Engen, K. J., & Bradlow, A. R. (2007). Sentence recognition in native- and foreign-language multi-talker background noise. *The Journal of the Acoustical Society of America*, *121*(1), 519–526. doi: [10.1121/1.2400666](https://doi.org/10.1121/1.2400666)
- Van Engen, K. J., & Peelle, J. E. (2014). Listening effort and accented speech. *Frontiers in Human Neuroscience*, *8*:577. doi: [10.3389/fnhum.2014.00577](https://doi.org/10.3389/fnhum.2014.00577)
- Van Kerkoerle, T., Self, M. W., Dagnino, B., Gariel-Mathis, M.-A., Poort, J., van der Togt, C., & Roelfsema, P. R. (2014). Alpha and gamma oscillations characterize feedback and feedforward processing in monkey visual cortex. *Proceedings of the National Academy of Sciences*, *111*(40), 14332–14341. doi: [10.1073/pnas.1402773111](https://doi.org/10.1073/pnas.1402773111)
- Vanthornhout, J., Decruy, L., Wouters, J., Simon, J. Z., & Francart, T. (2018). Speech Intelligibility Predicted from Neural Entrainment of the Speech Envelope. *Journal of the Association for Research in Otolaryngology*, *19*(2), 181–191. doi: [10.1007/s10162-018-0654-z](https://doi.org/10.1007/s10162-018-0654-z)
- Vetter, P., Bola, L., Reich, L., Bennett, M., Muckli, L., & Amedi, A. (2020). Decoding Natural Sounds in Early “Visual” Cortex of Congenitally Blind Individuals. *Current Biology*, *30*(15), 3039–3044.e2. doi: [10.1016/j.cub.2020.05.071](https://doi.org/10.1016/j.cub.2020.05.071)
- Vetter, P., Smith, F. W., & Muckli, L. (2014). Decoding sound and imagery content in early visual cortex. *Current Biology: CB*, *24*(11), 1256–1262. doi: [10.1016/j.cub.2014.04.020](https://doi.org/10.1016/j.cub.2014.04.020)
- Vettori, S., Dzhelyova, M., Van der Donck, S., Jacques, C., Steyaert, J., Rossion, B., & Boets, B. (2019). Reduced neural sensitivity to rapid individual face discrimination in autism spectrum disorder. *NeuroImage: Clinical*, *21*, 101613. doi: [10.1016/j.nicl.2018.101613](https://doi.org/10.1016/j.nicl.2018.101613)
- Vinken, K., Op de Beeck, H. P., & Vogels, R. (2018). Face Repetition Probability Does Not Affect Repetition Suppression in Macaque Inferotemporal Cortex. *The Journal of Neuroscience*, *38*(34), 7492–7504. doi: [10.1523/JNEUROSCI.0462-18.2018](https://doi.org/10.1523/JNEUROSCI.0462-18.2018)
- Vinken, K., & Vogels, R. (2017). Adaptation can explain evidence for encoding of

- probabilistic information in macaque inferior temporal cortex. *Current Biology*, 27(22), R1210–R1212. doi: [10.1016/j.cub.2017.09.018](https://doi.org/10.1016/j.cub.2017.09.018)
- Vogels, R. (2016). Sources of adaptation of inferior temporal cortical responses. *Cortex*, 80, 185–195. doi: [10.1016/j.cortex.2015.08.024](https://doi.org/10.1016/j.cortex.2015.08.024)
- Waldo, M., Gerhardt, G., Baker, N., Drebing, C., Adler, L., & Freedman, R. (1992). Auditory sensory gating and catecholamine metabolism in schizophrenic and normal subjects. *Psychiatry Research*, 44(1), 21–32. doi: [10.1016/0165-1781\(92\)90066-c](https://doi.org/10.1016/0165-1781(92)90066-c)
- Wang, L., Wu, E. X., & Chen, F. (2020). Robust EEG-Based Decoding of Auditory Attention With High-RMS-Level Speech Segments in Noisy Conditions. *Frontiers in Human Neuroscience*. 14:557534. doi: [10.3389/fnhum.2020.557534](https://doi.org/10.3389/fnhum.2020.557534)
- Wang, Xianhui, & Xu, L. (2021). Speech perception in noise: Masking and unmasking. *Journal of Otology*, 16(2), 109–119. doi: [10.1016/j.joto.2020.12.001](https://doi.org/10.1016/j.joto.2020.12.001)
- Wang, Xiaosha, Caramazza, A., Peelen, M. V., Han, Z., & Bi, Y. (2015). Reading Without Speech Sounds: VWFA and its Connectivity in the Congenitally Deaf. *Cerebral Cortex*, 25(9), 2416–2426. doi: [10.1093/cercor/bhu044](https://doi.org/10.1093/cercor/bhu044)
- Waters, D., Campbell, R., Capek, C. M., Woll, B., David, A. S., McGuire, P. K., ... MacSweeney, M. (2007). Fingerspelling, signed language, text and picture processing in deaf native signers: The role of the mid-fusiform gyrus. *NeuroImage*, 35(3), 1287–1302. doi: [10.1016/j.neuroimage.2007.01.025](https://doi.org/10.1016/j.neuroimage.2007.01.025)
- Webster, M. A. (2015). Visual Adaptation. *Annual Review of Vision Science*, 1(1), 547–567. doi: [10.1146/annurev-vision-082114-035509](https://doi.org/10.1146/annurev-vision-082114-035509)
- Weisberg, J., Koo, D. S., Crain, K. L., & Eden, G. F. (2012). Cortical plasticity for visuospatial processing and object recognition in deaf and hearing signers. *NeuroImage*, 60(1), 661–672. doi: [10.1016/j.neuroimage.2011.12.031](https://doi.org/10.1016/j.neuroimage.2011.12.031)
- Widmann, A., Schröger, E., & Maess, B. (2015). Digital filter design for electrophysiological data – a practical approach. *Journal of Neuroscience Methods*, 250, 34–46. doi: [10.1016/j.jneumeth.2014.08.002](https://doi.org/10.1016/j.jneumeth.2014.08.002)
- Willems, R. M., & Gerven, M. A. J. van. (2018). New fMRI Methods for the Study of Language. In S.-A. Rueschemeyer & M. G. Gaskell (Eds.), *The Oxford Handbook of Psycholinguistics* (2 ed.). Oxford: Oxford University Press. doi: [10.1093/oxfordhb/9780198786825.013.42](https://doi.org/10.1093/oxfordhb/9780198786825.013.42)
- Wolmetz, M., Poeppel, D., & Rapp, B. (2011). What Does the Right Hemisphere Know about Phoneme Categories? *Journal of Cognitive Neuroscience*, 23(3), 552–569. doi: [10.1162/jocn.2010.21495](https://doi.org/10.1162/jocn.2010.21495)
- Yan, T., Feng, Y., Liu, T., Wang, L., Mu, N., Dong, X., ... Zhao, L. (2017). Theta Oscillations Related to Orientation Recognition in Unattended Condition: A vMMN Study. *Frontiers in Behavioral Neuroscience*, 11, 166. doi: [10.3389/fnbeh.2017.00166](https://doi.org/10.3389/fnbeh.2017.00166)
- Yan, X., Liu-Shuang, J., & Rossion, B. (2019). Effect of face-related task on rapid individual face discrimination. *Neuropsychologia*, 129, 236–245. doi: [10.1016/j.neuropsychologia.2019.04.002](https://doi.org/10.1016/j.neuropsychologia.2019.04.002)

- Yusuf, P. A., Hubka, P., Tillein, J., & Kral, A. (2017). Induced cortical responses require developmental sensory experience. *Brain*, *140*(12), 3153–3165. doi: [10.1093/brain/awx286](https://doi.org/10.1093/brain/awx286)
- Yusuf, P. A., Hubka, P., Tillein, J., Vinck, M., & Kral, A. (2021). Deafness Weakens Interareal Couplings in the Auditory Cortex. *Frontiers in Neuroscience*, *14*, 625721. doi: [10.3389/fnins.2020.625721](https://doi.org/10.3389/fnins.2020.625721)
- Zangaladze, A., Epstein, C. M., Grafton, S. T., & Sathian, K. (1999). Involvement of visual cortex in tactile discrimination of orientation. *Nature*, *401*(6753), 587–590. doi: [10.1038/44139](https://doi.org/10.1038/44139)
- Zareian, B., Maboudi, K., Daliri, M. R., Abrishami Moghaddam, H., Treue, S., & Esghaei, M. (2020). Attention strengthens across-trial pre-stimulus phase coherence in visual cortex, enhancing stimulus processing. *Scientific Reports*, *10*(1), 4837. doi: [10.1038/s41598-020-61359-7](https://doi.org/10.1038/s41598-020-61359-7)
- Zendel, B. R., West, G. L., Belleville, S., & Peretz, I. (2019). Musical training improves the ability to understand speech-in-noise in older adults. *Neurobiology of Aging*, *81*, 102–115. doi: [10.1016/j.neurobiolaging.2019.05.015](https://doi.org/10.1016/j.neurobiolaging.2019.05.015)
- Zion Golumbic, E. M., Ding, N., Bickel, S., Lakatos, P., Schevon, C. A., McKhann, G. M., ... Schroeder, C. E. (2013). Mechanisms Underlying Selective Neuronal Tracking of Attended Speech at a ‘Cocktail Party.’ *Neuron*, *77*(5), 980–991. doi: [10.1016/j.neuron.2012.12.037](https://doi.org/10.1016/j.neuron.2012.12.037)
- Zoefel, B. (2018). Speech Entrainment: Rhythmic Predictions Carried by Neural Oscillations. *Current Biology*, *28*(18), R1102–R1104. doi: [10.1016/j.cub.2018.07.048](https://doi.org/10.1016/j.cub.2018.07.048)
- Zorzos, I., Kakkos, I., Ventouras, E. M., & Matsopoulos, G. K. (2021). Advances in Electrical Source Imaging: A Review of the Current Approaches, Applications and Challenges. *Signals*, *2*(3), 378–391. doi: [10.3390/signals2030024](https://doi.org/10.3390/signals2030024)



Unless otherwise expressly stated, all original material of whatever nature created by Evgenia Bednaya and included in this thesis, is licensed under a Creative Commons Attribution Noncommercial Share Alike 3.0 Italy License.

Check on Creative Commons site:

<https://creativecommons.org/licenses/by-nc-sa/3.0/it/legalcode>

<https://creativecommons.org/licenses/by-nc-sa/3.0/it/deed.en>

Ask the author about other uses.